ESTIMATING THE RELATIVE ENERGETIC COST OF FORAGING IN PACIFIC COAST FEEDING GROUP GREY WHALES FROM BIOLOGGING DATA

by

Kate M. Colson

B.Sc., The University of British Columbia, 2020

A THESIS SUBMITTED IN PARTIAL FULFILLMENT OF

THE REQUIREMENTS FOR THE DEGREE OF

MASTER OF SCIENCE

in

THE FACULTY OF GRADUATE AND POSTDOCTORAL STUDIES

(Oceans and Fisheries)

THE UNIVERSITY OF BRITISH COLUMBIA

(Vancouver)

August 2023

The following individuals certify that they have read, and recommend to the Faculty of Graduate and Postdoctoral Studies for acceptance, the thesis entitled:

Estimating the Relative Energetic Cost of Foraging in Pacific Coast Feeding Group Grey Whales from Biologging Data

submitted by	Kate M. Colson	in partial fulfilment of the requirements
for the degree of	Master of Science	
in	Oceans and Fisheries	

Examining Committee:

Andrew Trites, Professor, Institute for the Oceans and Fisheries, UBC
Supervisor

Leigh Torres, Associate Professor, Marine Mammal Institute, Oregon State University
Supervisory Committee Member

Evgeny Pakhomov, Professor, Institute for the Oceans and Fisheries, UBC
Additional Examiner

Additional Supervisory Committee Members:

David Cade, Post Doctoral Fellow, Hopkins Marine Station, Stanford University
Supervisory Committee Member

Christopher Harley, Professor, Institute for the Oceans and Fisheries, UBC
Supervisory Committee Member

Abstract

Biologging tags that record high-resolution tri-axial accelerometry data are proving to be integral to the study of foraging ecology of large, free-roaming marine mammals, such as whales. They have been applied to a number of baleen whale species that feed pelagically through lunges or ram filtration to quantitatively define behaviours and estimate energetic costs. However, few behavioural ecology studies using accelerometry data have been conducted on grey whales, a unique baleen whale that performs benthic suction feeding. Using suction cup tri-axial accelerometer tag deployments on 10 Pacific Coast Feeding Group (PCFG) grey whales along the Oregon and Washington coasts, I defined signals of foraging behaviour at both the broad state (dive) and foraging tactic (roll event) scales. I then estimated the relative energetic cost of these behaviours using energy expenditure proxies derived from the accelerometry data—Overall Dynamic Body Acceleration (ODBA; ms^{-2}), stroke rate (Hz), stroke amplitude (radians per s), and duration of dives with different foraging tactics performed (min). Hidden Markov Models (HMMs) defined three biologically distinct states—forage, search, and transit—using turn angle, dive duration, dive tortuosity and presence of roll events. Classification and Regression Tree (CART) models best defined the foraging tactics of headstands, benthic digs, and side swims using median pitch, depth to body length ratio, and absolute value of the median roll. These definitions of grey whale foraging signals using accelerometry data add to the quantitative descriptions of foraging behaviours previously described for baleen whales. Stroke rate identified foraging and headstanding as being the most energetically costly activities at the broad state and foraging tactic scales. These findings contribute to the foundational understanding of grey whale foraging energetics needed to assess the impacts of various conservation concerns on the fitness and interpret patterns of behaviour choice of this unique group of grey whales.

Lay Summary

Suction cup tags that record fine scale behaviour are important tools for studying baleen whales. However, this technology has not been used to describe the behavioural energetics of grey whales, a unique species of baleen whale that feeds on the sea floor. I used data from suction cup tags deployed on Pacific Coast Feeding Group (PCFG) grey whales to define foraging behaviours and estimate the relative energetic cost of these behaviours. My work adds to the quantitative definitions of foraging behaviours previously described in baleen whales and provides a foundational understanding of grey whale foraging energetics. These findings can help explain patterns of behavioural choices made by PCFG grey whales.

Preface

This thesis represents my original work. Co-supervised by Dr. Andrew W. Trites and Dr. Leigh G. Torres, I came up with the research questions and designed the study. Input from committee members Dr. David E. Cade and Dr. Christopher Harley was incorporated into the study design and analysis. John Calambokidis and Dr. David E. Cade helped deploy the tags used in this study, while I assisted with the tagging effort field work as an additional member of the Geospatial Ecology of Marine Megafauna Lab field team at Oregon State University with approval of the University of British Columbia Animal Care Committee (permit #A21-0254). I pre-processed the tag data with assistance from Dr. David E. Cade and conducted the statistical analyses with guidance from Dr. Enrico Pirotta and Dr. Leslie New. I formatted data chapters (Chapter 2 and Chapter 3) as manuscripts for submission to peer-reviewed journals.

Table of Contents

List of Tables

List of Figures

List of submitted files

Movie S1

Acknowledgements

I have so many people to thank for making my graduate experience a memorable one. First, thank you to my supervisors Dr. Andrew Trites and Dr. Leigh Torres. Andrew, I appreciate you helping me to think critically and making me a more competent researcher. Leigh, I am so grateful for all the opportunities you gave me to learn what it means to be a scientist and how to be successful in academia. I owe Dr. Dave Cade a debt of gratitude for patiently teaching me how to process tag data and for using his rockstar tagging skills to help collect the data for this research. Thank you to Dr. Chris Harley for helping me refocus on the bigger picture and always reminding me that he was there to help me achieve my goals.

I am indebted to Dr. Enrico Pirotta and Dr. Leslie New for all their advice on statistical analysis and their guidance in model building and interpretation. I learned so much from you both. I thank all the GRANITE collaborators for their valuable feedback through the various stages of this research and the GRANITE field team for memorable days on the water collecting amazing data.

I want to thank Pamela Rosenbaum for all the behind the scenes help needed to make progress on my thesis and get me graduated on time and John Calambokidis for sharing tag deployments from Washington and collaborating in the fieldwork efforts.

I am so fortunate that my master's degree made me a part of two labs, and I am so grateful for the support, advice and brainstorming from my MMRU and GEMM Lab mates. Working alongside you all has made the experience unforgettable.

Finally, I am eternally grateful for all the support I received from my friends and family. I would not be where I am today without you.

For my parents

Chapter 1: General introduction

Behaviour mediates how individuals interact with other individuals and their environment. As such, understanding a species' behavioural ecology is fundamental to determining the fitness implications of behaviour choice on a population. More specifically, behavioural ecology can provide a framework to understand the impact of human disturbance and overexploitation, explain the ecology of fear, determine locations of critical habitat, and predict responses to climate change (Dill, 2017), all of which are critical pieces of information to inform conservation efforts.

Feeding, fleeing, fighting and reproduction are the four F's representing the main components of behavioural ecology. Foraging behaviour has the added significance of being the only time that energy is being consumed to compensate for the energy expended during all other activities, including the foraging behaviour itself (Norberg, 1977). Foraging success determines body condition, which in turn affects reproductive output and ultimately population success (Lemos et al., 2020a). Therefore, not only is it important to be able to define foraging behaviour of a species, but it is also necessary to determine the cost of foraging, as this knowledge can ultimately be used to assess the impacts of threats and disturbance on a population.

Studying the behavioural ecology of marine animals, such as cetaceans, is challenging given the logistical constraints of species that perform most of their behaviours underwater. This has necessitated technological developments to undertake more in-depth behavioural studies (Nowacek et al., 2016). Unoccupied Aerial Systems (UAS; aka drones), for example, have progressed the study of cetacean behaviour beyond land- or boat-based focal follows by extending the observation capacity by a factor of three (Torres et al., 2018). However, observing behaviour from drone footage is constrained by water clarity, depth of the animal, and daylight observation, necessitating use of more advanced tools.

Not only is it logistically challenging to observe and classify cetacean behaviours, it is also difficult to estimate metabolic cost of behaviours in cetaceans. Two methods commonly used to measure the metabolic rates of small species of marine mammals, respirometry (Withers, 1977) and doubly labeled water (Schoeller and van Santen, 1982) require re-capturing an animal (doubly labelled water method) or obtaining measurements of gas exchange in a controlled environment (respirometry), both of which are logistically challenging when working with free-

ranging, large-bodied cetaceans. Estimates of energy expenditure can also be obtained from heart rate, but also requires a controlled environment for calibration that is difficult if not impossible to obtain in large diving marine mammals (Butler et al., 2004; Green, 2011). Respiration rate has thus become the most commonly applied method to estimate metabolic rate in cetaceans, although it requires many assumptions that can lead to inaccurate estimates (Fahlman et al., 2016).

Despite the challenges of studying the foraging behaviour and energetics in whales, the vulnerable state of many cetacean populations recovering from industrial whaling (Magera et al., 2013) makes understanding cetacean behavioural ecology and energetics vital for interpreting population dynamics of these species and informing management decisions.

Biologging methods in baleen whales

The development of biologging tags has revolutionized behavioural studies in cetaceans due to high frequency sampling rates and integration of multiple sensors (i.e., accelerometers, magnetometers, and gyroscopes) that allow for fine scale detection of behaviours and provide a minimally invasive means to estimate energy expenditure (Crossin et al., 2014; Watanabe and Goldbogen, 2021). Biologging tags do not face the daytime-only constraint that limits visual focal follows (e.g., Schwarz et al., 2021) and allow for the observation of the individual without needing a research vessel to be near the whale, which could potentially disrupt the observed behaviours. Additionally, given that most cetacean foraging behaviours occur at depth, the ability of biologging tags to record throughout a dive cycle provides unique and critical data that is not possible to collect from focal follows, even from drones (Wright et al., 2017).

Overall Dynamic Body Acceleration (ODBA) as a measure of body movement (Wilson et al., 2020) and stroke rate (Williams and Maresh, 2015) are helpful proxies for energy expenditure that are derived from accelerometry data. Higher ODBA and higher stroke rate correspond to elevated energetic costs and can be used to estimate metabolic rate when linked with oxygen consumption. ODBA has been linked to metabolism in many studies (Allen et al., 2022; Fahlman et al., 2013; Halsey et al., 2009; Jeanniard-du-Dot et al., 2017; John, 2020; Wilson et al., 2006). Stroke rate is more commonly linked to metabolic rate for cetaceans than ODBA, although most studies have primarily focused on odontocetes and pinnipeds (Allen et al.,

2022; Isojunno et al., 2018; Jeanniard-Du-Dot et al., 2016; Maresh et al., 2015; Martín López et al., 2015).

High-resolution accelerometry data from biologging tag deployments have proven useful for understanding the behavioural ecology of baleen whales. For example, biologging instrumentation and data have elucidated how the lunge feeding behaviour of rorquals (i.e., humpback, fin and blue whales) occurs in four phases (Cade et al., 2016; Shadwick et al., 2019), while the ram filtration behaviour of balaenids (i.e., right and bowhead whales) is linked to an optimal swim speed (Simon et al., 2009). Using tri-axial acceleration to describe the specialized foraging behaviours of these baleen whales has revealed behavioural patterns, as well as the energetic consequences of these behaviours (Goldbogen et al., 2012; Potvin et al., 2012) and exposure to threats feeding whales face based on their behaviour (Constantine et al., 2015; Ware et al., 2014).

Accelerometry-derived energy expenditure have benefited conservation efforts by estimating the energetic cost of entanglements from increased drag (van der Hoop et al., 2017) and increasing the precision of prey requirements estimated from bioenergetic models (Brodie et al., 2016). However, despite the clear advantage to utilizing biologging data when studying baleen whales, there has been no attempt to use high-resolution accelerometry data to aid in the study of grey whale foraging energetics.

Grey whale ecology and previous energetics research

Grey whales (*Eschrichtius robustus*) are a primarily benthic-feeding baleen whale species that inhabit the North Pacific Ocean. They belong to three populations: **1)** the Western North Pacific (WNP) population that feeds off the coast of Russia and breeds in the lagoons of Baja California, Mexico, with some individuals potentially breeding in the South China Sea (estimated population size of 230 individuals; Cooke et al., 2019); **2)** the Eastern North Pacific (ENP) population that feeds in the Arctic and breeds in the Mexican lagoons (estimated population size of 17,000 individuals; Eguchi et al., 2022); and **3)** the Pacific Coast Feeding Group (PCFG) that is a subset of the ENP population, which stops short of the Arctic to feed in Pacific Northwest waters, and also breeds in the Mexican lagoons (estimate population size of 212 individuals; Harris et al., 2022).

The dominant prey of grey whales varies between foraging grounds. ENP and WNP grey whales feed primarily on amphipods in their Arctic foraging ground (Moore et al., 2022; Nerini, 1984). In contrast, PCFG grey whales appear to primarily target epibenthic swarming mysids in the Pacific Northwest foraging (Feyrer and Duffus, 2011; Newell and Cowles, 2006), although this group of whales also feeds on a variety of prey including crab larvae and amphipods (Darling et al., 1998; Hildebrand et al., 2022). Grey whales employ a suction foraging behaviour that is unique in baleen whales (Goldbogen et al., 2017, 2013; Nerini, 1984).

Recent drone-based observations of PCFG grey whale behaviour established an ethogram including four distinct foraging tactics (Torres et al., 2018). One of these tactics is headstands, where the whale is positioned vertically in the water column with head down-fluke up, and another is side swims, where the whale is swimming rolled on its side (Torres et al., 2018), which further illustrates the unique foraging ecology of this group of grey whales. However, due to visibility limitations, the drone ethogram does not include benthic digs, the traditional foraging tactic performed by ENP and WNP grey whales where the whale rolls onto its side, and plows through the sediment to suction up benthic prey while leaving feeding pits in the seafloor (Johnson and Nelson, 1984; Nerini, 1984).

The variety of foraging behaviours used by PCFG grey whales appear to be a function of grey whale body length (Bird et al., *in prep*) and the type and density of prey consumed (Hildebrand et al., 2022). Prey quality is known to be similar if not higher in the PCFG foraging range than in the Arctic foraging grounds (Hildebrand et al., 2021), providing insight to the potential energetic gain from PCFG foraging. PCFG grey whales are also known to be shorter (Bierlich et al., 2023) and have lower, more variable body condition (Akmajian et al., 2021; Torres et al., 2022) than ENP grey whales. However, no study has considered the role of energetic cost of different foraging tactics in the choice of foraging tactic utilization.

The dependence of grey whales on benthic prey restricts them to feeding in shallow, coastal habitats where individuals are often in close contact with humans. The PCFG grey whale population especially has many major port cities of the Pacific Northwest in its foraging range. As a result, the major threats facing PCFG grey whales differ from those facing ENP and WNP grey whales. Most notably, human-related activities are suspected of reducing the ability of individual PCFG whales to obtain sufficient prey to meet their energetic needs.

Threats facing the PCFG population include disturbance of the benthos in PCFG feeding habitat due to expanding coastal infrastructure that may alter benthic productivity (COSEWIC, 2017). Similarly, boating disturbance from whale watching and other recreational vessels may also reduce the time and locations available for PCFG grey whales to feed (COSEWIC, 2017; Duffus, 1996; Sullivan and Torres, 2018). Additionally, risk of vessel strikes and entanglement may negatively impact the ability of PCFG grey whales to obtain sufficient energy (Scordino et al., 2020; Silber et al., 2021). Anthropogenic climate change poses another threat to PCFG grey whales as environmental changes such as marine heatwaves alter the zooplankton prey communities and negatively impact the ability of the population to replenish energy stores (Lemos et al., 2020a, 2020b). High rates of microplastic ingestion from the benthic suction feeding of grey whales can lead to lower nutrient absorption and bioaccumulation of toxic materials in individuals (Torres et al., 2023).

The identified threats facing PCFG grey whales are compounded by the documentation of two grey whale Unusual Mortality Events that have affected all grey whales in the North Pacific (UMEs; 1999-2000 and 2019-present) over the past two decades (Gulland et al., 2005; Raverty et al., 2020; Scordino et al., 2023) —and have been linked to malnutrition (Christiansen et al., 2021; Le Boeuf et al., 2000; Moore et al., 2003; Perryman et al., 2002; Perryman et al., 2020). The consequences of anthropogenic threats and elevated conservation concern for grey whales illustrate the need to understand foraging energetics of PCFG grey whales.

Evaluating the energetic consequences of anthropogenic threats on grey whales requires knowledge of fine-scale foraging behaviour. Unfortunately, foraging ecology studies of PCFG grey whales have so far been largely limited to day-time only focal follows that record broad behavioural states (e.g., forage, travel, rest) and lack fine scale details of foraging tactics performed within each dive (Hildebrand et al., 2022; Mallonee, 1991; Stelle et al., 2008; Sullivan and Torres, 2018; Wursig et al., 1986). Drone-based observations have provided finer-scale information, but have been limited by water clarity and battery capacity (Torres et al., 2018). The lack of behavioural definitions, descriptions of behavioural budgets, and behavioural energetic estimates has excluded PCFG grey whales from previous grey whale bioenergetics models and analyses that assist with management decisions (Agbayani, 2022; Villegas-Amtmann et al.,

2017, 2015). Obtaining fine-scale behavioural specific measures of energetic cost will allow more informed estimates of energetic cost of behaviours to be calculated for this species.

Thesis objectives

I used data from suction cup biologging tags with high-resolution accelerometers deployed on PCFG grey whales along the Oregon coast, USA to define grey whale foraging behaviour (Chapter 2) and estimate relative energetic costs of each behaviour (Chapter 3).

In Chapter 2, I quantified foraging signals in the biologging data at the broad state scale (e.g., forage, search, transit) using Hidden Markov Models and the foraging tactic scale (e.g., headstand, benthic dig, side swim) using Classification and Regression Trees. I then compared the foraging signals identified in grey whales to those previously used to describe foraging behaviour in other species of baleen whale. I expected the biologging data to use accelerometry-derived metrics similar to the residence in space and time framework used to distinguish between broad states in previous focal follow studies (Hildebrand et al., 2022; Sullivan and Torres, 2018) and the qualitative descriptions of body position used in drone ethograms (Torres et al., 2018) to distinguish between foraging tactics. In addition, I expected grey whale foraging will be predominantly benthic with periods showing the whale rolled on its side (Nerini, 1984). Finally, I expected the foraging signals from the grey whale biologging data to differ from the foraging signals described for other baleen whale species given the unique benthic suction feeding mechanism of grey whales (Goldbogen et al., 2017; Nerini, 1984).

I estimated the relative energetic cost of foraging for PCFG grey whales in Chapter 3 using the definitions of foraging behaviour identified in Chapter 2. I calculated multiple energy expenditure proxies from the accelerometry data, including ODBA (ms^{-2}), stroke rate (Hz), stroke amplitude (radians per s), and duration of dives (min) where different foraging tactics were performed, to estimate the relative energetic cost of foraging behaviours. I expected forage to be the most energetically expensive broad state as the whale must maneuver to capture elusive prey within a prey patch. In contrast, I expected transit to have the lowest energetic cost because it is a broad state with highly directional movement and a minimum cost of transport to increase swimming efficiency (Williams and Maresh, 2015). I further expected side swims to have the highest energetic cost compared to benthic digs and headstands given 1) recent evidence demonstrating an ontogenetic shift in PCFG grey whales from side swims to headstands with

maturity (Bird et al., *in prep*) and 2) benthic digs are the assumed primary foraging tactic of grey whales, especially in the Arctic foraging grounds (Nerini, 1984).

My research is the first to calculate biologging-derived estimates of energy expenditure in grey whales. It is therefore a starting point to using accelerometry-derived proxies in the field of energetics. My thesis also provides a foraging-energetics means to assess and mitigate the impacts of threats and disturbance facing grey whales.

Chapter 2: Detecting grey whale foraging signals in biologging data

Summary

Biologging tags that record high-resolution accelerometry data have quantitatively described lunges and continuous ram filtration behaviours in foraging baleen whales. However, foraging behaviours have not been similarly quantified for grey whales. We deployed suction cup biologging tags on Pacific Coast Feeding Group (PCFG) grey whales along the Oregon coast to quantify signals of foraging behaviour at both the broad state (dive) and foraging tactic (roll event) scales. Hidden Markov Models (HMMs) at the dive scale identified three biologically distinct states—forage, search, and transit—defined using turn angle, dive duration, dive tortuosity and presence of roll events. Classification and Regression Tree (CART) models best defined the roll events into foraging tactics used by grey whales (headstands, benthic digs, and side swims) based on body position variables (median pitch, depth to body length ratio, and absolute value of the median roll). These definitions of grey whale foraging signals using accelerometry data add to the quantitative descriptions of foraging behaviours previously described for baleen whales. The foraging behaviour signals of PCFG grey whales provide a means to examine the link between energetics and the physiological impact of threats (e.g., vessel disturbance and pollution) facing this group.

Introduction

High-resolution tri-axial accelerometry data from biologging tags have quantified the foraging kinematics and behaviour of many baleen whales (Cade et al., 2016; Goldbogen et al., 2017, 2013; Shadwick et al., 2019; Simon et al., 2009). Most notably, data from biologging instruments show that the lunge feeding behaviour of rorquals (i.e., humpback, fin and blue whales) occurs in four phases (Cade et al., 2016; Shadwick et al., 2019), while the ram filtration behaviour of balaenids (i.e., right and bowhead whales) requires optimal swim speeds (Simon et al., 2009). Tri-axial acceleration data can thus identify behavioural patterns, and can also be used to determine the energetic costs of these behaviours (Goldbogen et al., 2012; Potvin et al., 2012), and assess exposure to anthropogenic threats during foraging (Constantine et al., 2015; Ware et al., 2014).

Despite the success defining ram filtration and lunge feeding with biologging data, suction feeding, which is only performed by grey whales (*Eschrichtius robustus*) has yet to be

quantitatively described. Grey whales are primarily benthic or epi-benthic feeders that make up three populations. Two populations, known as the Western North Pacific (WNP) and Eastern North Pacific (ENP) populations, consume mostly amphipods that live in sandy substrates (Moore et al., 2022; Nerini, 1984)—while a third, the Pacific Coastal Feeding Group (PCFG) primarily consume epibenthic swarming mysids (Feyrer and Duffus, 2011; Newell and Cowles, 2006), although this group of whales also feeds on a variety of prey including crab larvae and amphipods (Darling et al., 1998; Hildebrand et al., 2022). PCFG grey whale foraging is often in association with reef habitat with and without kelp, although observations of sediment expulsions from the mouth following dives have also been recorded (Bird et al., *in prep*; Torres et al., 2018; L. Torres pers. obs.). All three populations employ a suction foraging behaviour that is unique among baleen whales (Goldbogen et al., 2017, 2013; Nerini, 1984) and is characterized by rolling to one side (usually the right) during the bottom phase of the dive, often in association with a negative pitch where the mouth is angled towards the benthos (Woodward and Winn, 2006).

To date, traditional and drone focal follows of PCFG grey whales during day-light hours have documented four broad behavioural states (forage, travel, rest and social) and four foraging tactics (e.g., headstands, side swims, upside down swims, and open mouth at the surface) (Hildebrand et al., 2022; Mallonee, 1991; Stelle et al., 2008; Sullivan and Torres, 2018; Torres et al., 2018; Wursig et al., 1986). Unfortunately, visibility limitations have precluded observing benthic digs, the traditional foraging tactic of grey whales (Nerini, 1984) whereby individuals roll onto their side, plow through the sediment to suction up benthic prey, and leave feeding pits in the seafloor (Johnson and Nelson, 1984; Nerini, 1984).

Biologging tags with tri-axial accelerometers deployed on foraging grey whales may be able to overcome the current limitations of surface observations by recording body position metrics, such as pitch and roll, to quantitatively define foraging tactics (Brown et al., 2013). These data can also be used to define behavioural states and determine behavioural budgets that include underwater activities, which are needed to determine the energy requirements of grey whales and assist with management decisions (Agbayani, 2022).

We deployed minimally-invasive suction cup biologging tags equipped with tri-axial accelerometers on PCFG grey whales on their foraging grounds in coastal waters of Oregon and

Washington, USA. We subsequently used Hidden Markov Models to quantitatively describe broad behavioural states (e.g., forage, search, travel), as well as Classification and Regression Trees to define foraging tactics performed during each dive. We also compare these biologging-derived definitions of foraging behaviour in grey whales to previously described foraging behaviour of other baleen whale species. Our analyses of the tri-axial accelerometry data yield rigorous, quantitative definitions of the primary behavioural states and multiple foraging tactics of grey whales, thus adding to the quantitative descriptions of baleen whale foraging behaviours that previously lacked grey whale data. Our work also provides baseline data needed to estimate the energetic cost of foraging and assess the impacts of threats on the foraging behaviour of this unique group of grey whales.

Methods

Data collection

Suction cup Custom Animal Tracking Solution (CATS; https://cats.is) video and inertial measurement unit (IMU) tags were deployed on grey whales from rigid hulled inflatable boats using an 8-m carbon fiber pole in August 2021, and July and September 2022 off the Oregon Coast between Waldport (44.418326, -124.092222) and Depoe Bay (44.835057, -124.064164). The timing and location of tagging efforts ensured that only PCFG grey whales, those observed in multiple years between 41^{o}N and 52^{o}N from 1 June to 30 November (International Whaling Commission, 2011), were included in the deployments. CATS tags were attached to the whales using 4 suction cups with oxidizing releases to ensure the tags released after suction failed. Tags were recovered using VHF (2021 & 2022) and Iridium signals (2022). The CATS tags integrated a video camera, hydrophone, 400 Hz accelerometer, 50 Hz magnetometer and gyroscope sensors, and 10 Hz pressure, temperature, light, and GPS sensors. All tag deployments were carried out under NOAA/NMSF permit #21678. The University of British Columbia Animal Care Committee approved the field work under permit #A21-0254.

An additional CATS tag deployment from a PCFG grey whale off Cape Flattery, Washington (48.3127, -124.6858) in September 2019 (J. Calambokidis, *unpublish. data*) was included in this analysis as this individual was previously sighted in the Oregon study area between Waldport and Depoe Bay (2016 (n = 1), 2017 (n = 4), 2018 (n = 5), L. Torres, *unpublish. data*), and was observed to be foraging in similar nearshore reef habitat with kelp as

the tags deployed in the Oregon Coast study area. Therefore, this deployment can complement the other tags deployed in this study to increase the sample size for analysis.

The tagged animals were identified using photo identification through comparison to PCFG grey whale catalogues held by the Geospatial Ecology of Marine Megafauna Lab at Oregon State University and Cascadia Research Collective (Olympia, Washington, USA). Genetic sex information was obtained for known individuals using previously collected tissue samples (Lang et al., 2014). A DJI Inspire 2 quadcopter with a Zenmuse X5 camera with a Micro Four Thirds (17.3 x 13 mm) sensor, 3840 x 2160-pixel resolution, a 25 mm focal length lens, and a Lightware SF11/C laser altimeter for recording altitude was used to conduct Unoccupied Aerial System (aka drone) focal follows of tagged animals.

Drone photogrammetry was used to calculate total length (TL; m) and body area index (BAI) measurements of tagged animals. TL was calculated as length from rostrum to fluke notch using MorphoMetriX (Torres and Bierlich, 2020). Asymptotic TL for PCFG grey whales is reported to be 12 m (Bierlich et al., 2023). BAI is a measure of body condition with low uncertainty that was calculated as surface area of the whale between 20% and 70% of the whale length and normalized by the total length of the individual (Bierlich et al., 2021; Burnett et al., 2018). Measurements of BAI for PCFG grey whales along the Oregon Coast range from 19.18 to 32.71 (mean = 26.79 ± 2.42 (s.d.), n = 374; K. Bierlich unpublish. data). The drone was used following previously established field methods (Bierlich et al., 2023; Lemos et al., 2020a; Torres et al., 2022). If a drone flight was unable to be conducted during tagging field work, drone photogrammetry measurements were obtained from flights within 15 days of tag deployment.

CATS tag data processing

All video and sensor data from the CATS tags were downloaded and imported into MATLAB (MathWorks v2021a) where they were pre-processed to align clock times, correct tag slips, and ensure sensor orientation in the whale frame (Cade et al., 2021). Pressure spikes from animals hitting the tag against the seafloor during benthic rolling behaviours were removed during this pre-processing stage and replaced with a linear interpolation of the pressure sensor data. All subsequent analysis of pre-processed data was conducted in R v4.2.3 (R Core Team, 2023).

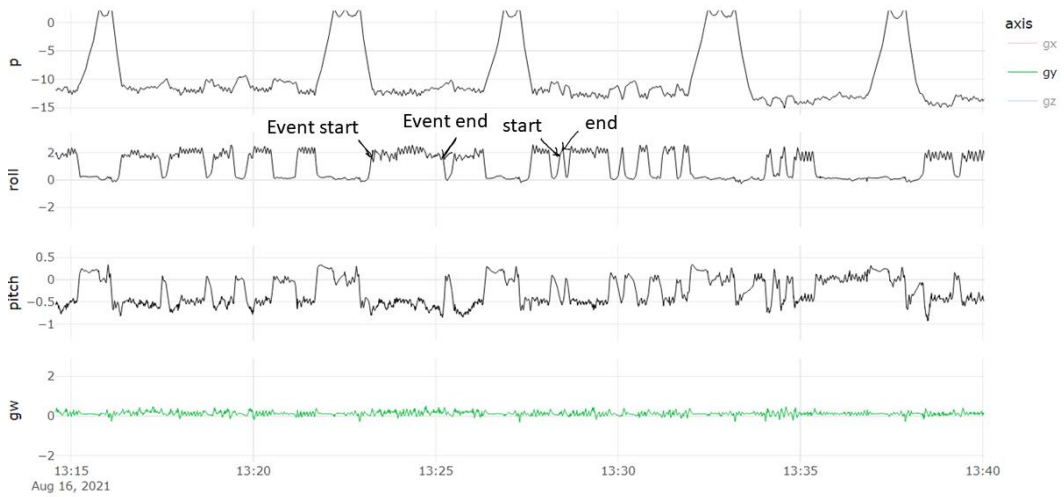

Figure 2.1. Example of pre-processed data derived from CATS tag deployment on a PCFG grey whale that was used to manually audit the dives and roll events. Note how inflection points were used to define the start and end of roll events.

The pre-processed data were manually audited to identify dives and periods of high roll (hereafter referred to as roll events) in the *catsr* package (Czapanskiy, 2022). Audits were performed using pressure sensor data for dives and roll data calculated from the X-axis of the accelerometry data for roll events. The first 15 minutes of each deployment were excluded to remove any influence of tagging on whale behaviour. Dives were defined as periods where the depth was greater than 1 m for longer than 30 sec, which eliminated short submergence periods during blow intervals where the whale remained close to the surface to maximize oxygen utilization for each breath (Sumich, 1983) and there was little potential for foraging activity (Stelle et al., 2008).. Periods of high roll (> 0.5 radians) were of interest as previous studies of grey whale foraging behaviour indicate that these animals often feed on their sides (Nerini, 1984; Torres et al., 2018; Woodward and Winn, 2006). Co-occurring video data from the tags were used to confirm this association by looking for evidence of foraging (e.g., sediment plumes, high density of zooplankton prey) during periods of high roll. Roll event start and stop times were determined as the first and last points of inflection in the elevated roll signal to exclude transitions into the roll events (**Figure 2.1**). By auditing dives and roll events, a multiscale classification of behaviour was conducted with dives corresponding to broad states and roll events corresponding to foraging tactics.

Pseudotracks, with an assumed average speed of 1.5 m/s, were constructed using the *tagtools* package (DeRuiter et al., 2022) to create a dead-reckoned track from the biologging speed and accelerometry data. An assumed average speed was used as PCFG grey whales did not achieve steep enough pitches during their dives to accurately calibrate the speed derived from acceleration as has been applied for other baleen whales (Cade et al., 2021). However, this assumption did not affect the relative positions of the individual along points of the pseudotrack or the tortuosity of the path taken by the individual (Wilson et al., 2007). The pseudotracks were used to determine the relative position at dive start times along the path the whale took during the deployment.

Descriptive summary metrics were calculated for each dive and roll event to differentiate between behaviours at each scale. Summary metrics were calculated using the *tagtools* package (DeRuiter et al., 2022). At the dive scale, these metrics included dive duration (s; the amount of time spent submerged from the start of the dive to the end), maximum dive depth (m; the deepest depth from the pressure sensor on the CATS tag), surface recovery period (s; duration of time at the surface from the end of the dive to the start of the next), ratio of surface to dive time (the ratio of the surface recovery time following the dive to the dive duration), the proportion of time during the dive spent in roll events, presence of roll events (i.e., if a roll event occurred during the dive), change in heading between dive start and dive end (degrees), and dive tortuosity (a unitless ratio of the stretched-out track length of the dive relative to the actual distance covered in the dive, ranging from 0 for movement in a perfectly straight line and 1 for extremely circuitous movement). At the roll event scale, these metrics included duration of the roll event (s; the time from the start of the high roll period to the end), maximum depth (m; the deepest depth from the pressure sensor on the CATS tag), depth to body length ratio (i.e., the depth of the animal from the CATS tag divided by the total length of the animal), absolute value of the median roll (degrees), absolute value of the ratio of the median roll to maximum roll, median pitch (degrees), change in heading between start of the roll event to the end (degrees), and relative speed (**see Appendix D for further description**). The depth to body length ratio used measurements of total length calculated from drone photogrammetry and was used to examine the potential limitation water depth may pose to foraging tactic use by grey whales that feed in nearshore habitats where the water depth is often shallower than the total lengths of the whales.

Behavioural classification

Broad states—Hidden Markov Models

Hidden Markov Models (HMMs) are a class of state-space models that use characteristics of the observed data (in this context, an animal's movement metrics) to classify a time series of underlying states while accounting for temporal autocorrelation (Morales et al., 2004). In ecology, these latent statistical states are then interpreted as the broad behavioural states of the individual. Here, we used the tag data to inform multivariate HMMs, using dives as the unit of analysis. The dive scale of analysis allowed for variable dive duration to be accounted for when determining broad behavioral states yet precluded the ability to detect surface behaviors (such as a possible resting behaviour) in the model. In particular, we aimed to classify forage, search, and transit states, which have been identified in previous PCFG grey whale focal follow studies (Hildebrand et al., 2022; Stelle et al., 2008; Sullivan and Torres, 2018). HMMs were fitted using the *momentuHMM* package (McClintock and Michelot, 2018).

Data streams were selected from the descriptive summary metrics calculated at the dive scale. The selection of data streams included in the model was guided by existing cetacean multivariate HMMs (DeRuiter et al., 2017), and modified in light of what is known about PCFG grey whale ecology. Specifically, we examined the histogram of each movement metric **(see Appendix A for histograms)** and selected those that had the most obvious breaks in their distribution, while ensuring there was no redundancy in their characterization of states (e.g., roll presence and proportion of dive spent rolling both describe the presence of a foraging tactic, so only one was included in the model). A discrete random effect of individual whale was not included due to the low sample size of deployments (McClintock, 2021).

The final set of data streams included in the HMM, and their distributions, are listed in **Table 2.2**. Step length was not included in the HMM due to its correlation with dive duration and mismatch with the dive time scale chosen for this model, as step length works best with a standard time interval as the unit of analysis (E. Pirotta pers. comm.). Maximum dive depth was also excluded from the model because it failed to identify the desired broad states (**see Appendix B for preliminary models**). Finally, the surface recovery period was removed from the model as we were unable to distinguish if the period at the surface is a recovery from the previous dive or preparation for the next. Two- and three-state HMMs were compared to determine if search

behaviour was distinguishable as a separate state using the biologging data. The final number of states to include in the model was chosen according to the suggestions of Pohle et al. (2017), including assessment of pseudo-residuals and biological relevance (**see Appendix C for pseudo-residual plots**).

To avoid convergence at local maxima, the HMMs were re-fit with random perturbations in the starting parameter values. The Viterbi-algorithm was used to estimate the most likely sequence of broad behavioural states (Zucchini et al., 2016).

Foraging tactics—Classification and Regression Trees

Classification and Regression Tree (CART) models are supervised machine learning algorithms that were used to define different foraging tactics in the biologging data. A subset of the roll event data (n = 236) were visually classified into foraging tactics using the TrackPlot data from the tag deployments (**see Appendix E for further description of validation method**) based on established qualitative descriptions of foraging tactics from drone observations (Torres et al., 2018) to check body orientation. Headstands, benthic digs, and side swims were observed in the biologging data. These visually classified events were split 80:20 into training and testing data sets.

Histograms of the summary metrics calculated for roll events were examined for each visually classified foraging tactic to determine the metrics with the clearest splits between the tactics **(see Appendix F for histograms)**; these metrics were then applied as input variables in the CART model. The chosen metrics included median pitch (degrees), absolute value of the median roll (degrees), and the depth to body length ratio. A more extreme negative median pitch indicated the individual was positioned more vertically in the water column with rostrum angled down in the sediment, while a median pitch closer to 0 indicates the individual was more horizontal. A higher absolute value of the median roll indicated that the individual was turned more on its side. A depth to body length ratio less than 1 indicated the roll event occurred at a depth that was shallower than the individual's total length. There was no need to determine correlation between the metrics as CART models account for collinearity.

A CART model was constructed using the training data. The *rpart* (Therneau and Atkinson, 2022) and *rpart.plot* (Milborrow, 2022) packages were used to build and visualize the classification tree. A pruned tree was also constructed using the minimum error of the

complexity parameter to create a more parsimonious model. The predictive accuracy of the CART model was evaluated using the testing data. A confusion matrix was generated to select the most accurate model. If the accuracy tests were the same between the original and the pruned model, the simplest model was selected.

A concern with CART models is over-sensitivity to the training data used to build the classification tree. Therefore, bootstrap aggregation (bagging) with 1,500 iterations of the CART model was conducted using the *ipred* package (Peters and Hothorn, 2023). The out of bag error, or prediction error, was calculated and an accuracy test on the confusion matrix was conducted to confirm the ability of the best CART model to assign foraging tactics given the complexity of interpreting results from bagged classification trees. The splitting rules from the most accurate CART model were then used to assign the non-visually classified roll events (n = 1,654) to a foraging tactic.

Behavioural budgets

Proportional activity budgets were calculated at the dive and roll event scale for all deployments combined and for each individual deployment. At the dive scale, the amount of time spent at the surface was compared to the amount of time at depth. The proportion of surface time was calculated as the sum of surface recovery periods for each deployment and divided by the total deployment duration, while the proportion of time at depth was calculated as the sum of the dive durations for each deployment, divided by the total deployment duration.

Proportional activity budgets were compared between day and night where day was assumed to be between 06:00 and 20:00 Pacific Daylight Time, based on the average sunrise and sunset times for Newport, Oregon in the summer (https://weatherspark.com/y/344/Average-Weather-in-Newport-Oregon-United-States-Year-Round).

Grey whales are known to have lateralization of their foraging behaviours (Woodward and Winn, 2006). Therefore, the sidedness of foraging tactics was examined across tagged individuals. Sidedness was coded as a binary variable with 0 indicating a left-sided roll (individual's left side is down) and 1 indicating a right-sided roll (individual's right side is down). Differences in sidedness values were explored between day and night.

Table 2.1. Biologging CATS tag deployment information for 10 PCFG grey whales tagged in 2019, 2021, and 2022.

Deployment ID	Genetic Sex	Tag on	Tag off	Tag on location	Deployment length (hh:mm:ss)	Total length (m)	Body area index (BAI)	No. roll events (N = 1890)	No. dives (N = 1,856)
A19	NA	9/1/19 15:05:52	9/1/19 16:41:18	Cape Flattery, WA	01:29:17	10.2*	NA	45	31
B21[a]	M	8/16/21 13:01:11	8/16/21 18:20:03	Lost Creek	03:00:34	12.0	22.74	137	78
C21[a]	NA	8/16/21 16:04:52	8/16/21 16:31:24	Alsea River Mouth	00:26:15	11.1	25.37	3	3
D21[b]	M	8/16/21 17:16:37	8/16/21 21:08:03	Alsea River Mouth	03:51:26	11.6	25.82	59	60
E22	F	7/21/22 9:50:30	7/22/22 10:38:49	Nye Beach	24:48:19	11.1	24.94	324	477
F22[c]	F	7/21/22 10:36:03	7/21/22 17:19:17	Flat Rock	06:43:14	10.4	26.94	288	141
G22	F	7/21/22 16:03:25	7/22/22 09:37:27	South Beach	17:34:02	11.6	27.39	370	298
H22	NA	9/12/22 13:13:35	9/12/22 18:00:00	Gull Rock	00:33:25	8.9	29.45	14	7
I22	F	9/12/22 12:49:02	9/13/22 11:54:58	Gull Rock	23:05:58	10.5	28.46	478	627
J22	F	9/12/22 11:49:02	9/12/22 19:12:53	Gull Rock	07:23:50	12.1	26.75	172	142

*Total length from outside of 15 day window around tag deployment.
[a]Tag without audio data.
[b]Tag without video data.
[c]Individual is the known calf of G22.

Results

Deployment summary

Nine CATS tags were successfully deployed on PCFG grey whales in 2021 (n = 3) and 2022 (n = 6). With the additional 2019 CATS tag deployment from the coast of Washington (J. Calambokidis, *unpublish. data*), these 10 deployments totaled 91.35 hours, with a mean deployment time of 9.14 hours (range = 0.44 hours to 24.81 hours; **Table 2.1**). Tags were deployed on five females, two males, and three whales of unknown sex, including a mother (G22) and her 8-year-old daughter (F22) on the same day.

The GPS data from the 2022 deployments was unable to be recovered. Deployment H22 had an abrupt stop in biologging data collection after ~0.5 hours despite the tag remaining on the animal. Deployment I22 had abrupt stops in data collection leading to gaps in the sensor data. Only the data following these gaps were included in the analysis for this deployment.

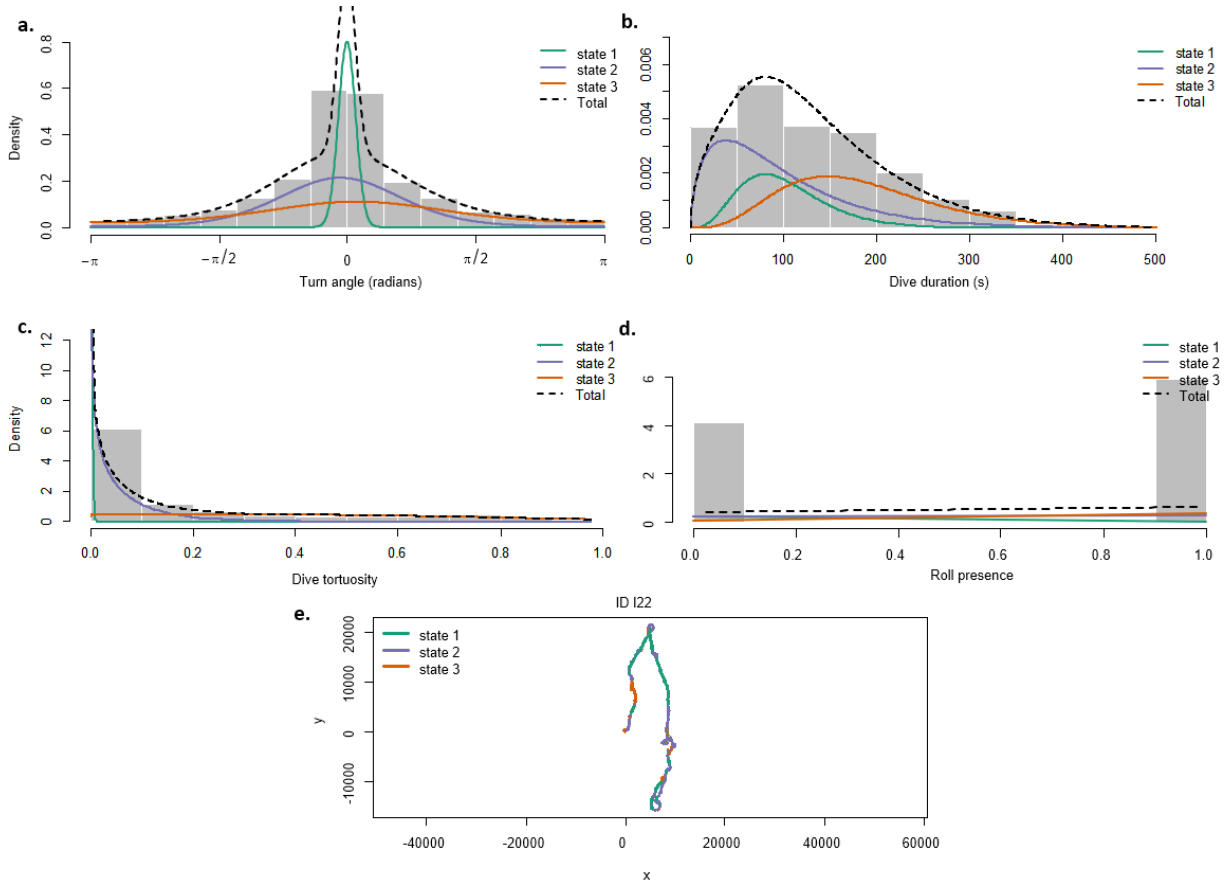

Figure 2.2. Hidden Markov Model (HMM) state-dependent distributions for all dives (n = 1,856) recorded on CATS tags deployed on PCFG grey whales based on (a) turn angle, (b) dive tortuosity, (c) dive duration, (d) and roll event presence. (e) Viterbi algorithm state assignments for one deployment's pseudotrack.

Based on the definitions of day and night, approximately 60.2 hours of sampling occurred during the day and 31.15 hours of sampling occurred at night. Four tags were considered to have behaviours performed at night—one deployment with a little over one hour of night sampling and three deployments with the full 10 hours of overnight sampling (**Table 2.1**). A total of 760 dives and 540 roll events occurred at night for all full overnight deployments combined, compared to 634 dives and 634 roll events during the day for these same deployments. An additional 18 dives and 20 roll events occurred at night in the one deployment with about an hour of night sampling, compared to the 42 dives and 39 roll events during the day.

Broad states

HMMs were constructed using 1,856 dives from CATS tags deployed on 10 individual whales. Dives of PCFG grey whales were best classified into three distinct and biologically

Table 2.2. State-dependent distribution parameters of the data streams estimated by the Hidden Markov Model (HMM) for the three states included in the deployments of CATS tags on PCFG grey whales (n = 1,856 dives).

Data stream	Distribution	State	Distribution parameters
Turn angle (radians)	von Mises	1	$\mu = -0.003$; $\kappa = 90.87$
		2	$\mu = -0.088$; $\kappa = 1.91$
		3	$\mu = 0.116$; $\kappa = 0.78$
Dive duration (s)	gamma	1	$\mu = 102.1$; $\sigma = 47.1$
		2	$\mu = 96.7$; $\sigma = 75.3$
		3	$\mu = 185.6$; $\sigma = 84.0$
Dive tortuosity	beta	1	$\alpha = 1.03$; $\beta = 791.08$
		2	$\alpha = 0.63$; $\beta = 10.74$
		3	$\alpha = 1.05$; $\beta = 1.46$
Roll presence	Bernoulli	1	$p = 0.005$
		2	$p = 0.550$
		3	$p = 0.980$

relevant states. Adding a third state to the HMM reduced the spread of the state-dependent distributions and resulted in more normally distributed pseudo-residuals compared to a two-state model (**see Appendix C for model comparison**). A rest state was not detected by the model, indicating that no dives had the characteristics of resting whales.

Dives classified under State 1 were characterized by turn angles close to 0^o, tortuosity close to zero, no roll events present, and an intermediate dive duration (**Figure 2.2**). These features suggest that this dive type corresponds to non-foraging, transit behaviour, used by whales when moving in a directed fashion.

State 2 dives had more variation in turn angle than State 1 dives, but less variation than State 3 (**Figure 2.2a**). Dive tortuosity for State 2 dives was concentrated around 0.1 and generally lower than 0.25, which was higher than State 1 dive tortuosity but included in the variation of tortuosity for State 3 dives (**Figure 2.2b**). Dives classified as State 2 had the shortest duration, albeit with high variation (**Figure 2.2c**), and were characterized by an intermediate probability of the presence of a roll event compared to the other two states (**Figure 2.2d**). The intermediate values for turn angle, dive tortuosity, and roll presence suggested that State 2 corresponds to search behaviour.

Dives classified as State 3 had the largest variation in turn angle, being the most likely to have turn angles greater than $\pm 90^o$ (**Figure 2.2a**). State 3 also had the highest variation in dive

Table 2.3. Transition probability matrix for the three states estimated by the Hidden Markov Model (HMM) based on dives (n = 1,856) recorded on CATS tag deployments on PCFG grey whales. Rows indicate the current state and columns indicate the proximate state.

	State 1	State 2	State 3
State 1	0.853	0.110	0.037
State 2	0.070	0.795	0.135
State 3	0.003	0.177	0.820

tortuosity and was the state most likely to have dive tortuosity greater than 0.25 (**Figure 2.2b**). State 3 dives had the longest duration and the highest probability of roll presence (**Figure 2.2c,d)**. Given these features, State 3 dives were indicative of forage behaviour.

The transition probability matrix of the final HMM indicated a high likelihood for a whale to remain in its current state (**Table 2.3**), which was especially true for the State 1 transit behaviour and the State 3 forage behaviour. The transition probability matrix supports State 2 search behaviour as an intermediate state based on the high likelihood of transition to or from both State 1 and State 3. A whale in State 1 transit behaviour was more likely to transition to State 3 forage behaviour than vice versa. For a whale in the State 2 search behaviour, there was approximately equal probability of transitioning to State 1 transit behaviour or State 3 forage behaviour.

Across all deployments (n = 1,856 dives), PCFG grey whales spent 43% of their dives searching, 36% of their dives foraging, and 21% of their dives transiting (**Table 2.4**). This pattern was consistent across most individual whales, except for E22, which spent the least proportion of dives searching (**Table 2.4**). Four individuals spent a noticeably higher proportion of time foraging (B21, C21, D21 and H22). The proportion of time spent in each state changed with time of day (**Table 2.4**). Across all deployments (n = 1,856 dives), the PCFG grey whales spent a higher proportion of time searching and a lower proportion of time foraging at night compared to the day. The proportion of transiting dives remained relatively constant between the day and night.

All tagged whales spent approximately 20% of their time at the surface compared to 80% at depth (**Table 2.5**). This 20:80 ratio holds for all whales except for one deployment (F22) that spent 37% of time at the surface and 63% of time diving. The percentage of time spent at the surface increased to approximately 30% at night compared to 20% during that day (**Table 2.5**). This pattern was driven by one deployment (G22) that spent 44% of the time at the surface at

Table 2.4. Percentage of dives from CATS tag deployments on PCFG grey whales estimated to correspond to each state defined by the Hidden Markov Model (HMM) during the full deployment and day (D) or night (N), for all deployments combined and each deployment. Day was considered to be 6am to 8pm PDT based on average sunrise and sunset times in the study region. Dashes indicate no available data for that deployment. The number of dives in each deployment is given in parentheses (n =).

Broad state	**All (n = 1,856)**		**A19 (n= 31)**		**B21 (n= 78)**		**C21 (n= 3)**		**D21 (n= 60)***		**E22 (n= 477)**		**F22 (n= 141)**		**G22 (n= 290)**		**H22 (n= 7)**		**I22 (n= 627)**		**J22 (n= 142)**	
Transit	0.21		0.10		0.18		0.00		0.00		0.35		0.04		0.06		0.00		0.28		0.04	
Search	0.43		0.55		0.18		0.00		0.22		0.21		0.42		0.52		0.14		0.59		0.49	
Forage	0.36		0.35		0.64		1.00		0.78		0.44		0.54		0.41		0.86		0.13		0.47	
Time of Day	**D (n = 1078)**	**N (n = 778)**	**D (n = 31)**	**N (n = 0)**	**D (n = 78)**	**N (n = 0)**	**D (n = 3)**	**N (n = 0)**	**D (n = 42)**	**N (n = 18)**	**D (n = 259)**	**N (n = 218)**	**D (n = 141)**	**N (n = 0)**	**D (n = 136)**	**N (n = 154)**	**D (n = 7)**	**N (n = 0)**	**D (n = 239)**	**N (n = 388)**	**D (n = 142)**	**N (n = 0)**
Transit	0.17	0.21	0.10	--	0.18	--	0.00	--	0.00	0.00	0.30	0.37	0.04	--	0.03	0.07	0.00	--	0.33	0.27	0.04	--
Search	0.36	0.53	0.55	--	0.18	--	0.00	--	0.31	0.00	0.19	0.21	0.42	--	0.51	0.53	0.14	--	0.39	0.63	0.49	--
Forage	0.47	0.26	0.35	--	0.64	--	1.00	--	0.69	1.00	0.51	0.42	0.54	--	0.47	0.40	0.86	--	0.27	0.10	0.47	--

*Indicates deployment with only 1 hour of night sampling.

Table 2.5. Percentage of time spent at the surface compared to diving for CATS tag deployments on PCFG grey whales during the full deployment and day (D) or night (N), for all deployments combined and each deployment. Dives were defined as periods where the depth was greater than 1 m for longer than 30 sec. Surface periods were defined as time spent at the surface between dives. Day was considered to be 6am to 8pm PST based on average sunrise and sunset times in the study region. Dashes indicate no available data for that deployment. The number of dives in each deployment is given in parentheses (n =).

	All (n = 1,856)		**A19 (n= 31)**		**B21 (n= 78)**		**C21 (n= 3)**		**D21 (n= 60)***		**E22 (n= 477)**		**F22 (n= 141)**		**G22 (n= 290)**		**H22 (n= 7)**		**I22 (n= 627)**		**J22 (n= 142)**	
Surface	0.23		0.22		0.13		0.20		0.23		0.16		0.18		0.37		0.10		0.24		0.23	
Depth	0.77		0.77		0.87		0.80		0.77		0.84		0.82		0.63		0.90		0.76		0.77	
Time of Day	**D (n = 1078)**	**N (n = 778)**	**D (n = 31)**	**N (n = 0)**	**D (n = 78)**	**N (n = 0)**	**D (n = 3)**	**N (n = 0)**	**D (n = 42)**	**N (n = 18)**	**D (n = 259)**	**N (n = 218)**	**D (n = 141)**	**N (n = 0)**	**D (n = 136)**	**N (n = 154)**	**D (n = 7)**	**N (n = 0)**	**D (n = 239)**	**N (n = 388)**	**D (n = 142)**	**N (n = 0)**
Surface	0.20	0.28	0.22	--	0.13	--	0.20	--	0.23	0.22	0.17	0.16	0.18	--	0.27	0.44	0.10	--	0.22	0.27	0.23	--
Depth	0.80	0.72	0.78	--	0.87	--	0.80	--	0.77	0.78	0.83	0.84	0.82	--	0.73	0.56	0.90	--	0.78	0.73	0.77	--

*Indicates deployment with only 1 hour of night sampling.

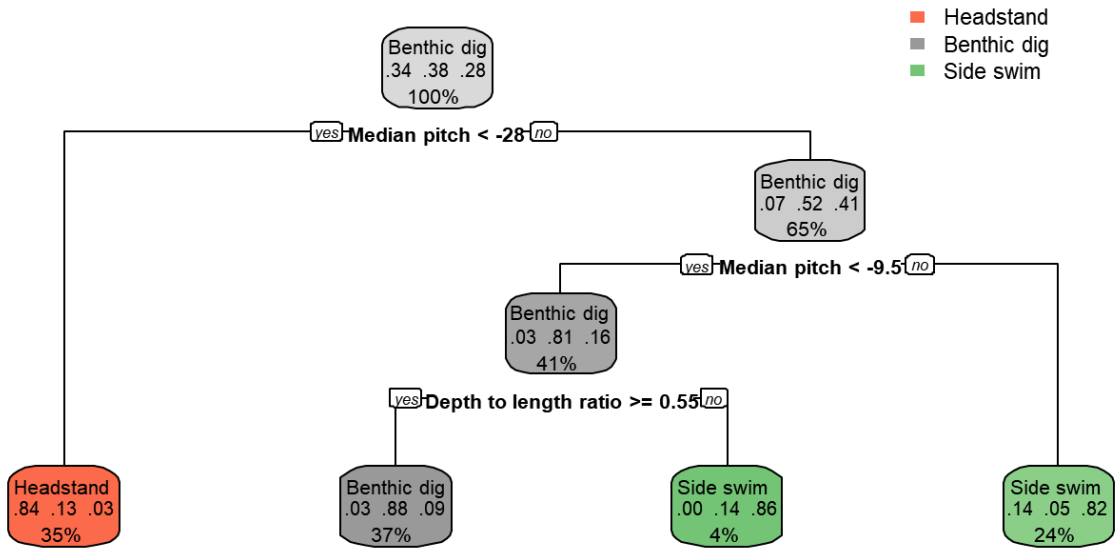

Figure 2.3. Classification and regression tree (CART) used to define foraging tactics for each roll event in CATS tag deployments on grey whales. The CART model was constructed using training data that was randomly selected from a subset of visually validated roll events. N = 189 roll events were included in the training data set used to create the CART model. A more extreme negative median pitch indicates the individual is positioned more vertically in the water column with rostrum angled down in the sediment, while a median pitch closer to 0 indicates the individual is more horizontal. The top row of each box denotes the dominant foraging tactic conforming to the prior splitting rule of the decision tree. The second row denotes the proportion of data belonging to each headstand, benthic dig, and side swim foraging tactic, respectively. The last row denotes the percentage of the total data set represented in each box.

night. Only one of the other full overnight deployments (I22) showed an increase in time spent at the surface at night.

Foraging tactics

The pruned tree was the best CART model to classify the training data set of visually validated roll event data into foraging tactics (**Figure 2.3**) as it was more parsimonious with the same accuracy as the unpruned tree. The pruned CART model was able to accurately predict 84.8% of foraging tactics in the testing data. Bagging results showed a low out of bag error of 0.1667 and a high accuracy of 89.1%, confirming the high accuracy of the CART model's foraging tactic classification. Post-hoc validation of the foraging tactics in 10 randomly selected dive series using the TrackPlot method (**see Appendix E for validation methods**) confirmed

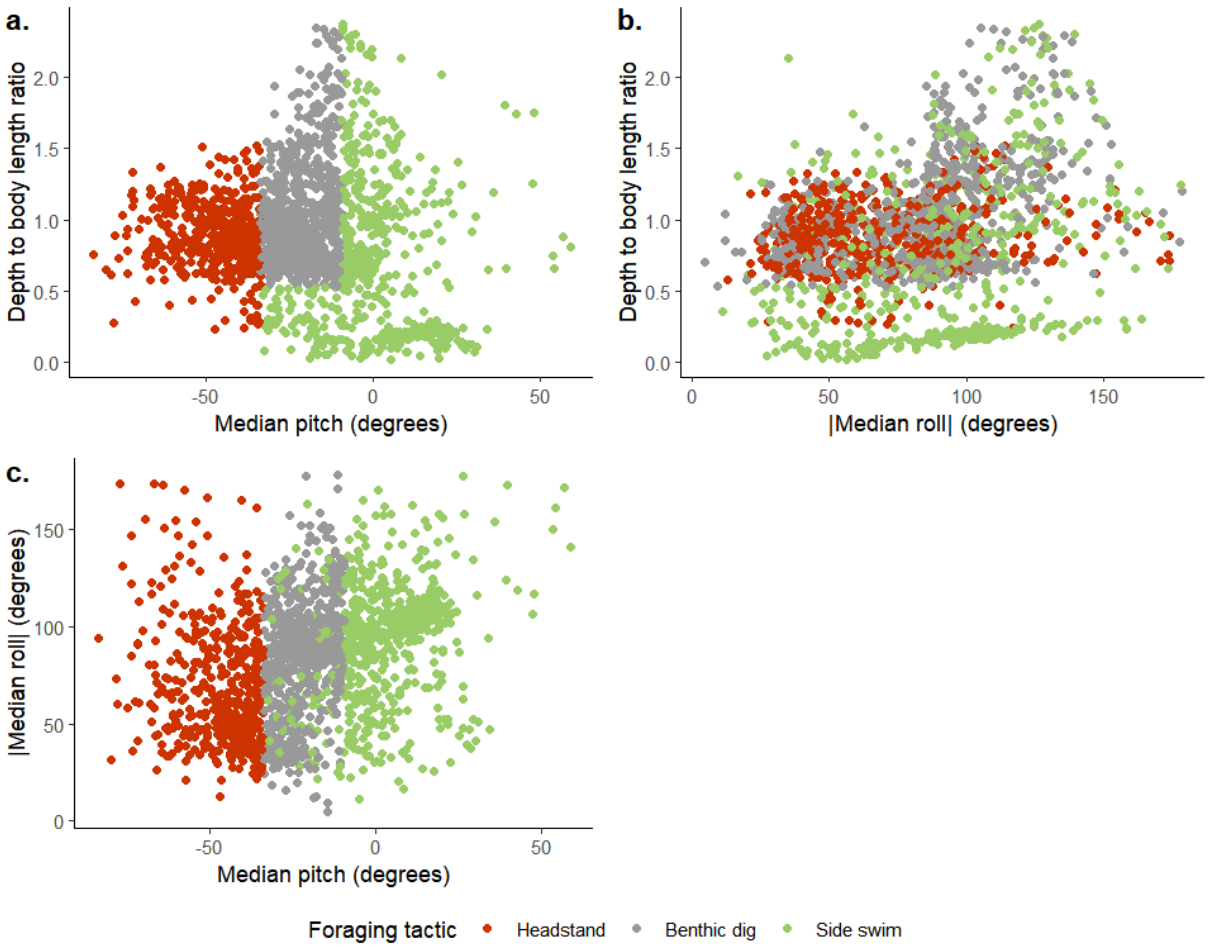

Figure 2.4. Distribution of foraging tactics relative to the variables used in the classification and regression tree model. The clear clusters in the median pitch and depth to body length ratio support the high importance of these variables in the classification tree.

that ignoring the autocorrelation structure of the foraging tactics in the CART model did not contribute to accuracy errors.

Median pitch was the most important variable in the CART model to correctly splitting the roll events into foraging tactics (64.7%), followed by the depth to body length ratio (19.3%), and finally by the absolute value of the median roll (10.1%). This variable importance is evident in **Figure 2.4** that illustrates clear breaks between foraging tactics relative to median pitch and depth to body length ratio, while the absolute value of the median roll is similar among all foraging tactics (**Table 2.6**).

Roll events with a median pitch more extreme than -27.9º were classified as headstands. Roll events with a median pitch between -27.9º and -9.5º and depth to body length ratio greater

Table 2.6. Summary table of metrics included in the classification and regression (CART model) defining the different foraging tactics from CATS tag deployments on PCFG grey whales. Values given as mean ± standard deviation. N is the number of roll events that correspond to each foraging tactic defined by the CART model.

Foraging tactic	Roll (degrees)	Pitch (degrees)	Depth to body length ratio
Headstand (n = 661)	68.7 ± 30.1	-42.8 ± 11.6	0.9 ± 0.3
Benthic dig (n = 582)	89.8 ± 27.2	-18.7 ± 5.4	1.1 ± 0.4
Side swim (n = 647)	93.8 ± 29.7	3.6 ± 12.9	0.6 ± 0.6

Table 2.7. Percentage of roll events and mean sidedness from CATS tag deployments on PCFG grey whales spent in each foraging tactic defined by the classification and regression tree (CART) model during the whole deployment and day (D) or night (N), for all deployments combined and each individual whale. Day was considered to be 6am to 8pm PDT based on average sunrise and sunset times in the study region. Sidedness values equal to 1 indicate rolling to the right and values equal to 0 indicate rolling to the left. Intermediate values suggest a mixture of right and left rolls. Dashes indicate that the foraging tactic was not present in the deployment. The number of foraging tactics in each deployment is given in parentheses (n =).

Foraging tactic	**All (n= 1890)**		**A19 (n= 45)**		**B21 (n= 137)**		**C21 (n= 3)**		**D21 (n= 59)***		**E22 (n= 324)**		**F22 (n= 288)**		**G22 (n= 370)**		**H22 (n= 14)**		**I22 (n= 478)**		**J22 (n= 172)**	
Headstand	0.31		0.64		0.34		1.00		0.44		0.72		0.13		0.21		0.00		0.16		0.32	
Benthic dig	0.35		0.02		0.53		0.00		0.03		0.09		0.74		0.71		0.00		0.02		0.40	
Side swim	0.34		0.33		0.14		0.00		0.53		0.19		0.13		0.08		1.00		0.82		0.28	
Time of Day	**D (n = 1330)**	**N (n = 560)**	**D (n = 45)**	**N (n = 0)**	**D (n = 137)**	**N (n = 0)**	**D (n = 3)**	**N (n = 0)**	**D (n = 39)**	**N (n = 20)**	**D (n = 236)**	**N (n = 88)**	**D (n = 288)**	**N (n = 0)**	**D (n = 231)**	**N (n = 139)**	**D (n = 14)**	**N (n = 0)**	**D (n = 165)**	**N (n = 313)**	**D (n = 172)**	**N (n = 0)**
Headstand	0.31	0.14	0.02	--	0.23	--	1.00	--	0.00	0.05	0.05	0.03	0.58	--	0.63	0.49	0.00	--	0.00	0.01	0.29	--
Benthic dig	0.44	0.28	0.64	--	0.59	--	0.00	--	0.21	0.95	0.78	0.73	0.28	--	0.30	0.40	0.00	--	0.36	0.06	0.41	--
Side swim	0.25	0.58	0.33	--	0.18	--	0.00	--	0.79	0.00	0.17	0.24	0.13	--	0.06	0.11	1.00	--	0.64	0.93	0.30	--
Sidedness																						
Headstand	0.93		1.00		1.00		1.00		0.00		0.86		0.92		0.95		--		0.75		0.86	
Benthic dig	0.97		1.00		1.00		--		1.00		1.00		0.93		0.98		--		0.95		0.90	
Side swim	0.51		0.93		0.88		--		0.97		0.92		0.87		0.40		0.00		0.30		1.00	

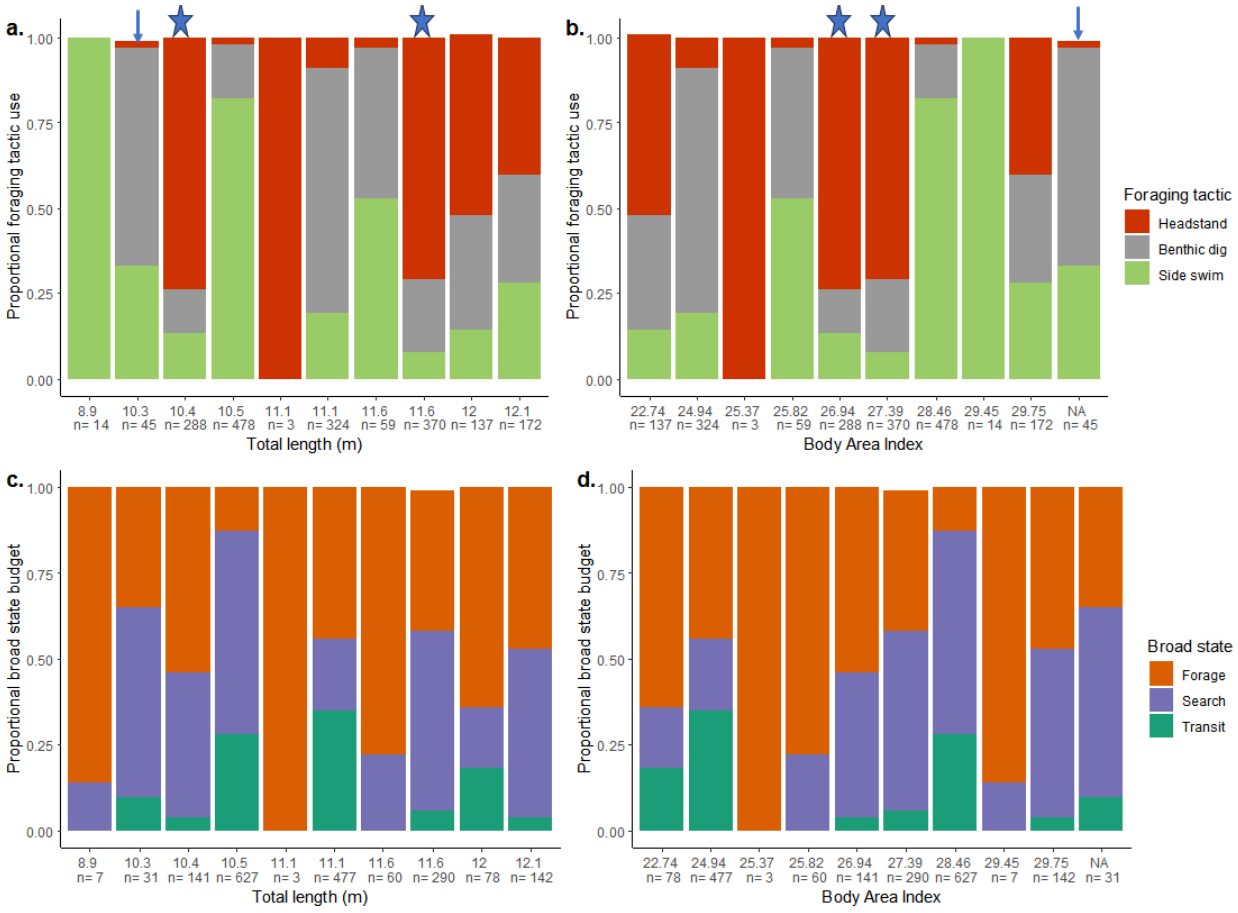

Figure 2.5. Proportional activity budgets at the foraging tactic (a,b) and broad state (c,d) scales from CATS tag deployments on PCFG grey whales across total lengths (m; a,c) and body area index (BAI; b,d) of the whales. Each bar represents an individual deployment. N represents the number of roll events (a,b) and dives (c,d) performed during the deployment. Stars represent the known mother-daughter pair and the arrow represents the Washington deployment.

than or equal to 0.55 were classified as benthic digs. Roll events with either median pitch less extreme than or equal to -9.5^{o}, or with median pitch between -27.9^{o} and -9.5^{o} and depth to body length ratio less than 0.55 were classified as side swims.

Across all deployments the foraging tactics were present in relatively equal proportions: 31% headstands, 35% benthic digs, and 34% side swims. However, there is high individual variation between deployments (**Table 2.7**). Three whales (A19, C21, and E22) performed headstands as their main foraging tactic. Four whales (B21, F22, G22, and J22) performed benthic digs as their main foraging tactic. One whale (D21) had relatively equal proportions of headstands and side swims as their main foraging tactics. The proportional activity budgets

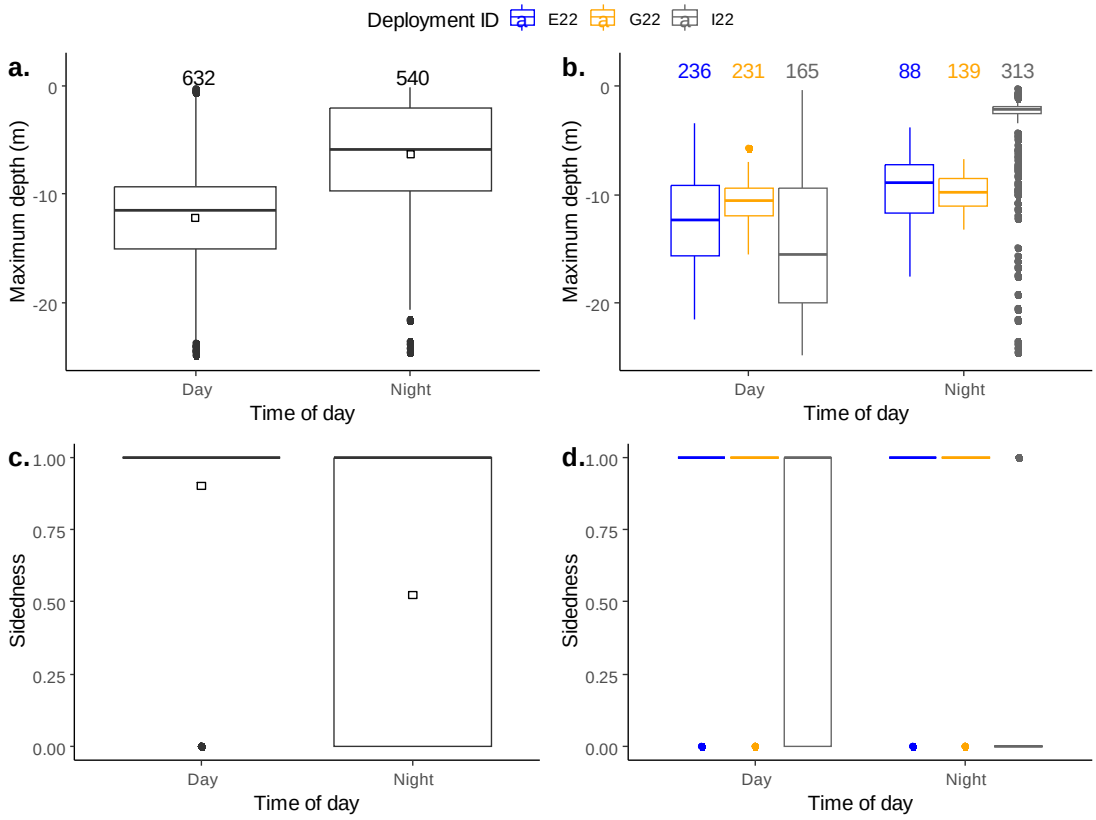

Figure 2.6. Maximum depth (m; a,b) and sidedness (c,d) of foraging tactics from CATS tag deployments on PCFG grey whales defined using a classification and regression tree (CART) model during day and night for three full overnight deployments. Numbers across the top indicate the number of roll events included in each boxplot. Day was considered to be 6am to 8pm PST based on average sunrise and sunset times in the study region. Sidedness values equal to 1 indicate rolling to the right and values equal to 0 indicate rolling to the left. Intermediate values suggest a mixture of right and left rolls. Panels a and c show the distribution of values for all three overnight deployments combined. Panels b and d show the distribution of each of the full overnight deployments, with the different colors representing unique deployments. The open square represents the mean value of all full overnight deployments (a,c). In all panels, the lines represent the median and dots denote outliers.

varied with total length and BAI (**Figure 2.5**). The whales that favored headstands and benthic digs were longer than 11 m. Whales with headstands as the main foraging tactic had relatively low BAI (< ~25) while individuals with benthic digs as the main foraging tactic had a mix of high and low BAI (~23-27). Two whales (H22 and I22) had side swims as their main foraging tactic, and these whales were shorter than 11 m and had relatively high BAI (> 28).

Diurnal patterns in foraging tactic use are evident. Across all deployments combined, the proportion of headstands and benthic digs decreased at night while the proportion of side swims increased (**Table 2.7**). Yet, foraging tactic use between day and night remained very

Table 2.8. Mean sidedness and maximum depth (m) of foraging tactics defined by a classification and regression tree (CART) model during day and night for full overnight deployments of CATS tags on PCFG grey whales. Day was considered to be 6am to 8pm PST based on average sunrise and sunset times in the study region. Sidedness values equal to 1 indicate rolling to the right and values equal to 0 indicate rolling to the left. Intermediate values suggest a mixture of right and left rolls. Dashes indicate that the foraging tactic was not present during that time of day for the deployment. Only whales with full overnight deployments were included. N represents the number of foraging tactics in the deployment for day and night, respectively.

Tactic		Er220721-81 (n= 324)		Er220721-83 (n= 370)		Er220912-82 (n= 478)	
		Day (n = 236)	Night (n = 88)	Day (n = 231)	Night (n = 139)	Day (n = 165)	Night (n = 313)
Headstand	sidedness	0.82	1.00	0.98	0.88	--	0.75
	depth	9.34	15.57	10.34	9.46	--	6.24
Benthic dig	sidedness	1.00	1.00	0.97	0.98	0.97	0.89
	depth	12.40	10.36	11.47	9.88	18.66	11.45
Side swim	sidedness	0.98	0.81	0.27	0.53	0.61	0.19
	depth	14.99	8.19	11.26	11.30	10.53	3.18

individualistic. Deployment D21 performed almost exclusively benthic digs during the night compared to mostly side swims during the day, while deployment I22 performed almost exclusively side swims at night compared to a 60:40 split of side swims and benthic digs during the day. Deployment E22 had little difference in foraging tactic use between the day and night, while deployment G22 shifted from a higher proportion of headstands during the day to a more equal proportion of headstands and benthic digs at night.

Headstands and benthic digs predominantly occurred during right-sided rolls, while side swims had more variation in the sidedness of the roll event (**Table 2.7**). This pattern of right-sided headstands and benthic digs and more left-sided side swims was consistent across individuals. The depth and lateralization of foraging tactics compared across the full overnight deployments (n = 1,172) indicates that grey whales tended to perform foraging tactics at shallower depths and roll more to the left at night (**Figure 2.6**). All overnight deployments showed a shallower depth of foraging tactic at night (mean depth = 9.51 m) than day (mean depth = 12.37 m), except for the headstands of deployment E22 (**Table 2.8**). The increase in left-sided rolls was most prevalent in side swims, although deployment G22 had more right-sided side swims at night (**Table 2.8**).

Discussion

The biologging data we obtained from suction cup tag deployments on 10 PCFG grey whales successfully defined behaviours at both the broad state and foraging tactic scales,

providing the first quantitative descriptions of grey whale behavior movements. Most notably, the HMMs defined three reasonably unique broad states at the dive scale that likely correspond to forage, search, and transit behaviours. These states were best described using turn angle between dive start points, dive duration, dive tortuosity and the presence of roll events within the dive. All of the tagged whales spent proportionally more time in the forage and search states than they did in the transit state, with only two individuals spending more than 20% of their time transiting. On average, the PCFG grey whales spent ~20% of their time at the surface, and 80% diving—and spent more time at night searching, as well as slightly more time at the surface.

CART models indicate that the foraging tactics of headstand, benthic dig, and side swim are best defined from accelerometry data using median pitch, the ratio of depth to body length, and the absolute value of the medial roll, with median pitch being the most important variable in the classification model. Across all whales, the proportion of foraging tactics used was approximately equal, but there was high individual variation in the preferred foraging tactic used. Foraging tactics occurred at shallower depths and included more left-sided rolls at night compared to during the day. This diurnal pattern of lateralization was most evident in side swims, which was the tactic most frequently used at night. However, high individual variation between foraging tactic proportion and lateralization were present in the biologging data.

The detection of a search state in the biologging data lends credence to the separation of search and forage behaviours for PCFG grey whales that have been proposed based on differences in dive cycle characteristics from qualitative broad state definitions (Mallonee, 1991; Stelle et al., 2008). Searching has also been described as a time- and distance-intensive behaviour (Hildebrand et al., 2022; Sullivan and Torres, 2018) where the whale spends a high amount of time and distance in an area. Thus, searching is a time when the whale expends energy with no energetic gains (Norberg, 1977) and is the basis of many foraging ecology theories attempting to describe how predators optimize their foraging behaviour in habitats of varying prey patch types and densities (Charnov, 1976; MacArthur and Pianka, 1966; Norberg, 1977). Optimal foraging theory predicts that when less prey are present in the prey patch, foraging time will increase if these lower quality patches are visited by predators (MacArthur and Pianka, 1966). However, foraging within a prey patch decreases the prey density. Thus, to maintain an optimal feeding strategy, the marginal value theorem predicts that in habitats with

low prey availability, predators will spend more time in each prey patch foraging, and less time moving between prey patches searching (Charnov, 1976). Overall, these theories predict that in times of low prey availability, animals will spend more time foraging and less time searching for "a better prey patch". Therefore, comparisons of time spent in the search state to the time in the forage state can be a proxy for prey availability based on theories of foraging ecology.

Body position variables—median pitch, depth to body length ratio, and median roll—were the most useful for quantitatively defining grey whale foraging tactics—a finding supported by their use in qualitative drone focal follows (Torres et al., 2018). Previous biologging studies on other baleen whale species used different accelerometry metrics to define foraging behaviour. These other metrics include swim speed and stroke rates for continuous ram filtration (Simon et al., 2009), and signals of high accelerometry and swim speed for lunges at depth (Cade et al., 2016; Goldbogen et al., 2008; Izadi et al., 2022; Shadwick et al., 2019; Simon et al., 2012) or high horizontal accelerometry and high pitch for lunges at the surface (Owen et al., 2016). Bottom side roll behaviour of humpback whales foraging on benthic sand lance is most similar to benthic suction feeding behaviour of grey whales and was detected using high roll and slow swim speed in tag accelerometry data (Ware et al., 2014). The similarity of metrics used to define bottom side roll behaviour in humpback whales (Ware et al., 2014) with those used to define grey whale foraging tactics in this study supports the contention that body position variables are useful for defining foraging behaviour of baleen whales feeding on benthic prey.

Our quantification of grey whale foraging tactics fills a knowledge gap in detection and quantitative description of foraging signals of eschrichtiids (grey whales), which can be combined with the thorough description of feeding methods by other baleen whales (Goldbogen et al., 2017) to provide quantified body movement descriptions for foraging tactics of all mysticete species groups. These newly established quantitative metrics to detect and define foraging in PCFG grey whales can enable other analyses that require quantified foraging behaviour data to support management and conservation efforts. For example, a bioenergetic model for ENP and WNP grey whale populations has been developed to assess the population consequences of disturbance to individual whales (Villegas-Amtmann et al., 2017, 2015). By quantifying PCFG grey whale foraging tactics, this unique group of grey whales a similar

analysis can now be conducted to inform management decisions regarding multiple threats facing this sub-group.

The proportional activity budgets we constructed from biologging data are similar to those previously constructed using other behavioural sampling techniques (i.e., theodolite focal follows (Sullivan and Torres, 2018), land-based observations (Mallonee, 1991; Stelle et al., 2008), drone focal follows (Torres et al., 2018)). We found that PCFG grey whales spend 36% of their time foraging, 43% searching, and 21% transiting, which fall within the range of values reported for these broad states from other parts of the PCFG range (Mallonee, 1991; Stelle et al., 2008; Sullivan and Torres, 2018). This study found that headstands, benthic digs, and side swims were present in approximately equal proportions, which differs from the only other study to assess foraging tactics that found headstands (including side digs) to be twice as common as side swims (Torres et al., 2018). This discrepancy highlights the benefits of the fine-scale data collected from biologging tags that allow a quantitative assessment of behavior. Patterns in individual variation of tactics also indicate that side swims are a less commonly used foraging tactic. Only two whales (H22 & I22) had side swim as the dominant foraging tactic, and these individuals were shorter than 11 m indicating that they likely had not reached maturity (Bierlich et al., 2023). This finding is consistent with the ontogenetic shift noted in PCFG grey whales that transition from side swims to headstands with increasing total length that is a proxy for age and maturity (Bird et al., *in prep*).

Biologging data can be used to explore the complex relationships between behaviour and body condition (Amo et al., 2007; Beale and Monaghan, 2004; Ransom et al., 2010). With our limited sample size, we documented that all grey whales with a BAI below average (i.e., <26.89; K. Bierlich pers. comm.) consistently made more foraging dives than search or transit. This pattern of skinnier whales spending more time foraging is somewhat similar to horses who forage more when in poorer body condition spent more time foraging than individuals in better body condition (Ransom et al., 2010). Body condition may also play a role in how animals respond behaviourally to disturbances, as shown for seabirds that react more readily to disturbances when they are in good body condition and can afford the added energetic cost of moving away (Beale and Monaghan, 2004). Given the intensity of vessel disturbance in the nearshore foraging range of the PCFG grey whales (COSEWIC, 2017; Duffus, 1996; Lemos et

al., 2022; Sullivan and Torres, 2018), disturbance impacts may reduce time spent foraging and thereby body condition, which in turn could impact the whales' ability to respond to the disturbance. Biologging data can play an integral role in disentangling these relationships between behaviour, body condition, and disturbance in future studies.

A surprising finding in the activity budgets was that the tag deployments on the whales that were a known mother (G22) and her daughter (F22) had very similar proportions of both broad states and foraging tactics (**Figure 2.5**). This suggests that there may be potential for vertical transmission of behaviours in PCFG grey whales, a group that shows high maternal recruitment (Calambokidis and Perez, 2017). Vertical transmission of foraging tactics and tool use have been documented in bottlenose dolphins (*Tursiops aduncus*) from mothers to primarily female offspring (Wild et al., 2019) and the importance of female-kinship for shared prey preferences has been demonstrated in humpback whales (Rendell et al., 2019). While there is limited data documenting maternal kinship in baleen whales (Rendell et al., 2019), and only two of our study animals had a known maternal relationship, this finding demonstrates how our study system of PCFG whales with strong site-fidelity and maternal recruitment presents a viable opportunity for future research to examine if vertical transmission of foraging tactics occurs in baleen whales.

The lack of social behaviour detected by the HMM is likely explained by the low probability of the tags being deployed long enough to capture social behaviours given the rarity of social interactions observed in the PCFG range (Stelle et al., 2008; Torres et al., 2018). The low number of social behaviours noted in PCFG grey whales increases in frequency in the early fall (late August, early September) towards the end of the foraging season (Stelle et al., 2008; Torres et al., 2018). About 31 hours to tag data was collected in early September, yet these deployments potentially occurred too early in the fall to have a high likelihood of recording data during social interactions.

The observed differences between day and night foraging behaviours suggest that the PCFG grey whales are visual predators (Torres, 2017) targeting zooplankton prey (likely mysids) that have a vertical expansion of their depth range at night (Alldredge and King, 1980; Mauchline, 1980). More dispersed prey and inability to rely on visual cues at night potentially require foraging PCFG grey whales to use more exploratory behaviour to detect prey in the dark,

leading to a higher proportion of the search state and side swims at night as this foraging tactic is performed in the mid-water column (Bird et al., *in prep*; Torres et al., 2018).

Decreased foraging depth and higher number of rolls to the left (right-eye up) during nighttime could also potentially result from an increased vertical distribution of prey and indicate that whales may track prey above them (Jaakkola et al., 2021). The overnight deployment with the most extreme change in depth and sidedness occurred when the moon was 97.58% illuminated (https://nineplanets.org/moon/phase/9-12-2022/), supporting the idea that with high moonlight, the whale was looking for the shadow of prey above them. The two other overnight deployments were when the moon was only 44.36% illuminated (https://nineplanets.org/moon/phase/7-21-2022/) and thus the decreased moonlight might explain why there were fewer notable changes in sidedness of foraging tactics between day and night.

PCFG grey whales were also found to slightly increase their surface time at night, from a 20:80 ratio during the day to a 30:70 ratio at night. This increase in surface time potentially indicates that whales spend more time resting at the surface during the night. This is further supported by the lack of resting dives detected by the HMM, suggesting that rest behavior may happen at the surface. Therefore, future work should focus on examining where and when PCFG grey whales rest.

Limitations and recommendations

Tagging studies are inherently limited by sample size and individual variation when generalizing to the larger population (Hays et al., 2016). However, this study illustrates the feasibility of using biologging data to define behavior states and foraging tactics of PCFG grey whales along the Oregon and Washington coast. Collection of a larger sample size of biologging data from PCFG whales would account for individual variability in behavioural classifications. Therefore, effort should be made to collect biologging data from grey whales throughout the PCFG foraging range, as well as the from the WNP and ENP populations foraging in the Arctic. Additionally, the whales we tagged were predominantly female (by chance) so other demographic units should be targeted in future tagging efforts to ensure that any behavioural differences in age and sex are captured in the biologging data.

Additionally, prey data should be integrated with the behavioural biologging data to develop metrics of foraging success. This approach would allow for an estimate of energetic gain

for each foraging tactic so that foraging efficiency can be calculated, and insight can be gained on which foraging strategies are the most successful (e.g., Savoca et al., 2021; Volpov et al., 2015; Ydesen et al., 2014). Estimates of prey consumption per foraging tactic have not been examined in grey whales, but can be obtained once prey densities have been determined and are combined with foraging energetics data (see Chapter 3) and measurements of prey quality (Hildebrand et al., 2021).

Conclusions

The 10 biologging tags deployed provide the first quantitative definitions of foraging behaviours of PCFG grey whales. These quantitative definitions of foraging behaviours provide a means to estimate foraging efficiency and analyze the drivers of foraging behaviour. Understanding the energetic costs of these behaviours will contribute to a better understanding of effects of disturbance and exposure to physiological threats such as boat strikes and pollution. Quantifiable definitions of foraging behaviour can also contribute to anticipating and diagnosing the causes of Unusual Mortality Events.

Chapter 3: Biologging-derived proxies estimate the relative energetic costs of grey whale foraging behaviours

Summary

Relatively little is known about the fine-scale energetic costs that grey whales incur to forage, travel and search for prey—or the consequences that disturbances have on their food requirements. One means to obtain measures of energetic cost is to calculate proxies of energy expenditure from movement variables recorded by sensors (accelerometers, magnetometers, and gyroscopes) mounted in biologging tags temporarily deployed on whales. In this study we attached suction-cupped biologging tags to 10 Pacific Coast Feeding Group (PCFG) grey whales, and calculated four proxies of energy expenditure—Overall Dynamic Body Acceleration (ODBA; ms^{-2}), stroke rate (Hz), stroke amplitude (radians per s), and duration of dives. Among the broad behavior states (i.e., forage, search, transit) and foraging tactics used by grey whales (i.e., headstands, benthic digs, and side swims), we found that foraging was more energetically costly than searching and transiting—and that headstanding was a more energetically expensive foraging tactic than benthic digs and side swims (based on stroke rates). We conclude that stroke rate is the best proxy to estimate energy expenditure for grey whales because it is the easiest to calculate, is the most comparable across tag deployments and studies, and has fewer limitations compared to the other proxies. These relative measures of energy expenditure calculated for different foraging behaviours represent an important foundational step toward better understanding grey whale foraging energetics, enabling assessment of prey requirements and energetic impacts of threats facing this species.

Introduction

A small group of grey whales (*Eschrichtius robustus*) known as the Pacific Coast Feeding Group (PCFG; ~210 individuals, Harris et al., 2022) forage over multiple years between Norther California and British Columbia (41^{o}N and 52^{o}N) from 1 June to 30 Nov (International Whaling Commission, 2011) rather than continue their migration north to Arctic foraging grounds with the larger Eastern North Pacific (ENP) grey whale population (~17,000 individuals; Eguchi et al., 2022). Additionally, PCFG grey whales use numerous foraging tactics, such as headstands and side swims (Torres et al., 2018) to forage on a variety of prey (Darling et

al., 1998; Hildebrand et al., 2021) in a mosaic of kelp and reef habitat (Torres et al., 2018) while ENP whales are thought to perform a traditional benthic dig to suction feed on benthic amphipods in soft-bottomed habitats (Johnson and Nelson, 1984; Moore et al., 2022; Nerini, 1984; Wursig et al., 1986). This small PCFG sub-group faces a number of unique threats associated with entanglement, boating disturbance, ship strikes, mircoplastic ingestion, and altered benthic productivity (COSEWIC, 2017; Duffus, 1996; Lemos et al., 2020a, 2020b; Scordino et al., 2020; Silber et al., 2021; Sullivan and Torres, 2018; Torres et al., 2023). The consequences of these threats likely include negative impacts on the foraging energetics of PCFG grey whales, and ultimately their health, survival, and birth rates. Unfortunately, relatively little is known about the fine-scale energetic costs of foraging and other behaviours of grey whales.

Annual food requirements have been calculated for grey whales using bioenergetics models that estimate the energetic costs of travelling (migration), breeding, and foraging as a function of average observed respiration rates (Agbayani, 2022; Villegas-Amtmann et al., 2017, 2015). These models provide useful estimates of prey requirements on broad spatial and temporal scales, but fail to provide insight into the energetic consequences of threats facing individual grey whales on finer spatial and temporal scales. Assessing fine scale energetic requirements of foraging needed by grey whales to support survival, growth, and reproduction, requires knowing the energetic costs associated with both broad states and foraging tactics.

Biologging tags that record high-resolution accelerometry data provide a minimally invasive means to measure energy expenditure of free-ranging animals (Watanabe and Goldbogen, 2021) with important conservation implications. Common metrics used to estimate energy expenditure of behaviors from biologging data in marine megafauna include overall dynamic body acceleration (ODBA), stroke rate, stroke amplitude and dive duration. ODBA is the sum of the specific acceleration in all three axes integrated over time and often used as a proxy for energetic expenditure (Brown et al., 2013; Gleiss et al., 2011; Halsey, 2017, 2011; Wilson et al., 2020). ODBA measures the acceleration of the body and is considered an effective way of determining energy expenditure when an animal's metabolic rate is majorly comprised of movement costs. ODBA has been linked to metabolic rate in many studies (Allen et al., 2022; Fahlman et al., 2013; Halsey et al., 2009; Jeanniard-du-Dot et al., 2017; John, 2020; Wilson et

al., 2006). Stroke rate, or the frequency of stroking, has been linked to metabolic rate in pinnipeds and cetaceans (Allen et al., 2022; Isojunno et al., 2018; Jeanniard-Du-Dot et al., 2016; Maresh et al., 2015; Martín López et al., 2015; Williams and Maresh, 2015), although the cetacean studies are primarily focused on odontocetes. Stroke amplitude is derived as a rotation rate from biologging data (Cade et al., 2020) and is often associated with indicating swimming intensity (Cade et al., 2020; Jeanniard-Du-Dot et al., 2016; Williams et al., 2015). The duration of dives can also be used as a proxy of energetic cost at the sub-dive behavioural scale (Jeanniard-Du-Dot et al., 2016; Ladds et al., 2017; Williams et al., 2004, 2017). It is assumed that animals will spend less time performing more energetically costly behaviors, thus potentially resulting in shorter dives based on the energetics of the behavior observed. These accelerometry-derived proxies of energy expenditure have aided conservation efforts for marine mammals by estimating entanglement costs (van der Hoop et al., 2017) and increasing precision of prey requirements from bioenergetic models (Brodie et al., 2016).

We deployed suction cup high-resolution accelerometry biologging tags on PCFG grey whales in their foraging grounds off the coast of Oregon, USA to calculate proxies of energy expenditure associated with broad behavior states (e.g., forage, search, transit) and specific foraging tactics (e.g., headstand, benthic dig, side swim) identified in prior analyses (Chapter 2). For each broad and fine scale behavior we calculate four metrics of energy expenditure (ODBA, stroke rate and amplitude, and dive duration) and compare results to determine the relative energetic costs of different behaviors and which metrics are the most consistent and useful for describing grey whale energetics. These biologging derived estimates of relative grey whale energy expenditure may have high utility in conservation contexts for a species facing regular disturbance from multiple threats and poses logistical challenges to measure metabolic rates through other methods.

Methods

Data collection

We deployed CATS (Custom Animal Tracking Solution, https://cats.is) video and inertial measurement unit (IMU) tags on ten PCFG grey whales, one in 2019, three in 2021 and six in 2022. All fieldwork was conducted under NOAA/NMFS permit #21678 and the University of British Columbia Animal Care Committee permit #A21-0254. Tagged animals were identified

Table 3.1. Biologging CATS tag deployments on PCFG grey whales.

Deployment ID	Genetic Sex	Tag on	Tag off	Tag on location	Deployment length (hh:mm:ss)	Total length (m)	Body area index (BAI)
A19	NA	9/1/19 15:05:52	9/1/19 16:41:18	Cape Flattery, WA	01:29:17	10.2	NA
B21[a]	M	8/16/21 13:01:11	8/16/21 18:20:03	Lost Creek	03:00:34	12.0	22.74
C21[a]	NA	8/16/21 16:04:52	8/16/21 16:31:24	Alsea River Mouth	00:26:15	11.1	25.37
D21[b]	M	8/16/21 17:16:37	8/16/21 21:08:03	Alsea River Mouth	03:51:26	11.6	25.82
E22	F	7/21/22 9:50:30	7/22/22 10:38:49	Nye Beach	24:48:19	11.1	24.94
F22[c]	F	7/21/22 10:36:03	7/21/22 17:19:17	Flat Rock	06:43:14	10.4	26.94
G22	F	7/21/22 16:03:25	7/22/22 09:37:27	South Beach	17:34:02	11.6	27.39
H22	NA	9/12/22 13:13:35	9/12/22 18:00:00	Gull Rock	00:33:25	8.9	29.45
I22	F	9/12/22 12:49:02	9/13/22 11:54:58	Gull Rock	23:05:58	10.5	28.46
J22	F	9/12/22 11:49:02	9/12/22 19:12:53	Gull Rock	07:23:50	12.1	26.75

[a]Tag without audio data.
[b]Tag without video data.
[c]Individual is the known calf of G22.

using photo identification, and genetic sex information was obtained for known individuals using previously collected tissue samples (Lang et al., 2014). Drone photogrammetry was used to calculate total length (m) and body area index (BAI) measurements of tagged animals from flights within 15 days of the deployment. Data from the CATS tags (400 Hz accelerometer, 50 Hz magnetometer and gyroscope sensors, and 10 Hz pressure sensors) were pre-processed according to the methods of Cade et al. (2021) — and dives and roll events were manually audited using the *catsr* package (Czapanskiy, 2022) in R v4.2.3 (R Core Team, 2023) and then classified into behaviours. Dives were defined into three broad states (forage, search, and transit) according to the Hidden Markov Model (Chapter 2). Roll events were assigned to foraging tactics (headstand, benthic dig, and side swim) according to the Classification and Regression Tree model described in Chapter 2. Deployment summary information can be found in **Table 3.1**.

Calculating energy expenditure proxies

All energy expenditure proxies were calculated from biologging data in R v4.2.3 (R Core Team, 2023) unless otherwise stated.

Overall Dynamic Body Acceleration (ODBA)

To remove the influence of gravity on the calculation of ODBA, accelerometer data were filtered at 25%, 50% and 70% of the dominant stroking frequency (dsf) for each deployment (**Table G1**). Different filter frequencies were calculated to test if choice of filter affected results. Dsf was calculated using the *dsf* function in the *tagtools* package (DeRuiter et al., 2022) on a dive series of the acceleration data where the whale was observed to be steady swimming. Complementary filtering of the full deployment was conducted using the *comp_filt* function in the *tagtools* package (DeRuiter et al., 2022).

ODBA was calculated from the high frequency acceleration data of the full deployment using the *odba* function in the *tagtools* package (DeRuiter et al., 2022). ODBA values within 0.2 m of the surface were replaced with NAs, as noise in the acceleration data from the tag breaking the surface confounds the true body movement signal (D. Cade pers. comm.). Then the mean ODBA for each dive and roll event was calculated. As ODBA depends on tag placement and animal size (Martin Lopez et al., 2022), ODBA values were standardized according to the following equation (Isojunno and Miller, 2015):

$$Standardized\ ODBA = \frac{Behaviour\ ODBA}{Median\ deployment\ ODBA} \times Median\ ODBA\ all\ deplyments$$

where all ODBA values are in ms^{-2} and median deployment ODBA values are reported in **Table G2**.

Stroke rate and amplitude

To calculate stroke rate, strokes were detected in the PCFG biologging data using a custom stroke finding algorithm in MATLAB (MathWorks, v2021a) as applied in Cade et al. (2020), based on *stroke_rate* and *dsf* scripts at animaltags.org and Martín López et al. (2015). The stroke detection code was applied to the y-axis of the gyroscope because this represents the axis where the up-down oscillatory swimming signal is observed. A 1-second low pass filter was chosen to separate the body and fluke rotations in the gyroscope signal. A deployment-specific

stroking threshold due to variable tag placement was chosen to exclude residual rotations after the whale had stopped fluking and to clearly define up- and down-strokes.

The stroke rate of each dive and roll event was calculated as the number of upstrokes that occurred during the behaviour divided by the duration of the behaviour. There is a known negative relationship between stroke rate and body length (Gough et al., 2021; Sato et al., 2007). Therefore, stroke rates were standardized according to the following equation:

$$Standardized\ stroke\ rate = \frac{Behaviour\ stroke\ rate}{Deployment\ dsf} \times Median\ dsf\ all\ deployments$$

where all stroke rates are in Hz and the dsf for each deployment is reported in **Table G1**.

In this study, stroke amplitude represents the speed of fluking (radians per s), or the rate of rotation in the y-axis of the gyroscope. Stroke amplitude was calculated as the maximum of the absolute values of the y-axis gyroscope data between each upstroke detected using the custom stroke finding algorithm described above. Stroke amplitude for each dive and roll event was calculated as the mean stroke amplitude that occurred during the behaviour. Stroke amplitude is dependent on tag placement and no standardization methods exist. Therefore, raw stroke amplitude values cannot be compared between deployments.

Dive duration

For each dive, the proportion of time spent performing each foraging tactic was calculated. If multiple foraging tactics were performed during a dive the dominant foraging tactic was chosen as the one that was performed for at least 50% of the dive time. Exploratory data analysis indicated that about 20% of the dives (199 out of 1,093) had multiple tactics performed during a single dive. Dive duration was calculated as the amount of time between the dive start (the point where the whale leaves the surface) and dive end (the point where the whale returns to the surface) following dive identification methods in Chapter 2.

Statistical analysis

All statistical analyses were conducted in R v4.2.3 (R Core Team, 2023). Significance levels for all tests were set to $\alpha = 0.05$.

Proxies of energy expenditure (i.e., dive duration, ODBA, and stroke rate) were compared between both broad states and foraging tactics using mixed effects models, with deployment as a random effect to account for the repeated measures on individuals. The models were fitted using the *lmerTest* package (Kuznetsova et al., 2017). Nested models with and

without fixed effects were compared using likelihood ratio tests to select whether the inclusion of the fixed factor for behaviour improved the null model with no fixed effects.

Linear mixed effects models were used to test for differences in dive duration and ODBA among different broad states and foraging tactics. Dive duration and ODBA were log-transformed to meet model assumptions of normally distributed errors and homogeneity of variance. The analysis for stroke rate was split into two models given the zero-inflation in the distribution of raw stroke rate values. This zero-inflation emerges from the raw stroke rate values capturing two components of stroking energy expenditure: 1) the likelihood of gliding within a behaviour, indicated by stroke rates of zero and 2) the stroke rate of a behaviour, when stroke rate was greater than zero. Therefore, a binary glide variable was created, where a value of 0 indicated stroking (stroke rate > 0) and a value of 1 indicated gliding (stroke rate = 0) to capture the non-fluking behaviour in the raw stroke rate data. The difference in probability of gliding between behaviours was assessed using a binomial generalized linear mixed model. For behaviours with a stroke rate greater than zero, linear mixed effects models were used to test for differences in stroke rate between different behaviours at the scale of broad state and foraging tactic. Stroke rate was log-transformed to meet model assumptions of normally distributed errors and homogeneity of variance.

Pairwise comparisons of the mean dive duration, ODBA, and non-zero stroke rate between behaviours were carried out using the estimated marginal means with the Tukey method for p-value adjustment when comparing a family of estimates using the *emmeans* package (Lenth, 2022). The differences in glide probability between behaviours were visualized by plotting the estimated effect of the behaviour factor using the *effects* package (Fox, 2003; Fox and Weisberg, 2019).

Differences in stroke amplitude between behaviours within each deployment were compared visually by plotting the data. General summaries of the number of deployments with the same patterns of stroke amplitude between behaviours were used to determine which behaviour had the highest stroke amplitude by majority rule. Only deployments with more than one behaviour were used in the summaries (n = 9 at broad state scale; n = 8 at foraging tactic scale). Stroke amplitude was reported as percent differences because raw values were not comparable across deployments. Broad state stroke amplitude was calculated as

$$Percent\ difference = \frac{(mean\ state\ stroke\ amplitude - mean\ transit\ stroke\ amplitude)}{mean\ transit\ stroke\ amplitude}$$

for n = 7 deployments except D21 and H22, where search stroke amplitude replaced transit stroke amplitude in the formula as these deployments did not have any transit data. Foraging tactic stroke amplitude was calculated as

$$Percent\ difference = \frac{(mean\ tactic\ stroke\ amplitude - \ mean\ transit\ stroke\ amplitude)}{mean\ transit\ stroke\ amplitude}$$

for n = 6 deployments except D21 and H22, where search stroke amplitude replaced transit stroke amplitude in the formula as these deployments did not have any transit data. The transit stroke amplitude was chosen as the baseline to compare to as this behaviour represents directional steady swimming (see Chapter 2). All stroke amplitudes included in the percent difference formulae were in radians per second.

Results

Broad states

The likelihood ratio test comparison of the nested models indicated that the models including broad state performed significantly better than the models without the fixed factor for all energy expenditure proxy models (**Table 3.2**).

The ODBA models and pairwise comparisons of the means for each broad behavior state showed that, for all filters, ODBA was significantly different between states (**Table 3.3**). ODBA was highest for the forage state using the 25% and 70% dsf filters, while ODBA was highest for the search state using the 50% dsf filter (**Table 3.4; Figure 3.1a-c**). ODBA was lowest for the transit state for all filters. The forage state ODBA was approximately 1.7-2.6 times that of the transit state (**Table 3.4**). The search state had the highest variation in ODBA, while the transit state had the lowest variation in ODBA (**Table 3.4**). This pattern in variation is also visible in **Figure 3.1**.

Exploration of the difference in ODBA between broad states across individual deployments suggested differences between individuals dependent on the filter used to calculate ODBA (**Figure 3.1d-f**). Apparent deviations of individual deployments from model results for all data combined suggest that selection of the filter used to calculate ODBA is critical when interpreting results.

Table 3.2. Results from comparison of linear mixed effects models constructed using the dives (n = 1,856) and roll events (n = 1,890) from CATS tag deployments on ten PCFG grey whales for different energy expenditure proxies, with and without broad state or foraging tactic as fixed effect, and with deployment included as a random effect. A significance level of 0.05 was used in analysis. Bolded models had higher performance. All non-binary variables were log-transformed to meet model assumptions. ODBA represents the Overall Dynamic Body Acceleration (ms^{-2}) calculated using three different filters 25% of the dominant stroke frequency (dsf; odba0.25), 50% dsf (odba0.5), and 70% dsf (odba0.7). ODBA was standardized to allow for comparison across deployments (Isojunno and Miller, 2015)**. Glide is the probability of gliding (i.e., having a stroke rate = 0) and stroke rate (Hz) represents all stroke rate values in the data greater than 0. Stroke rate was standardized by dsf to account for the negative relationship between stroke rate and body size** (Gough et al., 2021; Sato et al., 2007)**. Dive duration was only considered at the foraging tactic scale and is the length of the dive in seconds of dives dominated by each foraging tactic.**

Behavioural scale	Energy expenditure proxy	Model	Log Likelihood	Chi Sq	Df	P-value
Broad state (n = 1,856 dives)	odba0.25	~1	-1919.8			
		~state	-1497.7	844.22	2	< 2.2E-16
	odba0.5	~1	-1740.4			
		~state	-1459.2	562.28	2	< 2.2E-16
	odba0.7	~1	-1556.2			
		~state	-1341.8	428.73	2	< 2.2E-16
	glide	~1	-80.5			
		~state	-70.9	19.13	2	7.03E-05
	stroke rate	~1	-1639.4			
		~state	-1508.3	262.22	2	< 2.2E-16
Foraging tactic (n = 1,890 roll events)	odba0.25	~1	-1503.1			
		~tactic	-1453.4	99.573	2	<2.2e-16
	odba0.5	~1	-1338.6			
		~tactic	-1295.5	86.115	2	<2.2e-16
	odba0.7	~1	-1194.0			
		~tactic	-1172.5	43.092	2	4.39E-10
	glide	~1	-708.3			
		~tactic	-693.0	30.716	2	2.14E-07
	stroke rate	~1	-1135.5			
		~tactic	-1129.0	12.965	2	0.00153
	dive duration	~1	-1221.3			
		~tactic	-1155.5	131.73	2	<2.2e-16

The probability of gliding did not differ between broad behavioral states according to glide model results (**Figure 3.2a**). However, stroke rate was significantly different between broad states according to the model (**Table 3.3**). Pairwise comparisons of mean stroke rates indicate that significant differences in stroke rate were present between the forage state and the search and transit states (**Table 3.4**), with significantly higher stroke rates while in the forage state (**Figure 3.2b**). The observed differences among individual stroke rates were greatest in the forage state (**Table 3.4; Figure 3.2b,c**). Stroke rates were more consistent across individuals in the transit state (**Table 3.4; Figure 3.2b,c**).

Table 3.3. Results from energy expenditure proxy linear mixed effects models constructed using the dives (n = 1,856) and roll events (n = 1,890) from CATS tag deployments on ten PCFG grey whales with broad state or foraging tactic as fixed effect and deployment included as a random effect and pairwise comparisons of the means. A significance level of 0.05 was used in analysis. All variables were log-transformed to meet model assumptions. ODBA represents the Overall Dynamic Body Acceleration (ms^{-2}) calculated using three different filters 25% of the dominant stroke frequency (dsf; odba0.25), 50% dsf (odba0.5), and 70% dsf (odba0.7). ODBA was standardized to allow for comparison across deployments (Isojunno and Miller, 2015)**. Stroke rate (Hz) represents all stroke rate values in the data greater than 0. Stroke rate was standardized by dsf to account for the negative relationship between stroke rate and body size** (Gough et al., 2021; Sato et al., 2007)**. Dive duration was considered only at the foraging tactic scale and is the length of the dive in seconds of dives dominated by each foraging tactic.**

Broad state (n = 1,856 dives)	odba0.25 ~ state + (1|DeploymentID)	**ANOVA**	**F-statistic**	**df**	**p-value**
			538.47	2	<2.2e-16
		Comparison	**t.ratio**	**df**	**p-value**
		forage - search	7.622	1843	<0.0001
		forage - transit	31.726	1842	<0.0001
		search - transit	26.661	1840	<0.0001
	odba0.5 ~ state + (1|DeploymentID)	**ANOVA**	**F-statistic**	**df**	**p-value**
			330.64	2	<2.2e-16
		Comparison	**t.ratio**	**df**	**p-value**
		forage - search	4.807	1843	<0.0001
		forage - transit	24.532	1843	<0.0001
		search - transit	21.561	1840	<0.0001
	odba0.7 ~ state + (1|DeploymentID)	**ANOVA**	**F-statistic**	**df**	**p-value**
			243.1	2	<2.2e-16
		Comparison	**t.ratio**	**df**	**p-value**
		forage - search	5.018	1843	<0.0001
		forage - transit	21.287	1843	<0.0001
		search - transit	17.97	1841	<0.0001
	stroke rate ~ state + (1|DeploymentID)	**ANOVA**	**F-statistic**	**df**	**p-value**
			140.81	2	<2.2e-16
		Comparison	**t.ratio**	**df**	**p-value**
		forage - search	15.204	1821	<0.0001
		forage - transit	13.435	1820	<0.0001
		search - transit	0.802	1819	0.7021
Foraging tactic (n = 1,890 roll events)	odba0.25 ~ tactic + (1|DeploymentID)	**ANOVA**	**F-statistic**	**df**	**p-value**
			51.066	2	<2.2e-16
		Comparison	**t.ratio**	**df**	**p-value**
		headstand - benthic dig	0.041	1884	0.9991
		headstand - side swim	-7.844	1886	<0.0001
		benthic dig - side swim	-9.737	1885	<0.0001
	odba0.5 ~ tactic + (1|DeploymentID)	**ANOVA**	**F-statistic**	**df**	**p-value**
			43.997	2	< 2.2e-16
		Comparison	**t.ratio**	**df**	**p-value**
		headstand - benthic dig	-0.995	1885	0.5803
		headstand - side swim	-7.886	1886	<0.0001
		benthic dig - side swim	-8.708	1885	<0.0001

odba0.7 ~ tactic + (1|DeploymentID)	**ANOVA**	**F-statistic**	**df**	**p-value**
		21.755	2	4.56E-10
	Comparison	**t.ratio**	**df**	**p-value**
	headstand - benthic dig	-2.234	1885	0.0659
	headstand - side swim	-6.230	1885	<0.0001
	benthic dig - side swim	-5.367	1886	<0.0001
stroke rate ~ tactic + (1|DeploymentID)	**ANOVA**	**F-statistic**	**df**	**p-value**
		6.4718	2	0.001586
	Comparison	**t.ratio**	**df**	**p-value**
	headstand - benthic dig	3.556	1634	0.0011
	headstand - side swim	2.696	1636	0.0194
	benthic dig - side swim	-0.305	1633	0.9500
dive duration ~ tactic + (1|DeploymentID)	**ANOVA**	**F-statistic**	**df**	**p-value**
		69.887	2	< 2.2e-16
	Comparison	**t.ratio**	**df**	**p-value**
	headstand - benthic dig	-1.519	1066	0.2823
	headstand - side swim	7.033	1010	<0.0001
	benthic dig - side swim	11.739	1072	<0.0001

Table 3.4. Energy expenditure proxies (mean ± s.d.) from CATS tag deployments on PCFG grey whales for all deployments combined and within each deployment. N represents the number of dives in the biologging data assigned to each broad state using the Hidden Markov Model or number of roll events assigned to each foraging tactic using the Classification and Regression Tree model constructed in Chapter 2. ODBA stands for Overall Dynamic Body Acceleration (ms^{-2}) and was calculated using three different filters (25% of the dominant stroke frequency (dsf), 50% of the dsf, and 70% of the dsf). ODBA was standardized to correct for effects of tag placement. Stroke rate (Hz) was standardized to account for the relationship between body size and stroke rate. Broad state stroke amplitude was presented as the percent difference in stroke amplitude between the transit broad state and the forage or search broad state. Foraging tactic stroke amplitude was presented as the percent difference in stroke amplitude between the transit broad state and the foraging tactic. Percent difference in broad state and foraging tactic stroke amplitude was calculated from the search broad state in deployments D21 and H22, as these deployments did not include transit, and could not be calculated for deployment C21 as this deployment only included the forage broad state. Stroke amplitude was only presented for individual deployments as raw stroke amplitude values are not comparable between deployments. Dive duration (min) was only calculated at the foraging tactic scale to compare between dives dominated by different foraging tactics. Note that deployment C21 only includes the forage broad state and headstand foraging tactic while deployments D21 and H22 only include the forage and search broad states and H22 only includes the side swim foraging tactic. Dashes indicate no data available.

		Broad state			Foraging tactic		
Deploy. ID	**Energy expenditure proxy**	**Forage**	**Search**	**Transit**	**Headstand**	**Benthic dig**	**Side swim**
All	N	672	795	389	486	743	661
	ODBA (25% dsf; ms^{-2})	1.88 ± 1.43	1.82 ± 2.36	0.73 ± 1.25	2.38 ± 1.82	2.27 ± 1.82	4.39 ± 1.95
	ODBA (50% dsf; ms^{-2})	1.17 ± 1.45	1.21 ± 2.23	0.60 ± 1.35	1.52 ± 1.73	1.40 ± 1.77	2.61 ± 1.92
	ODBA (70% dsf; ms^{-2})	0.90 ± 1.43	0.89 ± 2.01	0.53 ± 1.46	1.13 ± 1.67	1.07 ± 1.73	1.70 ± 1.77
	Stroke rate (Hz)	0.34 ± 0.31	0.19 ± 0.16	0.14 ± 0.06	0.60 ± 0.55	0.36 ± 0.40	0.25 ± 0.29
	Dive duration (min)	--	--	--	2.60 ± 1.29	3.13 ± 1.40	1.48 ± 1.32
A19	N	11	17	3	1	29	15
	ODBA (25% dsf; ms^{-2})	2.48 ± 1.26	1.13 ± 1.55	0.76 ± 1.04	7.10	3.53 ± 1.82	3.32 ± 1.57
	ODBA (50% dsf; ms^{-2})	1.36 ± 1.26	0.72 ± 1.35	0.58 ± 1.05	2.77	1.63 ± 1.67	1.75 ± 1.62

Deploy. ID	Energy expenditure proxy	Broad state			Foraging tactic		
		Forage	Search	Transit	Headstand	Benthic dig	Side swim
A19	ODBA (70% dsf; ms^{-2})	1.04 ± 1.22	0.55 ± 1.21	0.49 ± 1.07	1.39	1.21 ± 1.60	1.20 ± 1.49
	Stroke rate (Hz)	0.14 ± 0.02	0.11 ± 0.02	0.11 ± 0.01	0.00	0.18 ± 0.19	0.13 ± 0.10
	Stroke amplitude (% diff)	0.50	0.06	0.00	-1.00	0.25	0.19
	Dive duration (min)	--	--	--	--	2.68 ± 1.25	2.27 ± 1.36
B21	N	50	14	14	31	81	25
	ODBA (25% dsf; ms^{-2})	2.63 ± 1.33	1.08 ± 2.12	0.59 ± 1.06	3.56 ± 1.55	3.56 ± 1.88	4.81 ± 1.79
	ODBA (50% dsf; ms^{-2})	1.68 ± 1.35	0.78 ± 1.93	0.48 ± 1.05	2.34 ± 1.62	2.18 ± 1.70	3.46 ± 1.68
	ODBA (70% dsf; ms^{-2})	1.27 ± 1.36	0.61 ± 1.79	0.41 ± 1.05	1.82 ± 1.55	1.61 ± 1.57	2.51 ± 1.73
	Stroke rate (Hz)	0.34 ± 0.08	0.30 ± 0.06	0.31 ± 0.03	0.33 ± 0.18	0.38 ± 0.21	0.46 ± 0.50
	Stroke amplitude (% diff)	0.81	0.19	0.00	0.57	0.48	0.24
	Dive duration (min)	--	--	--	2.84 ± 2.30	3.67 ± 1.74	2.06 ± 2.01
C21	N	3	0	0	3	0	0
	ODBA (25% dsf; ms^{-2})	1.29 ± 1.04	--	--	1.00 ± 1.07	--	--
	ODBA (50% dsf; ms^{-2})	0.84 ± 1.05	--	--	0.67 ± 1.05	--	--
	ODBA (70% dsf; ms^{-2})	0.67 ± 1.04	--	--	0.58 ± 1.05	--	--
	Stroke rate (Hz)	1.16 ± 0.04	--	--	1.30 ± 0.10	--	--
	Stroke amplitude (% diff)	--	--	--	--	--	--
	Dive duration (min)	--	--	--	3.47 ± 0.08	--	--
D21	N	49	13	0	1	27	31
	ODBA (25% dsf; ms^{-2})	1.38 ± 1.11	1.48 ± 1.36	--	12.55	1.28 ± 1.28	1.23 ± 1.51
	ODBA (50% dsf; ms^{-2})	0.94 ± 1.11	0.85 ± 1.26	--	10.91	0.90 ± 1.23	0.88 ± 1.42
	ODBA (70% dsf; ms^{-2})	0.75 ± 1.09	0.55 ± 1.28	--	8.76	0.76 ± 1.15	0.74 ± 1.38
	Stroke rate (Hz)	0.10 ± 0.01	0.07 ± 0.02	--	0.25	0.11 ± 0.02	0.10 ± 0.03
	Stroke amplitude (% diff)	0.00	0.00	--	12.1	0.00	-0.19
	Dive duration (min)	--	--	--	--	2.88 ± 0.20	2.92 ± 0.63
E22	N	211	98	168	14	248	62
	ODBA (25% dsf; ms^{-2})	1.60 ± 1.26	0.99 ± 1.48	0.85 ± 1.19	1.88 ± 1.63	1.63 ± 1.43	2.05 ± 1.63
	ODBA (50% dsf; ms^{-2})	0.93 ± 1.22	0.75 ± 1.38	0.79 ± 1.23	1.07 ± 1.39	0.94 ± 1.32	1.11 ± 1.48
	ODBA (70% dsf; ms^{-2})	0.71 ± 1.25	0.63 ± 1.46	0.75 ± 1.35	0.85 ± 1.39	0.71 ± 1.33	0.74 ± 1.52
	Stroke rate (Hz)	0.15 ± 0.03	0.11 ± 0.03	0.13 ± 0.03	0.16 ± 0.05	0.16 ± 0.08	0.17 ± 0.15
	Stroke amplitude (% diff)	0.19	0.05	0.00	0.05	0.19	0.14
	Dive duration (min)	--	--	--	3.61 ± 2.07	3.43 ± 1.44	2.92 ± 1.35
F22	N	76	59	6	168	82	38
	ODBA (25% dsf; ms^{-2})	1.93 ± 1.17	1.00 ± 1.68	0.58 ± 1.09	2.23 ± 1.58	2.41 ± 1.57	2.83 ± 1.62
	ODBA (50% dsf; ms^{-2})	1.30 ± 1.19	0.70 ± 1.52	0.48 ± 1.11	1.57 ± 1.49	1.68 ± 1.53	2.03 ± 1.57
	ODBA (70% dsf; ms^{-2})	1.00 ± 1.20	0.57 ± 1.44	0.43 ± 1.09	1.17 ± 1.46	1.26 ± 1.54	1.48 ± 1.63
	Stroke rate (Hz)	0.32 ± 0.04	0.32 ± 0.06	0.40 ± 0.04	0.46 ± 0.44	0.30 ± 0.31	0.25 ± 0.27
	Stroke amplitude (% diff)	0.67	0.33	0.00	0.47	0.20	0.00
	Dive duration (min)	--	--	--	2.60 ± 64	2.09 ± 0.88	1.83 ± 0.73

Deploy. ID	Energy expenditure proxy	Broad state			Foraging tactic		
		Forage	Search	Transit	Headstand	Benthic dig	Side swim
G22	N	120	152	18	214	126	30
	ODBA (25% dsf; ms^{-2})	1.69 ± 1.32	1.23 ± 1.65	0.68 ± 1.23	2.39 ± 1.97	2.29 ± 1.99	5.26 ± 1.46
	ODBA (50% dsf; ms^{-2})	1.08 ± 1.31	0.79 ± 1.57	0.50 ± 1.19	1.42 ± 1.84	1.48 ± 1.90	2.83 ± 1.48
	ODBA (70% dsf; ms^{-2})	0.84 ± 1.27	0.63 ± 1.52	0.41 ± 1.19	1.04 ± 1.73	1.12 ± 1.80	2.03 ± 1.48
	Stroke rate (Hz)	0.67 ± 0.32	0.20 ± 0.20	0.15 ± 0.14	0.62 ± 0.52	0.70 ± 0.41	0.48 ± 0.54
	Stroke amplitude (% diff)	0.00	-0.05	0.00	-0.05	0.21	-0.11
	Dive duration (min)	--	--	--	2.30 ± 1.06	2.84 ± 1.38	2.11 ± 1.33
H22	N	6	1	0	0	0	14
	ODBA (25% dsf; ms^{-2})	1.27 ± 1.17	1.00	--	--	--	1.53 ± 1.30
	ODBA (50% dsf; ms^{-2})	0.78 ± 1.16	0.68	--	--	--	0.99 ± 1.36
	ODBA (70% dsf; ms^{-2})	0.62 ± 1.19	0.51	--	--	--	0.84 ± 1.36
	Stroke rate (Hz)	0.11 ± 0.01	0.11	--	--	--	0.11 ± 0.06
	Stroke amplitude (% diff)	0.47	0.00	--	--	--	0.60
	Dive duration (min)	--	--	--	--	--	2.66 ± 0.51
I22	N	81	371	175	4	79	395
	ODBA (25% dsf; ms^{-2})	3.35 ± 1.31	3.09 ± 2.41	0.66 ± 1.21	5.58 ± 1.92	3.67 ± 1.43	6.23 ± 1.54
	ODBA (50% dsf; ms^{-2})	2.16 ± 1.32	1.99 ± 2.32	0.48 ± 1.16	3.46 ± 2.16	2.48 ± 1.40	3.60 ± 1.57
	ODBA (70% dsf; ms^{-2})	1.63 ± 1.31	1.38 ± 2.09	0.40 ± 1.15	2.41 ± 2.29	1.95 ± 1.36	2.18± 1.51
	Stroke rate (Hz)	0.17 ± 0.03	0.17 ± 0.06	0.12 ± 0.03	0.32 ± 0.39	0.18 ± 0.06	0.19 ± 0.11
	Stroke amplitude (% diff)	0.50	0.33	0.00	0.42	0.58	0.25
	Dive duration (min)	--	--	--	1.35	3.13 ± 1.11	1.05 ± 1.15
J22	N	67	70	5	50	71	51
	ODBA (25% dsf; ms^{-2})	1.73 ± 1.39	1.23 ± 1.55	0.56 ± 1.23	2.32 ± 1.92	2.44 ± 1.90	2.77 ± 1.65
	ODBA (50% dsf; ms^{-2})	1.13 ± 1.35	0.83 ± 1.46	0.46 ± 1.12	1.38 ± 1.75	1.54 ± 1.86	1.67 ± 1.58
	ODBA (70% dsf; ms^{-2})	0.88 ± 1.32	0.65 ± 1.41	0.40 ± 1.13	1.03 ± 1.63	1.15 ± 1.80	1.27 ± 1.51
	Stroke rate (Hz)	0.74 ± 0.43	0.34 ± 0.37	0.08 ± 0.10	1.28 ± 0.65	0.90 ± 0.66	0.71 ± 0.55
	Stroke amplitude (% diff)	-0.34	-0.24	0.00	-0.17	-0.24	-0.41
	Dive duration (min)	--	--	--	3.57 ± 1.37	2.63 ± 1.38	1.86 ± 0.79

Deployments with higher stroke rates also tended to have greater variability in their stroke rate for each broad state (**Table 3.4; Figure 3.2c**). Five of nine deployments had the highest stroke rate in the forage state, which agreed with the results from the stroke rate model for all deployments combined. Two of nine deployments appeared to have equivalent stroke rate for the forage and search states, while two deployments suggested there were no differences in stroke rate between broad states.

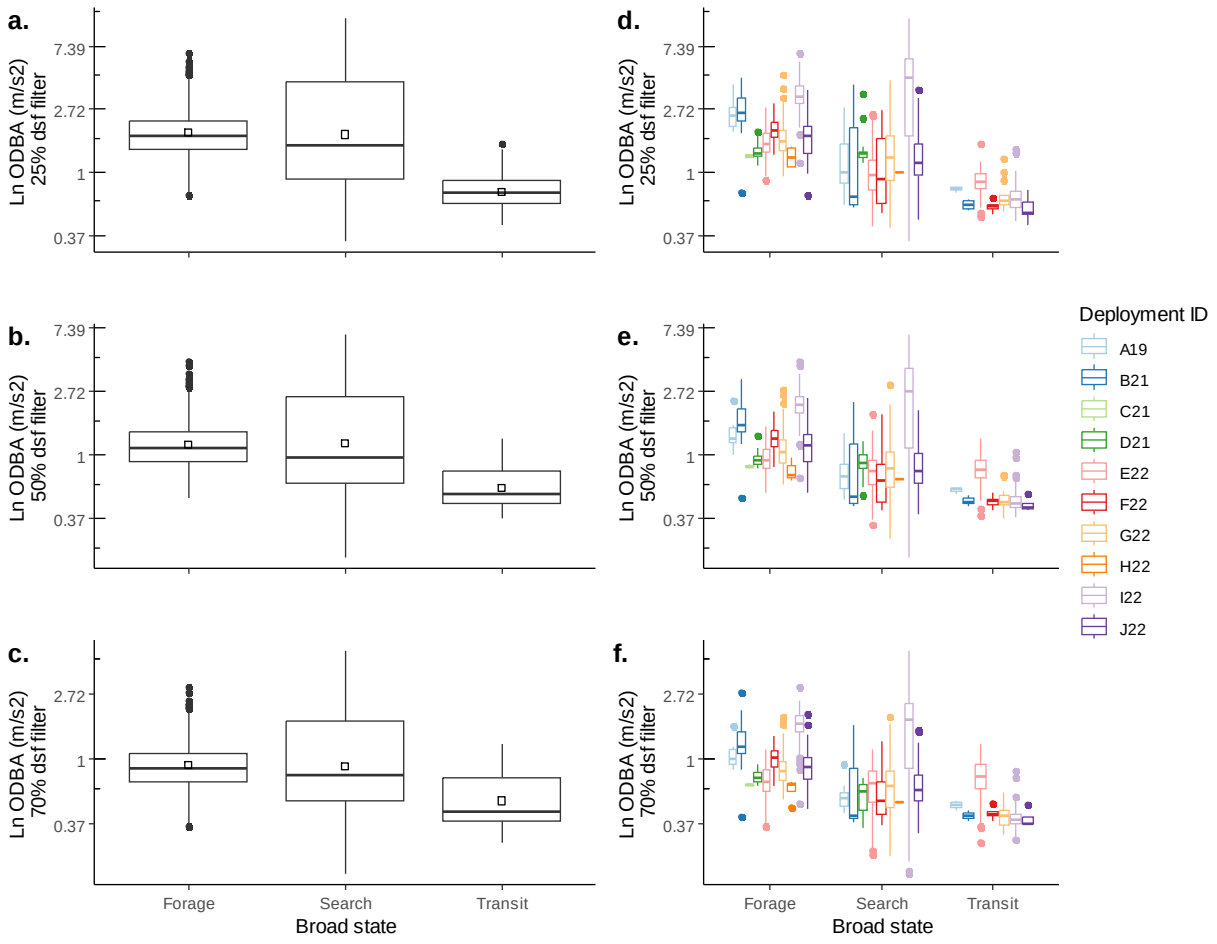

Figure 3.1. Overall Dynamic Body Acceleration (ODBA; ms-2) for three broad behavior states calculated from CATS tag deployments on ten PCFG grey whales (n = 1,856 dives), compared across all deployments (a,b,c) and across individual deployments (d,e,f) calculated using a filter of 25% dominant stroking frequency (dsf; a,d), 50% dsf (b,e), and 70% dsf (c, f). ODBA was standardized to account for differences in tag placement following the methods of (Isojunno and Miller, 2015)**. Open box represents the mean ODBA for each broad state. Note that in the model comparing ODBA between broad states, data were log-transformed. Each color represents a different deployment. Note that deployment C21 only includes the forage broad state while deployments D21 and H22 only include forage and search broad states.**

The results from the stroke amplitude analysis within each deployment suggested stroke amplitude was highest in the forage state, with this result supported by five of seven deployments with all broad states included (**Table 3.4; Figure 3.2d**). For the two deployments with only forage and search states identified, stroke amplitude was not significantly different between these broad states (**Table 3.4; Figure 3.2d**).

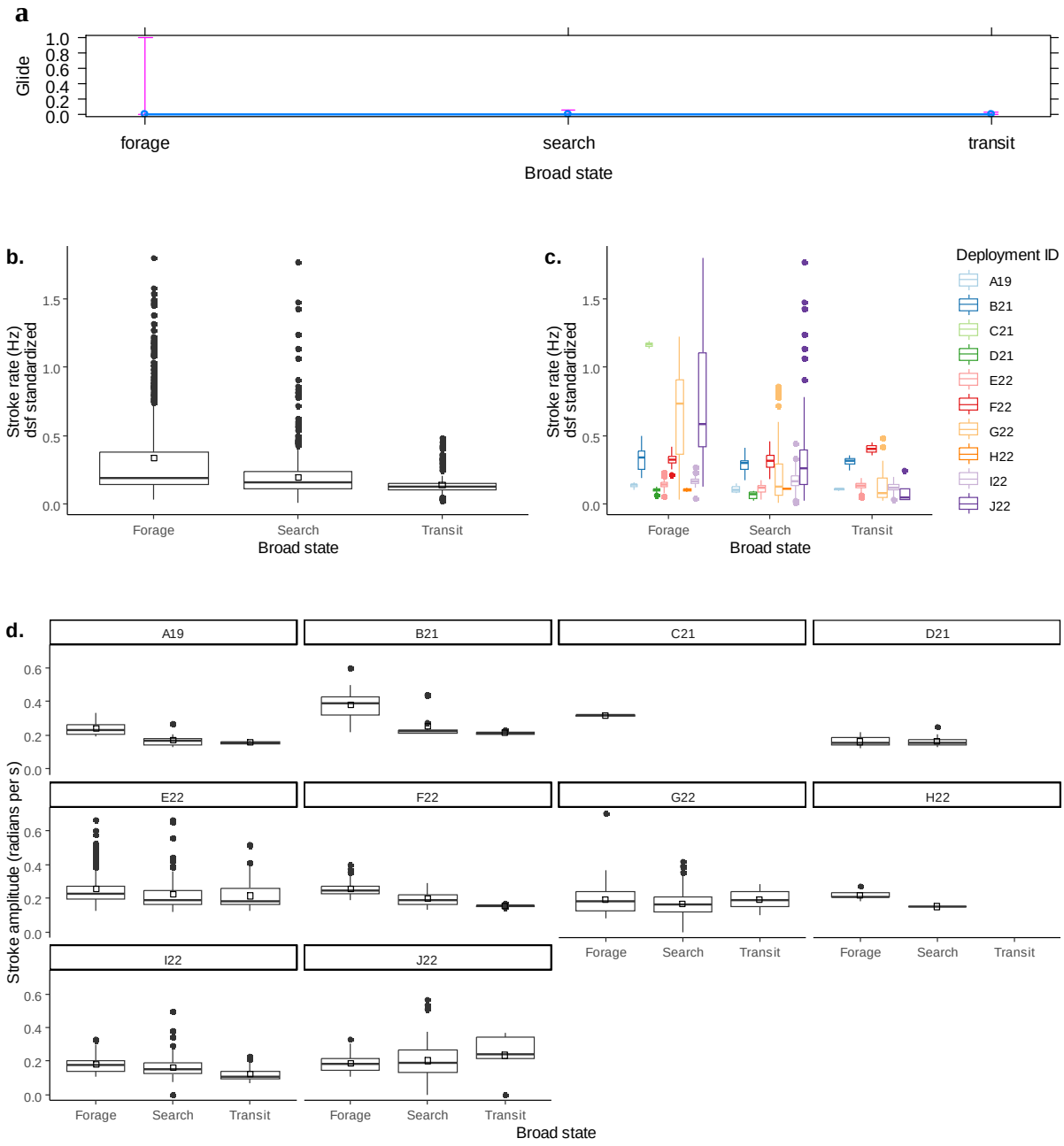

Figure 3.2. Broad state stroke metrics of predicted glide probability (a), stroke rate (Hz) compared between broad states (b) and across individual deployments (c) and stroke amplitude (radians per s; d) calculated from CATS tag deployments on ten PCFG grey whales (n = 1,856 dives). Predicted glide probability from the fitted generalized linear mixed model is shown on the probability scale by the blue dot with pink error bars representing the 95% confidence interval around the predicted effect (a). Stroke rate was standardized by the dominant stroking frequency (dsf) to account for the negative relationship between stroke rate and body length. The open box represents the mean stroke rate of each broad state (b). Note that in the model comparison, zero-values were excluded, and stroke rate was log-transformed. Each color represents a different deployment (c). Stroke amplitude values cannot be compared across deployments and the open box represents the mean stroke amplitude for that broad state within the deployment (d). Note that deployment

C21 only includes the forage broad state while deployments D21 and H22 only include forage and search broad states.

Foraging tactics

Likelihood ratio tests for nested model comparison showed that the models including foraging tactic perform significantly better than the models without the fixed factor for all energy expenditure proxies (**Table 3.2**).

The ODBA models indicate that foraging tactic significantly affected ODBA calculated with all filters. Pairwise comparisons of the mean ODBA indicate that ODBA calculated with all filters was significantly different between side swims and the other foraging tactics (**Table 3.3**), with higher ODBA for the side swim foraging tactic compared to headstands and benthic digs (**Figure 3.3a-c**). The mean ODBA values for side swims were approximately 1.5-1.8 times higher than headstands and 1.6-1.9 times higher than benthic digs (**Table 3.4**). Side swims had the highest calculated variation in ODBA, while headstands had the lowest calculated variation in ODBA (**Table 3.4**).

Exploration of ODBA patterns by individual deployment indicated that individual effects on ODBA values for foraging tactics varied by the filter used to calculate ODBA, with more consistency between patterns within deployments as the dsf filter was increased (**Table 3.4; Figure 3.3d-f**). A variety of within-deployment patterns existed for ODBA calculated with the 25% dsf and 50% dsf filters (**Figure 3.3d,e**)—the highest ODBA for side swims (two of eight deployments 25% dsf vs three of eight deployments 50% dsf), the highest ODBA for headstands (two of eight deployments 25% dsf and 50% dsf), no difference in ODBA between foraging tactics (one of eight deployments 25% dsf and 50% dsf), and ODBA differing between side swims and one other tactic (three of eight deployments 25% dsf vs two of eight deployments 50% dsf). ODBA calculated with the 70% dsf filter had the highest consistency in the patterns observed (**Figure 3.3f**), with the highest ODBA during side swims for three of eight deployments, the highest ODBA in headstands in one of eight deployments, and no difference in ODBA between foraging tactics for four of eight deployments.

Visual examination of the glide model outputs indicates that side swims had a higher glide probability than benthic digs and headstands, while the estimated glide probability was comparable between headstands and benthic digs (**Figure 3.4a**). The stroke rate model and pairwise comparisons indicated that headstands have a significantly different stroke rate

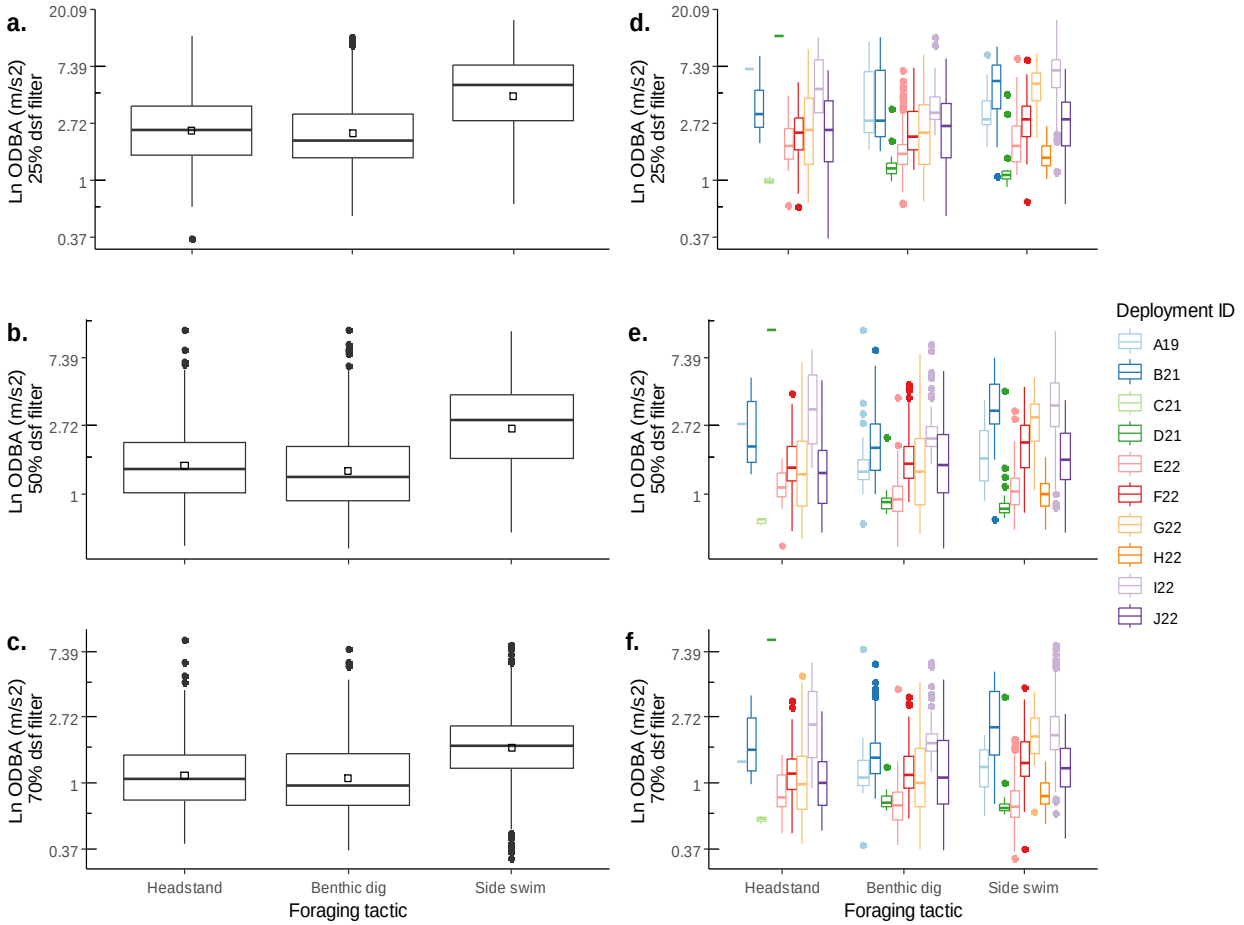

Figure 3.3. Foraging tactic Overall Dynamic Body Acceleration (ODBA; ms-2) calculated from CATS tag deployments on ten PCFG grey whales (n = 1,890 roll events), compared between foraging tactics (a,b,c) and across individual deployments (d,e,f) calculated using a filter of 25% dominant stroking frequency (dsf; a,d), 50% dsf (b,e), and 70% dsf (c,f). ODBA was standardized to account for differences in tag placement following the methods of (Isojunno and Miller, 2015)**. Open box represents the mean ODBA for each foraging tactic. Note that in the model comparing ODBA between foraging tactics, data were log-transformed. Each color represents a different deployment. Note that deployment C21 only has the headstand foraging tactic while deployment H22 only has the side swim foraging tactic.**

compared to the other foraging tactics (**Table 3.3**). The mean stroke rate of headstands was approximately 1.7 times that of benthic digs and 2.4 times that of side swims (**Table 3.4; Figure 3.4b**).

Exploratory analysis revealed high individual effects in the patterns of stroke rate across foraging tactics within deployments (**Table 3.4; Figure 3.4c**). Only two of eight deployments supported the overall pattern of headstands having higher stroke rates than benthic digs and side

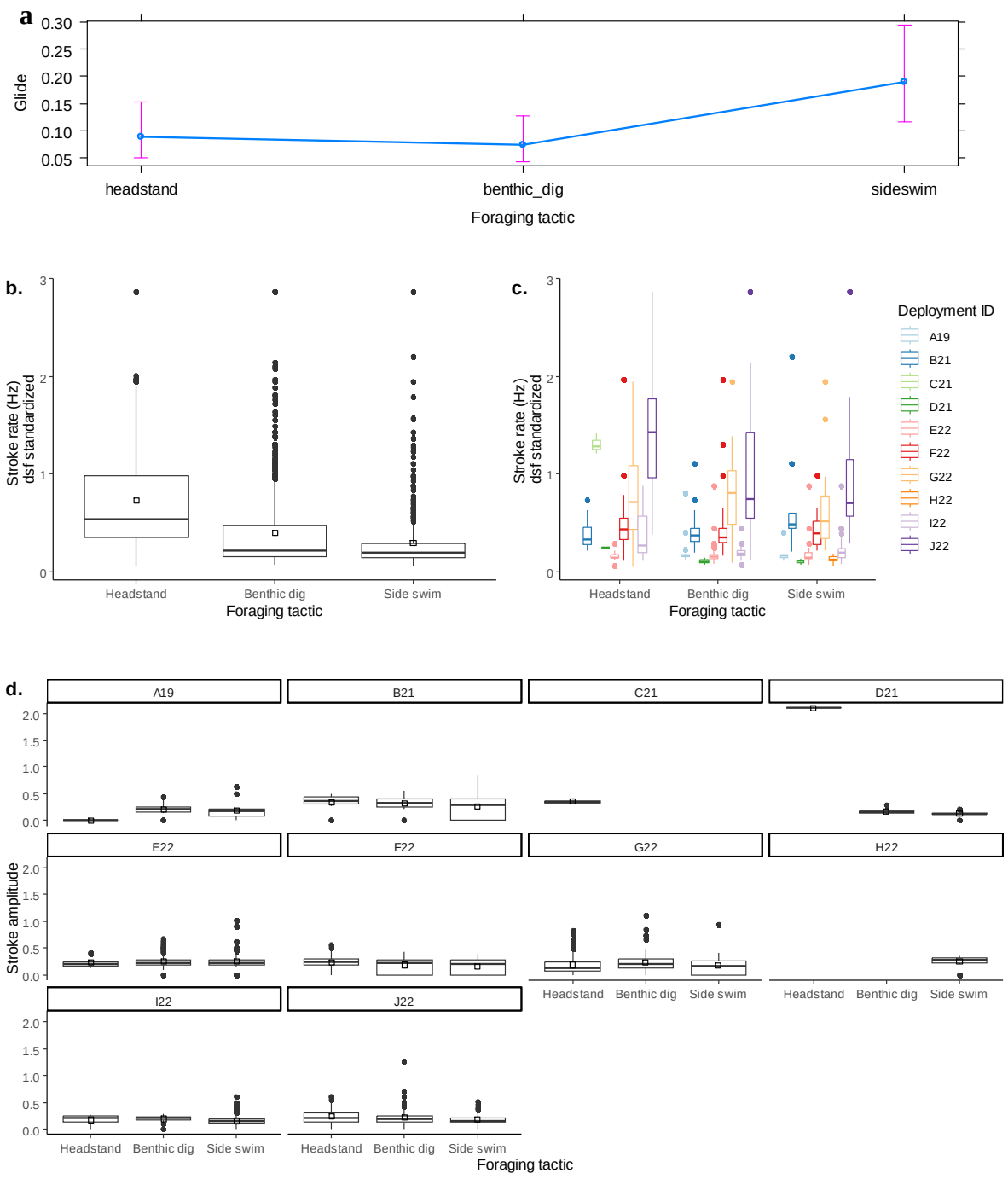

Figure 3.4. Foraging tactic stroke metrics of predicted glide probability (a), stroke rate (Hz) compared between foraging tactics (b) and across individual deployments (c) and stroke amplitude (radians per s; d) calculated from ten CATS tag deployments on PCFG grey whales (n = 1,890 roll events). Predicted glide probability from the fitted generalized linear mixed model is shown on the probability scale by the blue dot with pink error bars representing the 95% confidence interval around the predicted effect (a). Stroke rate was standardized by the dominant stroking frequency (dsf) to account for the negative relationship between stroke rate and body length. The open box represents the mean stroke rate of each foraging tactic (b). Note

that in the model comparison, zero-values were excluded, and stroke rate was log-transformed. Each color represents a different deployment (c). Stroke amplitude values cannot be compared across deployments and the open box represents the mean stroke amplitude for that foraging tactic within the deployment (d). Note that deployment C21 only has the headstand foraging tactic while deployment H22 only has the side swim foraging tactic.

swims. The deviation from the stroke rate model results in the remaining deployments suggests high individual differences in fluking patterns while performing foraging tactics.

Grey whale stroke rates for both benthic digs and side swims were higher than bowhead whale stroke rates during continuous ram filtration feeding, but similar (if not slightly lower) than lunge stroke rates for humpback and Bryde's whales (**Table 3.5**). Grey whale side swim stroke rates were most similar to the lunge stroke rates of blue whales, a species that is approximately twice as long as grey whales (**Table 3.5**). Headstands are the foraging tactic where the stroke rate is elevated compared to other tactics of other species with similar dsf, total length, and tactic duration, while the side swim tactic has stroke rates that are below average when compared to other species (**Figure 3.5**).

High individual differences in patterns of ODBA and stroke rate within deployments were also reflected in stroke amplitude. Comparison of stroke amplitude for each foraging tactic within deployments does not show a consistent pattern (**Table 3.4; Figure 3.4d**).

The dive duration model indicated a significant effect of foraging tactic and pairwise comparisons of the mean showed that the duration of dives dominated by side swims were significantly different from dives dominated by other foraging tactics (**Table 3.3**). Dives dominated by side swims were approximately half the duration of those dominated by other foraging tactics (**Table 3.4; Figure 3.6a**).

Exploratory analysis indicated that individual patterns of dive duration for dives dominated by different foraging tactics were consistent across deployments (**Table 3.4; Figure 3.6b**). Four of eight deployments supported the model result for all tags combined, suggesting that dives dominated by side swims were shortest. One of eight deployments suggested that dives dominated by side swims were only shorter than dives dominated by benthic digs and three of eight deployments suggested that the dominant tactic of a dive does not influence the dive duration.

Table 3.5. Comparison of foraging tactic stroke rates (Hz) between baleen whale species. Asterisks indicate species of similar length to grey whales. Dominant stroke frequency (dsf) and total length from each source was used to account for the negative relationship between stroke rate and body length (Gough et al., 2021; Sato et al., 2007)**. Tactic duration represents the interval over which stroke rate was calculated for each foraging tactic.**

Species	Foraging tactic	Stroke rate (Hz)	Dsf (Hz)	Total length (m)	Tactic duration (s)	Reference
Grey	Side swim	0.25 ± 0.29	0.16	10.79	26	This study
	Benthic dig	0.36 ± 0.40	0.16	11.22	71	This study
	Headstand	0.60 ± 0.55	0.16	11.23	20	This study
Bowhead*	Ram filtration	0.12 ± 0.08	0.07	9.60	--	(Simon et al., 2009)
Humpback*	Lunge	0.34 ± 0.011	0.24	11.06	10	(Gough et al., 2021)
	Lunge	0.45 ± 0.05	0.26	--	--	(Simon et al., 2012)
Bryde's*	Lunge	0.42 ± 0.010	0.24	12.04	10	(Gough et al., 2021)
	Lunge	~ 0.35	--	--	30	(Izadi et al., 2022)
Fin	Lunge	0.32 ± 0.018	0.24	18.90	10	(Gough et al., 2021)
	Lunge	0.27 ± 0.04	0.30	--	16	(Goldbogen et al., 2006)
Blue	Lunge	0.24 ± 0.004	0.18	22.41	10	(Gough et al., 2021)
	Lunge	~ 0.3	--	--	20	(Goldbogen et al., 2011)
Antarctic minke	Lunge	0.49 ± 0.008	0.38	7.30	10	(Gough et al., 2021)
Sei	Lunge	0.30	0.22	16.62	10	(Gough et al., 2021)

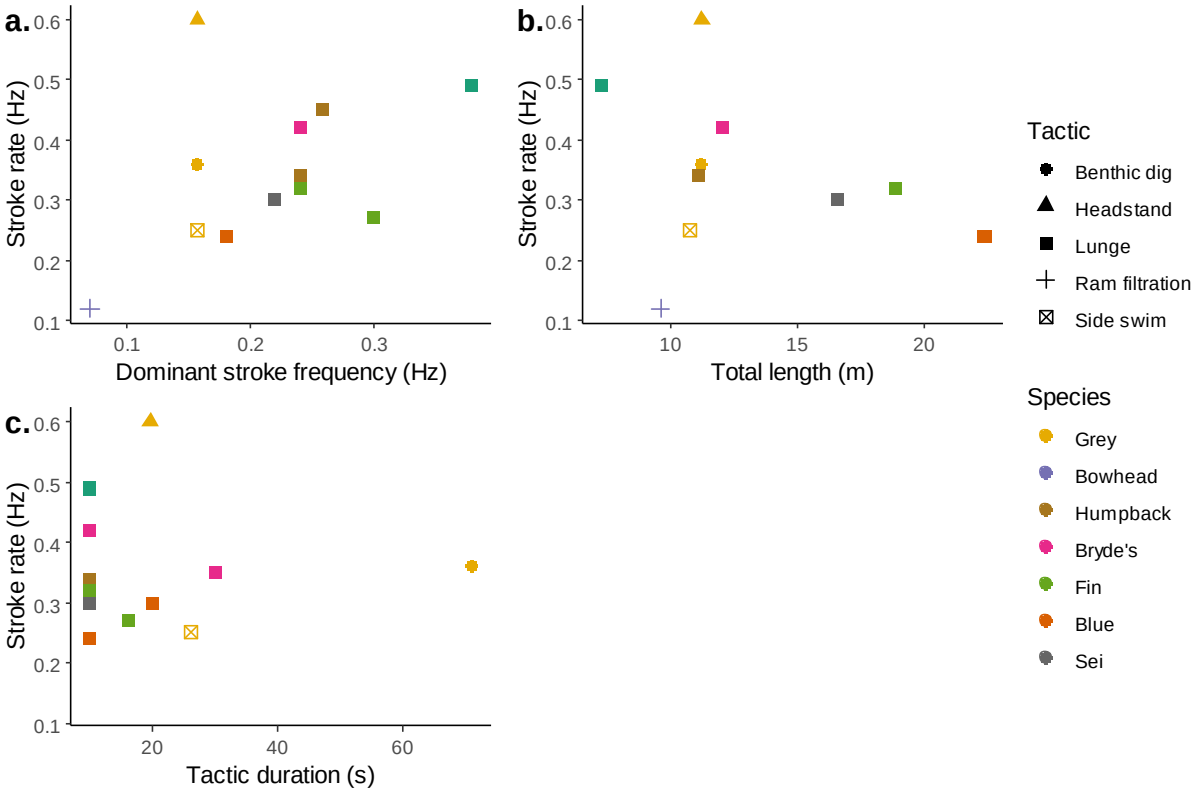

Figure 3.5. Comparison of stroke rate between baleen whale species performing different foraging tactics accounting for dominant stroke frequency (a), total length (b), and foraging tactic duration (c) using published data and the results from this study.

Discussion

Biologging-derived proxies of energy expenditure were used for the first time to estimate the relative energetic cost of different foraging behaviours in grey whales. We conclude that stroke rate was the best proxy for inferring relative energy expenditure in PCFG grey whales. Stroke rates were higher for the forage state compared to search or transit and the headstand foraging tactic compared to benthic digs and side swims. The inferred higher energetic cost of forage and headstand behaviours indicate a high susceptibility of PCFG grey whales to changes in prey quality and quantity that may reduce the net energetic gain from performing high energy foraging tactics.

We calculated multiple proxies of energy expenditure from biologging data and evaluated these proxies in similar ways, creating a unique opportunity to comment on the most effective energy expenditure proxy. At the broad state scale, ODBA suggested that forage (25% and 70% dsf filters) and search (50% dsf filter) are the most energetically costly states, and that transit is

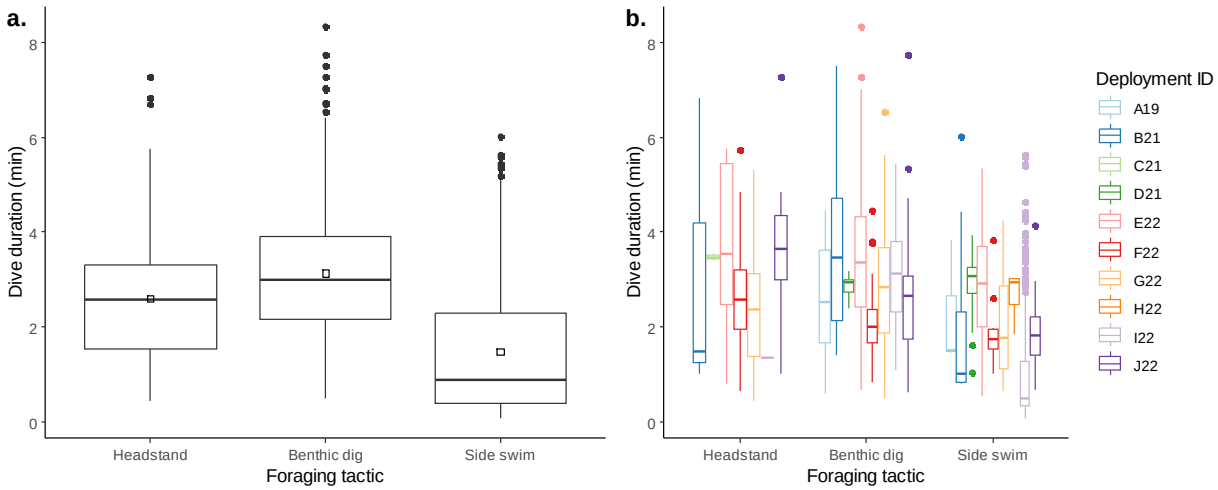

Figure 3.6. Dive duration (min) of dives with different dominant foraging tactics compared across (a) and within deployments (b) calculated from ten CATS tag deployments on PCFG grey whales. Dominant forging tactics were defined as the tactic that accounted for at least half of the time spent rolled during the dive. The open box represents the mean dive duration for each foraging tactic. Note that in the model comparison, dive duration was log-transformed. Each color represents a different deployment. Note that deployment A19 does not have any dives dominated by the headstand foraging tactic, deployment C21 only has dives dominated by the headstand foraging tactic, and deployment H22 only has dives dominated by the side swim foraging tactic.

the least (all dsf filters), while stroke rate and amplitude both suggested that foraging is the most energetically costly state. At the foraging tactic scale, ODBA and dive duration suggested side swims were the most energetically expensive foraging tactic, while the glide probability suggested sides swims were the least expensive foraging tactic. Stroke rate suggested headstands were the most energetically expensive tactic and stroke amplitude was inconclusive, therefore suggesting stroke amplitude is not a useful proxy for estimating energy expenditure of foraging tactics in grey whales.

The differences in the foraging tactic determined to be most energetically expensive by each energy expenditure proxy is likely driven by the signals captured by each proxy. For instance, stroke rate is an isolation of the fluking signal while ODBA captures body movement in all three axes. Therefore, ODBA captures the energy from each fluke beat in addition to any other acceleration signal detected by the sensor and is likely to be more sensitive to other movements in addition to fluking, suggesting that these metrics can hint at the differing mechanics of side swims and headstands. Side swims, in addition to fluking, have jaw snapping and pectoral fin sculling (**Movie S1**; L. Torres *unpublish data*) that likely contribute to the

elevated body movement and higher ODBA values of this foraging tactic. Headstands, on the other hand, likely require more fluking to address buoyancy control and hold the individual's extremely pitched position in the water column (see Chapter 2) than to propel the body through the water column, leading to a higher stroke rate than side swims.

Based on our results, we conclude that stroke rate is the best proxy and should be used in future analyses of energy expenditure in grey whales. Stroke rate was easiest to calculate and compare between individual deployments and with studies of other baleen whales. Stroke rate also did not require additional computational steps (e.g., complimentary filtering to calculate ODBA) that introduce additional sources of error and more individual effects. Stroke rate also does not incorporate any noise in the signal that is due to contact with the benthos while feeding that is likely to occur with ODBA, and can include surface behaviours as this proxy does not need to account for the tag breaking the surface. Unlike the dive duration proxy, stroke rate does not depend on the targeted prey (Stelle et al., 2008 citing Guerro, 1989), prey patch quality (Charnov, 1976; MacArthur and Pianka, 1966), dive depth and other confounding factors that are incorporated with dive duration. Stroke amplitude cannot be compared across deployments, and the lack of a consistent pattern across individuals at the foraging tactic scale suggests that stroke amplitude is not a useful proxy of energy expenditure. The limitations of the other proxies further support stroke rate as being the most useful proxy to estimate energy expenditure.

Overall, the biologging proxies of energetic expenditure find transit to be the least costly state, which is consistent with focal follow studies that use respiration metrics as a proxy. Longer blow intervals (i.e., the time submerged between breaths during the surface period following a dive), which indicate a lower metabolic cost (Fahlman et al., 2017), were found during travel and non-foraging behaviours compared to foraging behaviour (including searching) for grey whales (Mallonee, 1991; Stelle et al., 2008; Wursig et al., 1986). The respiration metrics used in these studies could not distinguish a difference in energetic cost between forage and search states, although this is likely related to the inability to effectively define forage and search as separate behaviours (Mallonee, 1991; Wursig et al., 1986).

The stroke rate of side swims and benthic digs was compared to the stroke rate of other baleen whale foraging behaviours as this proxy is comparable across studies and to species of similar size (Gough et al., 2021; Sato et al., 2007). Side swims represent the foraging tactic that

is most similar to the continuous ram filtration feeding and lunges that target pelagic zooplankton prey or small schooling fishes through forward movement. While benthic digs are not as comparable to these pelagic strategies, this tactic represents the traditional feeding tactic of grey whales (Nerini, 1984), and the fluke is assumed to have full range of motion given the body orientation of the whale (see Chapter 2), thus warranting comparison of energetic costs of benthic digs with published values for other baleen whale foraging behaviours. The higher stroke rate of side swims and benthic digs is two to three times higher compared to the ram filtration stroke rate (Simon et al., 2009), suggesting a higher energetic cost of these grey whale foraging tactics compared to the typical feeding behaviour of balaenids (e.g., bowheads and right whales). The side swim stroke rate was about 25-44% lower than the lunge stroke rate of similarly sized rorquals (e.g., humpback and Bryde's whales) while benthic digs had a similar stroke rate, ranging from 6% higher to 20% lower than lunges. Overall, these results suggest that the grey whale side swims are less energetically costly than lunges, but benthic digs may be more similar in energetic cost to lunges. The similar energetic cost between benthic digs and lunges may stem from a similar forward momentum needed to plow through the sediment in benthic digs as for the acceleration needed for a successful lunge.

An interesting finding is that headstands seem to be at the extreme of energetic cost, and is a foraging tactic that is unique to the PCFG foraging grounds (Torres et al., 2018). It is not clear why PCFG grey whales utilize a different foraging ground than ENP whales. Caloric density of prey is similar or higher in the PCFG range compared to the Arctic (Hildebrand et al., 2021), suggesting that either prey patches are denser and more numerous in the PCFG range compared to the Arctic, or capture efficiencies are higher in headstands compared to other foraging tactics to compensate for the increased energetic cost of the headstands. It is also possible that the PCFG grey whales are forced to utilize headstands to exploit the epi-benthic prey in a foraging habitat composed of a reef mosaic. In other words, the transition to headstands with increased length (Bird et al., *in prep*) is due to an inability of longer whales to maneuver around rocky reefs. As such, they must increasingly rely on the stationary headstand tactic to exploit rocky reefs, despite the elevated relative energetic cost. More data is needed on the prey density in both foraging grounds and capture efficiency of each foraging tactic for the drivers of PCFG foraging ground utilization to be fully understood.

The skinnier and shorter morphology of PCFG grey whales compared to the ENP (Bierlich et al., 2023; Torres et al., 2022) are also interesting to examine in the context of these results as it is unclear if these morphological differences indicate that the PCFG represents an ecological trap or an ecological opportunity. In other words, do the higher energetic cost of side swims and headstands potentially indicate these morphological differences are due to nutritional stress (i.e., an ecological trap), or does the morphology of PCFG grey whales allow this group to exploit a different foraging ground through the use of unique, adapted foraging tactics (i.e., an ecological opportunity). The elevated cost of side swims and headstands could indicate that overall grey whales are better suited for benthic foraging rather than the headstand and side swim foraging tactics used by the PCFG (Woodward et al., 2006), supporting the ecological trap theory. Yet, the site-fidelity and maternal recruitment to the PCFG range by whales that regularly employ these feeding tactics (Bird et al. *in prep*) indicates the viability of these foraging tactics and thus supports the ecological opportunity theory. A better understanding of prey density and capture efficiency for each foraging tactic is needed to be able to fully address these hypotheses.

Body length and body condition are thought to be important morphological variables that affect individual behaviour. However, the standardization method for the energy expenditure proxies we used to account for tag positioning (ODBA) and body size (stroke rate) removes some of the morphological impacts on the energetic cost of different behaviours (**Figure H1a,b**). The small sample size of deployments further limits the ability to detect differences in association with morphology. Therefore, it is possible that a larger sample size of deployments is needed to account for the morphological differences and high individual variation in how individuals perform behaviours that in turn impact the estimated energetic cost. This is especially true for the PCFG where energetics may provide a mechanism for explaining the observed specialization between whales of different lengths (Bird et al. *in prep*).

Future directions

The energy expenditure proxies calculated in this study must be linked to oxygen consumption to be infer metabolic rate and hence determine if the differences in the proxies between behaviours truly impact the energetic cost. Future aims should work to link these biologging-derived energy expenditure proxies to oxygen consumption to estimate a field metabolic rate for PCFG grey whales. Recent work refining estimates of tidal volume from free-

range grey whales will benefit from the fine-scale behavioural energetics estimates (Sumich et al., *in revision*). Additionally, this study only obtained these biologging proxies from PCFG grey whales, based on the assumption that the benthic dig included in the biologging data is in fact representative of the traditional benthic dig predominantly used by ENP and WNP grey whales. Therefore, future efforts should focus on deploying biologging tags on these populations to compare energy expenditure proxies across the grey whale foraging groups.

Other drivers of behavioural energetics, such as morphology, foraging habitat, and targeted prey, anthropogenic disturbance, were not evaluated by these biologging proxies. Therefore, future studies should include a larger sample size to tease apart the morphological impacts on energetic cost of behaviours that was not feasible in this study. Additionally, prey type and density should be included in models estimating the differences in energetic cost of behaviours and capture efficiency of different foraging tactics should be investigated to determine if this is driving the use of higher energy tactics in the PCFG foraging grounds. Biologging-derived energy expenditure proxies estimated in this study can be used in future work constructing energy landscapes, or the energetic cost of moving through variable habitat (Wilson et al., 2012), for PCFG grey whales when linking prey and habitat to the cost of foraging, as this can provide information about protecting critical foraging habitat.

A criticism of biologging studies is that the data are rarely connected to fitness impacts on the population (Crossin et al., 2014). Therefore, future work should link the biologging-derived energetic cost of behaviours to the fitness metrics, such as body condition and reproductive success, to address questions of which foraging tactics related to the highest foraging success.

Conclusions

For the first time, biologging-derived energy expenditure proxies were used to estimate the relative energetic cost of grey whale behaviour states and foraging tactics. Foraging was more energetically expensive than transiting or searching, and headstand was a more energetically costly foraging tactic than benthic dig and side swim (based on our recommended energy expenditure proxy of stroke rate). Despite the high stroke rate of headstands, this remains a prominent foraging tactic observed in the PCFG foraging grounds, indicating that despite the elevated stroke rate, this foraging tactic likely yields a higher capture efficiency of prey within

the PCFG foraging range than other tactics assessed. This theory is supported by the ontogenetic shift observed in PCFG whales transitioning from higher probability of side swims to headstands with length/age (Bird et al., *in prep*). If the elevated stroke rate in headstands is used to overcome buoyancy, then older whales likely develop a mechanism to further counteract buoyancy and can make headstands even more efficient.

Overall, our study contributes to a foundational understanding of foraging energetics in a species of conservation concern (COSEWIC, 2017). Estimates of foraging energetics provides fundamental groundwork to understand the mechanisms that underlie behavioural choices. These relative estimates of energy expenditure also provide a means to estimate fitness impacts on the PCFG grey whales which are showing signs of nutritional stress (Akmajian et al., 2021; Bierlich et al., 2023; Torres et al., 2022) and allow for this unique group to be included in grey whale bioenergetics models to better understand the energy requirements for this population.

Chapter 4: General discussion

Summary of findings

This study is the first to quantitatively define foraging signals (Chapter 2) and estimate the relative energetic cost of behaviours (Chapter 3) in grey whales from biologging data. At the dive scale, I was able to define an intermediate search state in addition to forage and transit states using turn angle, dive duration, dive tortuosity, and presence of roll events in the dive. I found that PCFG grey whales spent a higher proportion of their time in forage and search states compared to transit, which was expected because the data came from whales on their foraging grounds, indicating that transit should be limited to moving between areas of intensive feeding. Headstands, benthic digs, and side swims were defined using body position variables (e.g., pitch, roll, and water depth to body length ratio) and occurred in relatively equal proportions for all deployments combined, although there was high individual preference across deployments. Stroke rate was found to be the best biologging-derived proxy of energy expenditure to use moving forward, as it was the easiest to calculate, the most comparable across deployments and studies, and had fewer limitations than the other proxies used in Chapter 3. Foraging and headstanding were found to be the most energetically costly behaviours at the broad state and foraging tactic scale according to stroke rate.

Strengths and weaknesses

The quantitative behavioural definitions I derived from the biologging data benefited from the long-term field program established with the PCFG grey whales. Previous land-based and drone focal follow studies greatly informed the summary metrics used to detect foraging in the biologging data. The turn angle and dive tortuosity signals used to differentiate between broad states were similar to those in the residence in space and time index used in previous focal follow studies (Hildebrand et al., 2022; Sullivan and Torres, 2018). However, the roll presence metric extended beyond focal follows, and was used as a proxy for foraging tactics performed at depth that could not be detected with the depth limitation imposed on the focal follow methods.

Drone ethograms suggested that the pitch and roll of the animal were going to be helpful for defining foraging tactics. However, the CART model constructed using the biologging data did not rely as heavily on roll. Instead, the biologging data used the depth to body length ratio, which captured how the water column depth limited the foraging tactics able to be used, which is

not possible to quantify from drone focal follows. The complementary data available for this population from drone focal follows also allowed for validation of the behavioural classification using the biologging data.

An additional strength of using biologging data is that it was not limited by the visibility constraints of focal follow methods. Biologging data were able to quantitatively describe benthic digs, which were not included in the drone ethogram as this foraging tactic occurs at depth where the drone cannot detect it (Torres et al., 2018). The biologging tags were also able to record night time grey whale behaviour for the first time.

During night, I found the proportion of searching and side swims increased, foraging tactics were shallower and more left-rolled, and the amount of surface time slightly increased. These results suggest that grey whales use visual cues to detect their prey, leading to more exploratory search behaviour at night and higher use of side swims at night. The shallower and more left-rolled foraging tactics are interesting given that grey whales are known to be benthic foragers with significant right-side lateralization (Woodward and Winn, 2006). This suggests that either PCFG grey whales forage in shallower habitats at night or become more pelagic feeders at night. Cetaceans have been documented to use their right eye to track prey (Jaakkola et al., 2021) and a quasi-diel vertical migration has been described for mysids (Alldredge and King, 1980; Mauchline, 1980), supporting the idea that PCFG grey whales forage more pelagically at night and roll left to track prey above them.

Another strength of my study is the calculation of multiple energy expenditure proxies defined from the biologging data that were all used in similar ways to compare the relative energetic cost between foraging behaviours. Very few studies have included multiple accelerometry-derived proxies of energetic cost (i.e., ODBA, stroke rate, stroke amplitude, and duration of dives). Comparing these different proxies gave me a unique opportunity to comment on the utility of each metric.

Based on the variability of the within deployment comparisons of ODBA calculated with different complementary filters (as well as the need to remove surface influence and the sensitivity of ODBA to noise from interactions with the benthos), I concluded that ODBA is not an ideal energy expenditure proxy for grey whales. Similarly, raw values of stroke amplitude cannot be compared across deployments and the lack of consistent patterns within deployments

suggests stroke amplitude is not an effective proxy. Duration of dives with different foraging tactics performed should also not be used to estimate energetic cost as there are many confounding factors (e.g., prey density and type, habitat, etc.) that influence dive duration. Ultimately, stroke rate was found to be the best proxy of energy expenditure because it was easiest to calculate and compare not only within deployments but across studies and different species.

The biggest caveat to keep in mind when interpreting the results from my study is the small numbers of deployments (n = 10). Even though my unit of analysis was hundreds to thousands of roll events and dives within each deployment, and my analysis accounted for the repeated measurement on individuals, it is important to keep in mind that only 10 individual grey whales were included in this study from limited parts of the PCFG range and most individuals were from the same demographic unit. The patterns of high individual variability in behaviour choice (Chapter 2) and high variation in energy expenditure proxies (Chapter 3) suggest that larger sample sizes are needed in future work.

A final caveat concerns the assumption that the benthic dig captured in the biologging data from PCFG grey whale deployments were the same as the benthic dig performed in the Arctic. However, it is unclear if the benthic dig performed in the PCFG range is truly used to forage on invertebrates buried in the benthos or if this tactic is used to target benthic swarms of mysids hovering above the sediment. For this assumption to be validated, high-resolution accelerometry tags need to be deployed on ENP and WNP grey whales foraging on Arctic feeding grounds.

Future directions

The quantitative definitions of foraging behaviour I established, and the estimates of relative energetic cost of behaviours I calculated lay the groundwork for future biologging studies of grey whales to fulfill the motivation of this project for including PCFG grey whales in existing grey whale bioenergetics models (Agbayani, 2022; Villegas-Amtmann et al., 2017, 2015). Future work should focus on linking the habitat and prey data with the behavioural and energetics data to determine how foraging behaviour changes with different prey densities and types as well as with habitat. Additionally, by linking foraging behaviour with prey, an estimate of net energy gain can be obtained, and the capture efficiencies of different tactics can be

evaluated. These net energy gain and capture efficiency parameters will be important to include in future PCFG grey whale bioenergetic models.

Another parameter necessary for a PCFG grey whale bioenergetics is the field metabolic rate. To achieve this from the data collected for my study, the energy expenditure proxies calculated need to be linked with oxygen consumption. Therefore, future work should focus on the relationship between stroke rate, the recommended energy expenditure proxy from this study, with measures of oxygen consumption. This is likely to come from respiration rates, which can become more accurate with better estimates of tidal volume from watching video footage of blowholes during exhalations and inhalations (Sumich et al., *in revision*). This footage of blowholes can come from tag videos or drone focal follows.

A major criticism of biologging studies is the lack of connection of the data to fitness impacts on the population (Crossin et al., 2014). The well-studied nature of the PCFG grey whales lends themselves nicely to rectifying this as long-term data and high resighting of individuals in this population allow for extensive knowledge on reproductive histories and changes in body condition. Therefore, pairing this data set with biologging data from individuals would allow for individual behavioural choices to be linked with their fitness and be explained by the behavioural energetics.

Conclusions

This is the first study to quantitatively define foraging behaviour in PCFG grey whales, and estimate the relative energetic cost of foraging using high-resolution accelerometry data from biologging tags. It establishes the effectiveness of biologging data in behavioural ecology and lays the groundwork to further estimate parameters needed for a PCFG grey whale bioenergetics model. The results of my research can be used to construct an energy landscape (Wilson et al., 2012) to identify critical foraging habitats for PCFG grey whales, and ultimately help to mitigate the impacts of the various conservation threats facing this species.

References

Agbayani, S. V. (2022). *Energy requirements of grey whales* (pp.111). [Unpublished Master's thesis]. University of British Columbia.

Akmajian, A. M., Scordino, J. J., Gearin, P. J., & Gosho, M. (2021). Body condition of gray whales (*Eschrichtius robustus*) feeding on the Pacific Coast reflects local and basin-wide environmental drivers and biological parameters. *Journal of Cetacean Research and Management*, *22*(232), 87–110.

Alldredge, A. L., & King, J. M. (1980). Effects of moonlight on the vertical migration patterns of demersal zooplankton. *Journal of Experimental Marine Biology and Ecology*, *44*(2), 133–156. https://doi.org/10.1016/0022-0981(80)90150-1

Allen, A. S., Read, A. J., Shorter, K. A., Gabaldon, J., Blawas, A. M., Rocho-Levine, J., & Fahlman, A. (2022). Dynamic body acceleration as a proxy to predict the cost of locomotion in bottlenose dolphins. *Journal of Experimental Biology*, *225*(4). https://doi.org/10.1242/jeb.243121

Amo, L., López, P., & Martín, J. (2007). Habitat deterioration affects body condition of lizards: A behavioral approach with *Iberolacerta cyreni* lizards inhabiting ski resorts. *Biological Conservation*, *135*(1), 77–85. https://doi.org/10.1016/j.biocon.2006.09.020

Barraquand, F., & Benhamou, S. (2008). Animal movements in heterogeneous landscapes: Identifying profitable places and homogeneous movement bouts. *Ecology*, *89*(12), 3336–3348. https://doi.org/10.1890/08-0162.1

Beale, C. M., & Monaghan, P. (2004). Behavioural responses to human disturbance: A matter of choice? *Animal Behaviour*, *68*(5), 1065–1069. https://doi.org/10.1016/j.anbehav.2004.07.002

Bierlich, K. C., Hewitt, J., Bird, C. N., Schick, R. S., Friedlaender, A., Torres, L. G., … Johnston, D. W. (2021). Comparing uncertainty associated with 1-, 2-, and 3D aerial

photogrammetry-based body condition measurements of baleen whales. *Frontiers in Marine Science*, *8*, 1–16. https://doi.org/10.3389/fmars.2021.749943

Bierlich, K. C., Kane, A., Hildebrand, L., Hildebrand, I., Bird, C. N., Fernandez Ajo, A., … Torres, L. G. (2023). Downsized: Gray whales using an alternative foraging ground have smaller bodies. *Biology Letters*, *19*. https://doi.org/https://doi.org/10.1098/rsbl.2023.0043

Bird, C. N., Pirotta, E., New, L., Bierlich, K. C., Donnelly, M., Hildebrand, L., … Torres, L. G. (*in prep*). Growing into it: Evidence of an ontogenetic shift in gray whale use of foraging tactics. *Functional Ecology*.

Brodie, S., Taylor, M. D., Smith, J. A., Suthers, I. M., Gray, C. A., & Payne, N. L. (2016). Improving consumption rate estimates by incorporating wild activity into a bioenergetics model. *Ecology and Evolution*, *6*(8), 2262–2274. https://doi.org/10.1002/ece3.2027

Brown, D. D., Kays, R., Wikelski, M., Wilson, R., & Klimley, A. P. (2013). Observing the unwatchable through acceleration logging of animal behavior. *Animal Biotelemetry*, *1*(1). https://doi.org/10.1186/2050-3385-1-20

Burnett, J. D., Lemos, L., Barlow, D., Wing, M. G., Chandler, T., & Torres, L. G. (2018). Estimating morphometric attributes of baleen whales with photogrammetry from small UASs: A case study with blue and gray whales. *Marine Mammal Science*, *35*(1), 108–139. https://doi.org/10.1111/mms.12527

Butler, P. J., Green, J. A., Boyd, I. L., & Speakman, J. R. (2004). Measuring metabolic rate in the field: The pros and cons of the doubly labelled water and heart rate methods. *Functional Ecology*, *18*(2), 168–183. https://doi.org/10.1111/j.0269-8463.2004.00821.x

Cade, D. E., Friedlaender, A. S., Calambokidis, J., & Goldbogen, J. A. (2016). Kinematic diversity in rorqual whale feeding mechanisms. *Current Biology*, *26*(19), 2617–2624. https://doi.org/10.1016/j.cub.2016.07.037

Cade, D. E., Gough, W. T., Czapanskiy, M. F., Fahlbusch, J. A., Kahane-Rapport, S. R., Linsky, J. M. J., … Goldbogen, J. A. (2021). Tools for integrating inertial sensor data with video

bio-loggers, including estimation of animal orientation, motion, and position. *Animal Biotelemetry*, *9*. https://doi.org/10.1186/s40317-021-00256-w

Cade, D. E., Levenson, J. J., Cooper, R., De La Parra, R., Webb, D. H., & Dove, A. D. M. (2020). Whale sharks increase swimming effort while filter feeding, but appear to maintain high foraging efficiencies. *Journal of Experimental Biology*, *223*. https://doi.org/10.1242/jeb.224402

Calambokidis, J., & Perez, A. (2017). Sightings and follow-up of mothers and calves in the PCFG and implications for internal recruitment. In *Paper SC/A17/GW/04 Presented to International Whaling Commission Scientific Committee*.

Castellini, M. (2012). Life under water: Physiological adaptations to diving and living at sea. *Comprehensive Physiology*, *2*(3), 1889–1919. https://doi.org/10.1002/cphy.c110013

Charnov, E. (1976). Optimal foraging, the marginal value theorem. *Theoretical Population Biology*, *9*, 739–752.

Christiansen, F., Rodríguez-González, F., Martínez-Aguilar, S., Urbán, J., Swartz, S., Warick, H., … Bejder, L. (2021). Poor body condition associated with an unusual mortality event in gray whales. *Marine Ecology Progress Series*, *658*, 237–252. https://doi.org/10.3354/meps13585

Constantine, R., Johnson, M., Riekkola, L., Jervis, S., Kozmian-Ledward, L., Dennis, T., … Aguilar de Soto, N. (2015). Mitigation of vessel-strike mortality of endangered Bryde's whales in the Hauraki Gulf, New Zealand. *Biological Conservation*, *186*, 149–157. https://doi.org/10.1016/j.biocon.2015.03.008

Cooke, J. G., Sychenko, O., Burdin, A., Weller, D., Bradford, A., Lang, A., & Brownell, R. L. (2019). Population assessment update for Sakhalin gray whales. In *Western Gray Whale Advisory Panel, 20th Panel*.

COSEWIC. (2017). *COSEWIC assessment and status report on the Grey Whale* Eschrichtius robustus, *Northern Pacific Migratory population, Pacific Coast Feeding Group population*

and the Western Pacific population, in Canada. Retrieved from www.sararegistry.gc.ca/status/status_e.cfm

Crossin, G. T., Cooke, S. J., Goldbogen, J. A., & Phillips, R. A. (2014). Tracking fitness in marine vertebrates: Current knowledge and opportunities for future research. *Marine Ecology Progress Series*, *496*, 1–17. https://doi.org/10.3354/meps10691

Czapanskiy, M. (2022). *catsr: Tools for using CATS PRH files in R*.

Darling, J. D., Keogh, K. E., & Steeves, T. E. (1998). Gray whale (*Eschrichtius robustus*) habitat utilization and prey species off Vancouver Island, B.C. *Marine Mammal Science*, *14*(4), 692–720. https://doi.org/10.1111/j.1748-7692.1998.tb00757.x

DeRuiter, S. L., Johnson, M., Sweeney, D., McNamara-Oh, Y. J., Fynewever, S., Tejevbo, (Oghenkevwe) Racheal, & Marques, T. (2022). *tagtools: Tools for Working with Data from High-Resolution Biologging Tags*. Retrieved from https://github.com/animaltags/tagtools_r

DeRuiter, S. L., Langrock, R., Skirbutas, T., Goldbogen, J. A., Calambokidis, J., Friedlaender, A. S., & Southall, B. L. (2017). A multivariate mixed Hidden Markov Model for blue whale behaviour and responses to sound exposure. *Annals of Applied Statistics*, *11*(1), 362–392. https://doi.org/10.1214/16-AOAS1008

Dill, L. M. (2017). Behavioural ecology and marine conservation: A bridge over troubled water? *ICES Journal of Marine Science*, *74*(6), 1514–1521. https://doi.org/10.1093/icesjms/fsx034

Duffus, D. A. (1996). The recreational use of grey whales in southern Clayoquot Sound, Canada. *Applied Geography*, *16*(3), 179–190. https://doi.org/10.1016/0143-6228(96)00002-1

Eguchi, T., Lang, A. R., & Weller, D. W. (2022). *Abundance and migratory phenology of eastern North Pacific gray whales 2021/2022*. Retrieved from https://doi.org/10.25923/x88y-8p07

Fahlman, A., Hoop, J. Van Der, Moore, M. J., Levine, G., & Brodsky, M. (2016). Estimating energetics in cetaceans from respiratory frequency: Why we need to understand physiology.

Biology Open, *5*, 436–442. https://doi.org/10.1242/bio.017251

Fahlman, A., Moore, M. J., & Garcia-Parraga, D. (2017). Respiratory function and mechanics in pinnipeds and cetaceans. *Journal of Experimental Biology*, *220*(10), 1761–1773. https://doi.org/10.1242/jeb.126870

Fahlman, A., Svärd, C., Rosen, D. A. S., Wilson, R. P., & Trites, A. W. (2013). Activity as a proxy to estimate metabolic rate and to partition the metabolic cost of diving vs. breathing in pre- and post-fasted Steller sea lions. *Aquatic Biology*, *18*(2), 175–184. https://doi.org/10.3354/ab00500

Feyrer, L. J., & Duffus, D. A. (2011). Predatory disturbance and prey species diversity: The case of gray whale (*Eschrichtius robustus*) foraging on a multi-species mysid (family *Mysidae*) community. *Hydrobiologia*, *678*(1), 37–47. https://doi.org/10.1007/s10750-011-0816-z

Fox, J. (2003). Effect displays for generalized linear models. *Journal of Statistical Software*, *8*(15), 1–27. https://doi.org/10.2307/271037

Fox, J., & Weisberg, S. (2019). *An R companion to applied regression* (3rd ed.). Retrieved from https://socialsciences.mcmaster.ca/jfox/Books/Companion/index.html

Gleiss, A. C., Wilson, R. P., & Shepard, E. L. C. (2011). Making overall dynamic body acceleration work: On the theory of acceleration as a proxy for energy expenditure. *Methods in Ecology and Evolution*, *2*(1), 23–33. https://doi.org/10.1111/j.2041-210X.2010.00057.x

Goldbogen, J. A., Cade, D. E., Calambokidis, J., Friedlaender, A. S., Potvin, J., Segre, P. S., & Werth, A. J. (2017). How baleen whales feed: The biomechanics of engulfment and filtration. *Annual Review of Marine Science*, *9*, 367–386. https://doi.org/10.1146/annurev-marine-122414-033905

Goldbogen, J. A., Calambokidis, J., Croll, D. A., Harvey, J. T., Newton, K. M., Oleson, E. M., … Shadwick, R. E. (2008). Foraging behavior of humpback whales: Kinematic and respiratory patterns suggest a high cost for a lunge. *Journal of Experimental Biology*, *211*(23), 3712–3719. https://doi.org/10.1242/jeb.023366

Goldbogen, J. A., Calambokidis, J., Croll, D. A., Mckenna, M. F., Oleson, E., Potvin, J., … Tershy, B. R. (2012). Scaling of lunge-feeding performance in rorqual whales: Mass-specific energy expenditure increases with body size and progressively limits diving capacity. *Functional Ecology*, *26*(1), 216–226. https://doi.org/10.1111/j.1365-2435.2011.01905.x

Goldbogen, J. A., Calambokidis, J., Oleson, E., Potvin, J., Pyenson, N. D., Schorr, G., & Shadwick, R. E. (2011). Mechanics, hydrodynamics and energetics of blue whale lunge feeding: Efficiency dependence on krill density. *Journal of Experimental Biology*, *214*(4), 698–699. https://doi.org/10.1242/jeb.054726

Goldbogen, J. A., Calambokidis, J., Shadwick, R. E., Oleson, E. M., McDonald, M. A., & Hildebrand, J. A. (2006). Kinematics of foraging dives and lunge-feeding in fin whales. *Journal of Experimental Biology*, *209*(7), 1231–1244. https://doi.org/10.1242/jeb.02135

Goldbogen, J. A., Friedlaender, A. S., Calambokidis, J., McKenna, M. F., Simon, M., & Nowacek, D. P. (2013). Integrative approaches to the study of baleen whale diving behavior, feeding performance, and foraging ecology. *BioScience*, *63*(2), 90–100. https://doi.org/10.1525/bio.2013.63.2.5

Gough, W. T., Smith, H. J., Savoca, M. S., Czapanskiy, M. F., Fish, F. E., Potvin, J., … Goldbogen, J. A. (2021). Scaling of oscillatory kinematics and Froude efficiency in baleen whales. *Journal of Experimental Biology*, *224*(13). https://doi.org/10.1242/jeb.237586

Green, J. A. (2011). The heart rate method for estimating metabolic rate: Review and recommendations. *Comparative Biochemistry and Physiology - A Molecular and Integrative Physiology*, *158*(3), 287–304. https://doi.org/10.1016/j.cbpa.2010.09.011

Gulland, F., Pérez-Cortés, H., Urbán, J. R., Rojas-Bracho, L., Ylitalo, G., Weir, J., … Rowles, T. (2005). Eastern North Pacific gray whale (*Eschrichtius robustus*) unusual mortality event, 1999-2000. In *U.S. Department of Commerce. NOAA Technical Memorandum NMFS-AFSC-150*. Retrieved from http://www.afsc.noaa.gov/publications/AFSC-TM/NOAA-TM-AFSC-150.pdf

Halsey, L. G. (2017). Relationships grow with time: A note of caution about energy expenditure-proxy correlations, focussing on accelerometry as an example. *Functional Ecology*, *31*(6), 1176–1183. https://doi.org/10.1111/1365-2435.12822

Halsey, L. G., Shepard, E. L. C., Quintana, F., Gomez Laich, A., Green, J. A., & Wilson, R. P. (2009). The relationship between oxygen consumption and body acceleration in a range of species. *Comparative Biochemistry and Physiology - A Molecular and Integrative Physiology*, *152*(2), 197–202. https://doi.org/10.1016/j.cbpa.2008.09.021

Halsey, L. G., Shepard, E. L. C., & Wilson, R. P. (2011). Assessing the development and application of the accelerometry technique for estimating energy expenditure. *Comparative Biochemistry and Physiology - A Molecular and Integrative Physiology*, *158*(3), 305–314. https://doi.org/10.1016/j.cbpa.2010.09.002

Harris, J., Calambokidis, J., Perez, A., & Mahoney, P. J. (2022). *Recent trends in the abundance of seasonal gray whales (*Eschrichtius robustus*) in the Pacific Northwest, 1996-2020*. Retrieved from https://repository.library.noaa.gov/

Hays, G. C., Ferreira, L. C., Sequeira, A. M. M., Meekan, M. G., Duarte, C. M., Bailey, H., … Thums, M. (2016). Key questions in marine megafauna movement ecology. *Trends in Ecology and Evolution*, *31*(6), 463–475. https://doi.org/10.1016/j.tree.2016.02.015

Hildebrand, L., Bernard, K. S., & Torres, L. G. (2021). Do gray whales count calories? Comparing energetics values of gray whale prey across two different feeding grounds in the Eastern North Pacific. *Frontiers in Marine Science*, *8*. https://doi.org/10.3389/fmars.2021.683634

Hildebrand, L., Sullivan, F. A., Orben, R. A., Derville, S., & Torres, L. G. (2022). Trade-offs in prey quantity and quality in gray whale foraging. *Marine Ecology Progress Series*, *695*, 189–201. https://doi.org/10.3354/meps14115

International Whaling Commission. (2011). Report of the Scientific Committee. *Journal of Cetacean Research Management*, *12*, 1–75.

Isojunno, S., Aoki, K., Curé, C., Kvadsheim, P. H., & O'Malley Miller, P. J. (2018). Breathing patterns indicate cost of exercise during diving and response to experimental sound exposures in long-finned pilot whales. *Frontiers in Physiology*, *9*. https://doi.org/10.3389/fphys.2018.01462

Isojunno, S., & Miller, P. J. O. (2015). Sperm whale response to tag boat presence: Biologically informed hidden state models quantify lost feeding opportunities. *Ecosphere*, *6*(1). https://doi.org/10.1890/ES14-00130.1

Izadi, S., Aguilar de Soto, N., Constantine, R., & Johnson, M. (2022). Feeding tactics of resident Bryde's whales in New Zealand. *Marine Mammal Science*, 1–14. https://doi.org/10.1111/mms.12918

Jaakkola, K., Loyer, C., Guarino, E., Donegan, K., & McMullen, C. (2021). Do dolphins really have a rightward lateralization for action? The importance of behavior-specific and orientation-neutral coding. *Behavioural Brain Research*, *401*. https://doi.org/10.1016/j.bbr.2020.113083

Jeanniard-du-Dot, T., Guinet, C., Arnould, J. P. Y., Speakman, J. R., & Trites, A. W. (2017). Accelerometers can measure total and activity-specific energy expenditures in free-ranging marine mammals only if linked to time-activity budgets. *Functional Ecology*, *31*(2), 377–386. https://doi.org/10.1111/1365-2435.12729

Jeanniard-Du-Dot, T., Trites, A. W., Arnould, J. P. Y., Speakman, J. R., & Guinet, C. (2016). Flipper strokes can predict energy expenditure and locomotion costs in free-ranging northern and Antarctic fur seals. *Scientific Reports*, *6*. https://doi.org/10.1038/srep33912

John, J. S. W. (2020). *Energetics of rest and locomotion in diving marine mammals: Novel metrics for prediciting the vulnerability of threatened cetacean, pinniped, and sirenian species* (pp.126). [PhD disseration]. University of California Santa Cruz.

Johnson, K. R., & Nelson, C. H. (1984). Side-scan sonar assessment of gray whale feeding in the Bering Sea. *Science*, *225*(4667), 1150–1152. https://doi.org/10.1126/science.225.4667.1150

Kuznetsova, A., Brockhoff, P. B., & Christensen, R. H. B. (2017). lmerTest package: Tests in linear mixed effects models. *Journal of Statistical Software*, *82*(13), 1–26. https://doi.org/10.18637/JSS.V082.I13

Ladds, M. A., Rosen, D. A. S., Slip, D. J., & Harcourt, R. G. (2017). Proxies of energy expenditure for marine mammals: An experimental test of " the time trap ." *Scientific Reports*, *7*(11815), 1–10. https://doi.org/10.1038/s41598-017-11576-4

Lang, A. R., Calambokidis, J., Scordino, J., Pease, V. L., Klimek, A., Burkanov, V. N., … Taylor, B. L. (2014). Assessment of genetic structure among eastern North Pacific gray whales on their feeding grounds. *Marine Mammal Science*, *30*(4), 1473–1493. https://doi.org/10.1111/mms.12129

Le Boeuf, B. J., Perez-Cortes, M. H., Urban, R. J., Mate, B. R., & Ollervides, U. F. (2000). High gray whale mortality and low recruitment in 1999: potential causes and implications. *Journal of Cetacean Research and Management*, *2*, 85–99.

Lemos, L. S., Burnett, J. D., Chandler, T. E., Sumich, J. L., & Torres, L. G. (2020a). Intra- and inter-annual variation in gray whale body condition on a foraging ground. *Ecosphere*, *11*(4). https://doi.org/10.1002/ecs2.3094

Lemos, L. S., Haxel, J. H., Olsen, A., Burnett, J. D., Smith, A., Chandler, T. E., … Torres, L. G. (2022). Effects of vessel traffic and ocean noise on gray whale stress hormones. *Scientific Reports*, *12*(1). https://doi.org/10.1038/s41598-022-14510-5

Lemos, L. S., Olsen, A., Smith, A., Chandler, T. E., Larson, S., Hunt, K., & Torres, L. G. (2020b). Assessment of fecal steroid and thyroid hormone metabolites in eastern North Pacific gray whales. *Conservation Physiology*, *8*(1). https://doi.org/10.1093/conphys/coaa110

Lenth, R. V. (2022). *emmeans: Estimated Marginal Means, aka Least-Squares Means*. Retrieved from https://cran.r-project.org/package=emmeans

MacArthur, R. H., & Pianka, E. R. (1966). On optimal use of a patchy environment. *The*

American Naturalist, *100*(916), 603–609.

Magera, A. M., Mills Flemming, J. E., Kaschner, K., Christensen, L. B., & Lotze, H. K. (2013). Recovery trends in marine mammal populations. *PloS One*, *8*(10). https://doi.org/10.1371/journal.pone.0077908

Mallonee, J. S. (1991). Behaviour of gray whales (*Eschrichtius robustus*) summering off the northern California coast, from Patrick's Point to Crescent City. *Canadian Journal of Zoology*, *69*(3), 681–690. https://doi.org/10.1139/z91-100

Maresh, J. L., Adachi, T., Takahashi, A., Naito, Y., Crocker, D. E., Horning, M., … Costa, D. P. (2015). Summing the strokes: Energy economy in northern elephant seals during large-scale foraging migrations. *Movement Ecology*, *3*(22). https://doi.org/10.1186/s40462-015-0049-2

Martin Lopez, L. M., Aguilar De Soto, N., Madsen, P. T., & Johnson, M. (2022). Overall Dynamic Body Acceleration measures activity differently on large vs small aquatic animals. *Methods in Ecology and Evolution*, *13*(2), 447–458. https://doi.org/10.1111/j.2041-210x.2010.00016.x

Martín López, L. M., Miller, P. J. O., Aguilar De Soto, N., & Johnson, M. (2015). Gait switches in deep-diving beaked whales: Biomechanical strategies for long-duration dives. *Journal of Experimental Biology*, *218*(9), 1325–1338. https://doi.org/10.1242/jeb.106013

Mauchline, J. (1980). The biology of mysids and euphausiids. *Advances in Marine Biology*, *18*, 1–681.

McClintock, B. T. (2021). Worth the effort? A practical examination of random effects in hidden Markov models for animal telemetry data. *Methods in Ecology and Evolution*, *12*(8), 1475–1497. https://doi.org/10.1111/2041-210X.13619

McClintock, B. T., & Michelot, T. (2018). momentuHMM: R package for generalized hidden Markov models of animal movement. *Methods in Ecology and Evolution*, *9*(6), 1518–1530. https://doi.org/10.1111/2041-210X.12995

Milborrow, S. (2022). *rpart.plot: Plot "rpart" Models: An Enhanced Version of "plot.rpart."* Retrieved from https://cran.r-project.org/package=rpart.plot

Moore, S. E., Clarke, J. T., Okkonen, S. R., Grebmeier, J. M., Berchok, C. L., & Stafford, K. M. (2022). Changes in gray whale phenology and distribution related to prey variability and ocean biophysics in the northern Bering and eastern Chukchi seas. *Plos One*, *17*(4). https://doi.org/10.1371/journal.pone.0265934

Moore, S. E., Grebmeier, J. M., & Davies, J. R. (2003). Gray whale distribution relative to forage habitat in the northern Bering Sea: Current conditions and retrospective summary. *Canadian Journal of Zoology*, *81*(4), 734–742. https://doi.org/10.1139/z03-043

Morales, J. M., Haydon, D. T., Frair, J., Holsinger, K. E., & Fryxell, J. M. (2004). Extracting more out of relocation data: Building movement models as mixtures of random walks. *Ecology*, *85*(9), 2436–2445. https://doi.org/10.1890/03-0269

Nerini, M. (1984). A review of gray whale feeding ecology. In M. Lou Jones, S. L. Swartz, & S. Leatherwood (Eds.), *The gray whale: Eschrichtius robustus* (pp. 423–450). https://doi.org/10.1016/B978-0-08-092372-7.50024-8

Newell, C. L., & Cowles, T. J. (2006). Unusual gray whale Eschrichtius robustus feeding in the summer of 2005 off the central Oregon coast. *Geophysical Research Letters*, *33*(22). https://doi.org/10.1029/2006GL027189

Norberg, R. A. (1977). An ecological theory on foraging time and energetics and choice of optimal food-searching method. *Journal of Animal Ecology*, *46*(2), 511–529.

Nowacek, D. P., Christiansen, F., Bejder, L., Goldbogen, J. A., & Friedlaender, A. S. (2016). Studying cetacean behaviour: New technological approaches and conservation applications. *Animal Behaviour*, *120*, 235–244. https://doi.org/10.1016/j.anbehav.2016.07.019

Owen, K., Dunlop, R. A., Monty, J. P., Chung, D., Noad, M. J., Donnelly, D., … Mackenzie, T. (2016). Detecting surface-feeding behavior by rorqual whales in accelerometer data. *Marine Mammal Science*, *32*(1), 327–348. https://doi.org/10.1111/mms.12271

Perryman, W. L., Donahue, M. A., Perkins, P. C., & Reilly, S. B. (2002). Gray whale calf production 1994-2000: Are observed fluctuations related to changes in seasonal ice cover? *Marine Mammal Science*, *18*(1), 121–144. https://doi.org/10.1111/j.1748-7692.2002.tb01023.x

Perryman, W. L., Joyce, T., Weller, D. W., & Durban, J. W. (2020). Environmental factors influencing eastern North Pacific gray whale calf production 1994–2016. *Marine Mammal Science*, (September 2020), 448–462. https://doi.org/10.1111/mms.12755

Peters, A., & Hothorn, T. (2023). *ipred: Improved Predictors*. Retrieved from https://cran.r-project.org/package=ipred

Pohle, J., Langrock, R., van Beest, F. M., & Schmidt, N. M. (2017). Selecting the number of states in Hidden Markov Models: Pragmatic solutions illustrated using animal movement. *Journal of Agricultural, Biological, and Environmental Statistics*, *22*(3), 270–293. https://doi.org/10.1007/s13253-017-0283-8

Potvin, J., Goldbogen, J. A., & Shadwick, R. E. (2012). Metabolic expenditures of lunge feeding rorquals across scale: Implications for the evolution of filter feeding and the limits of maximum body size. *PLoS ONE*, *7*(9). https://doi.org/10.1371/journal.pone.0044854

R Core Team. (2023). *R: A Language and Environment for Statistical Computing*. Retrieved from https://www.r-project.org/

Ransom, J. I., Cade, B. S., & Hobbs, N. T. (2010). Influences of immunocontraception on time budgets, social behavior, and body condition in feral horses. *Applied Animal Behaviour Science*, *124*(1–2), 51–60. https://doi.org/10.1016/j.applanim.2010.01.015

Raverty, S. A., Duignan, P. J., Greig, D. J., Huggins, J., Burek, K., Garner, M., … Fauquier, D. (2020). Post mortem findings of a 2019 gray whale Unusual Mortality Event in the Eastern North Pacific. *SC/68B/IST/05*, p. 31. Retrieved from www.journal.uta45jakarta.ac.id

Rendell, L., Cantor, M., Gero, S., Whitehead, H., & Mann, J. (2019). Causes and consequences of female centrality in cetacean societies. *Philosophical Transactions of the Royal Society*

B: Biological Sciences, *374*(1780). https://doi.org/10.1098/rstb.2018.0066

Sato, K., Watanuki, Y., Takahashi, A., Miller, P. J. O., Tanaka, H., Kawabe, R., … Naito, Y. (2007). Stroke frequency, but not swimming speed, is related to body size in free-ranging seabirds, pinnipeds and cetaceans. *Proceedings of the Royal Society B: Biological Sciences*, *274*(1609), 471–477. https://doi.org/10.1098/rspb.2006.0005

Savoca, M. S., Czapanskiy, M. F., Kahane-Rapport, S. R., Gough, W. T., Fahlbusch, J. A., Bierlich, K. C., … Goldbogen., J. A. (2021). Baleen whale prey consumption based on high resolution foraging measurements. *Nature*, *599*, 85–90. https://doi.org/10.1038/s41586-021-03991-5

Schoeller, D. A., & van Santen, E. (1982). Measurement of energy expenditure in free-living humans by using doubly labeled water. *Journal of Applied Physiology*, *53*(4), 955–959. https://doi.org/10.1093/jn/118.11.1278

Schwarz, J. F. L., Mews, S., DeRango, E. J., Langrock, R., Piedrahita, P., Páez-Rosas, D., & Krüger, O. (2021). Individuality counts: A new comprehensive approach to foraging strategies of a tropical marine predator. *Oecologia*, *195*(2), 313–325. https://doi.org/10.1007/s00442-021-04850-w

Scordino, J., Bickham, J., Brandon, J. R., Brownell, R. L. J., Burdin, A., Doniol-Valcroze, T., … Weller, D. W. (2023). Update on gray whale status since 2020 implementation review. *Paper SC/69A/IST/04 Presented to the Scientific Committee of the International Whaling Commission*, 22.

Scordino, J., Litovka, D., Kim, H. W., Urbán, J., & Cottrell, P. (2020). Ship strikes and entanglements of gray whales in the North Pacific Ocean, 1924-2018: Revised. *Paper SC/68B/IST/08 Presented to International Whaling Commission Scientific Committee*.

Shadwick, R. E., Potvin, J., & Goldbogen, J. A. (2019). Lunge feeding in rorqual whales. *Physiology*, *34*, 409–418. https://doi.org/10.1152/physiol.00010.2019

Silber, G. K., Weller, D. W., Reeves, R. R., Adams, J. D., & Moore, T. J. (2021). Co-occurrence

of gray whales and vessel traffic in the North Pacific Ocean. *Endangered Species Research*, *44*, 177–201. https://doi.org/10.3354/ESR01093

Simon, M., Johnson, M., & Madsen, P. T. T. (2012). Keeping momentum with a mouthful of water: Behavior and kinematics of humpback whale lunge feeding. *Journal of Experimental Biology*, *215*(21), 3786–3798. https://doi.org/10.1242/jeb.071092

Simon, M., Johnson, M., Tyack, P., & Madsen, P. T. (2009). Behaviour and kinematics of continuous ram filtration in bowhead whales (*Balaena mysticetus*). *Proceedings of the Royal Society B: Biological Sciences*, *276*(1674), 3819–3828. https://doi.org/10.1098/rspb.2009.1135

Stelle, L. L., Megill, W. M., & Kinzel, M. R. (2008). Activity budget and diving behavior of gray whales (*Eschrichtius robustus*) in feeding grounds off coastal British Columbia. *Marine Mammal Science*, *24*(3), 462–478. https://doi.org/10.1111/j.1748-7692.2008.00205.x

Sullivan, F. A., & Torres, L. G. (2018). Assessment of vessel disturbance to gray whales to inform sustainable ecotourism. *Journal of Wildlife Management*, *82*(5), 896–905. https://doi.org/10.1002/jwmg.21462

Sumich, J. L. (1983). Swimming velocities, breathing patterns, and estimated costs of locomotion in migrating gray whales, *Eschrichtius robustus*. *Canadian Journal of Zoology*, *61*(3), 647–652. https://doi.org/10.1139/z83-086

Sumich, J. L., Alberston, G., Torres, L. G., Bird, C. N., Bierlich, K. C., & Harris, C. (*in revision*). Using audio and UAS-based video for estimating tidal lung volumes of active adult gray whales (*Eschrichtius robustus*). In *Marine Mammal Science*.

Therneau, T., & Atkinson, B. (2022). *rpart: Recursive Partitioning and Regression Trees*. Retrieved from https://cran.r-project.org/package=rpart

Torres, L. G. (2017). A sense of scale: Foraging cetaceans' use of scale-dependent multimodal sensory systems. *Marine Mammal Science*, *33*(4), 1170–1193.

https://doi.org/10.1111/mms.12426

Torres, L. G., Bird, C. N., Rodriguez-Gonzalez, F., Christiansen, F., Bejder, L., Lemos, L., … Bierlich, K. C. (2022). Range-wide comparison of gray whale body condition reveals contrasting sub-population health characteristics and vulnerability to environmental change. *Frontiers in Marine Science*, *9*. https://doi.org/10.3389/fmars.2022.867258

Torres, L. G., Brander, S. M., Parker, J. I., Bloom, E. M., Norman, R., Brocklin, J. E. Van, … Hildebrand, L. (2023). Zoop to poop: Assessment of microparticle loads in gray whale zooplankton prey and fecal matter reveal high daily consumption rates. *Frontiers in Marine Science*, *10*. https://doi.org/10.3389/fmars.2023.1201078

Torres, L. G., Nieukirk, S. L., Lemos, L., & Chandler, T. E. (2018). Drone up! Quantifying whale behavior from a new perspective improves observational capacity. *Frontiers in Marine Science*, *5*. https://doi.org/10.3389/fmars.2018.00319

Torres, W., & Bierlich, K. (2020). MorphoMetriX: a photogrammetric measurement GUI for morphometric analysis of megafauna. *Journal of Open Source Software*, *5*(45). https://doi.org/10.21105/joss.01825

van der Hoop, J. M., Nowacek, D. P., Moore, M. J., & Triantafyllou, M. S. (2017). Swimming kinematics and efficiency of entangled North Atlantic right whales. *Endangered Species Research*, *32*(1), 1–17. https://doi.org/10.3354/esr00781

Villegas-Amtmann, S., Schwarz, L. K., Gailey, G., Sychenko, O., & Costa, D. P. (2017). East or west: The energetic cost of being a gray whale and the consequence of losing energy to disturbance. *Endangered Species Research*, *34*, 167–183. https://doi.org/10.3354/esr00843

Villegas-Amtmann, S., Schwarz, L. K., Sumich, J. L., Costa, D. P., & Peters, D. P. C. (2015). A bioenergetics model to evaluate demographic consequences of disturbance in marine mammals applied to gray whales. *Ecosphere*, *6*(10). https://doi.org/10.1890/ES15-00146.1

Volpov, B. L., Hoskins, A. J., Battaile, B. C., Viviant, M., Wheatley, K. E., Marshall, G., … Arnould, J. P. Y. (2015). Identification of prey captures in Australian fur seals

(Arctocephalus pusillus doriferus) using head-mounted accelerometers: Field validation with animal-borne video cameras. *PLoS ONE*, *10*(6). https://doi.org/10.1371/journal.pone.0128789

Ware, C., Wiley, D. N., Friedlaender, A. S., Weinrich, M., Hazen, E. L., Bocconcelli, A., … Abernathy, K. (2014). Bottom side-roll feeding by humpback whales (*Megaptera novaeangliae*) in the southern Gulf of Maine, U.S.A. *Marine Mammal Science*, *30*(2), 494–511. https://doi.org/10.1111/mms.12053

Watanabe, Y. Y., & Goldbogen, J. A. (2021). Too big to study? The biologging approach to understanding the behavioural energetics of ocean giants. *Journal of Experimental Biology*, *224*(13). https://doi.org/10.1242/jeb.202747

Wild, S., Allen, S. J., Krutzen, M., King, S. L., Gerber, L., & Hoppitt, W. J. E. (2019). Multi-network-based diffusion analysis reveals vertical cultural transmission of sponge tool use within dolphin matrilines. *Biology Letters*, *15*(7). https://doi.org/10.1098/rsbl.2019.0227

Williams, T. M., Fuiman, L. A., & Davis, R. W. (2015). Locomotion and the cost of hunting in large, stealthy marine carnivores. *Integrative and Comparative Biology*, *55*(4), 673–682. https://doi.org/10.1093/icb/icv025

Williams, T. M., Fuiman, L. A., Horning, M., & Davis, R. W. (2004). The cost of foraging by a marine predator, the Weddell seal *Leptonychotes weddellii*: Pricing by the stroke. *Journal of Experimental Biology*, *207*(6), 973–982. https://doi.org/10.1242/jeb.00822

Williams, T. M., Kendall, T. L., Richter, B. P., Ribeiro-french, C. R., John, J. S., Odell, K. L., … Stamper, M. A. (2017). Swimming and diving energetics in dolphins : a stroke-by-stroke analysis for predicting the cost of flight responses in wild odontocetes. *Journal of Experimental Biology*, *220*, 1135–1145. https://doi.org/10.1242/jeb.154245

Williams, T. M., & Maresh, J. L. (2015). Exercise energetics. In M. A. Castellini & J.-A. Mellish (Eds.), *Marine mammal physiology: Requisites for ocean living* (pp. 334–349). Boca Raton , FL: CRC Press.

Wilson, R. P., Börger, L., Holton, M. D., Scantlebury, D. M., Gómez-Laich, A., Quintana, F., … Shepard, E. L. C. (2020). Estimates for energy expenditure in free-living animals using acceleration proxies: A reappraisal. *Journal of Animal Ecology*, *89*(1), 161–172. https://doi.org/10.1111/1365-2656.13040

Wilson, R. P., Liebsch, N., Davies, I. M., Quintana, F., Weimerskirch, H., Storch, S., … McMahon, C. R. (2007). All at sea with animal tracks; methodological and analytical solutions for the resolution of movement. *Deep-Sea Research Part II: Topical Studies in Oceanography*, *54*, 193–210. https://doi.org/10.1016/j.dsr2.2006.11.017

Wilson, R. P., Quintana, F., & Hobson, V. J. (2012). Construction of energy landscapes can clarify the movement and distribution of foraging animals. *Proceedings of the Royal Society B: Biological Sciences*, *279*(1730), 975–980. https://doi.org/10.1098/rspb.2011.1544

Wilson, R. P., White, C. R., Quintana, F., Halsey, L. G., Liebsch, N., Martin, G. R., & Butler, P. J. (2006). Moving towards acceleration for estimates of activity-specific metabolic rate in free-living animals: The case of the cormorant. *Journal of Animal Ecology*, *75*(5), 1081–1090. https://doi.org/10.1111/j.1365-2656.2006.01127.x

Withers, P. C. (1977). Measurement of VO2, VCO2, and evaporative water loss with a flow through mask. *Journal of Applied Physiology*, *42*(1), 120–123. https://doi.org/10.1152/jappl.1977.42.1.120

Woodward, B. L., & Winn, J. P. (2006). Apparent lateralized behavior in gray whales feeding off the Central British Columbia coast. *Marine Mammal Science*, *22*(1), 64–73. https://doi.org/10.1111/j.1748-7692.2006.00006.x

Woodward, B. L., Winn, J. P., & Fish, F. E. (2006). Morphological specializations of baleen whales associated with hydrodynamic performance and ecological niche. *Journal of Morphology*, *267*, 1284–1294. https://doi.org/10.1002/jmor

Wright, B. M., Ford, J. K. B., Ellis, G. M., Deecke, V. B., Shapiro, A. D., Battaile, B. C., & Trites, A. W. (2017). Fine-scale foraging movements by fish-eating killer whales (Orcinus

orca) relate to the vertical distributions and escape respones of salmonid prey (Oncorhyncus spp.). *Movement Ecology*, *5*. https://doi.org/10.1186/s40462-017-0094-0

Wursig, B., Wells, R. S., & Croll, D. A. (1986). Behavior of gray whales summering near St. Lawrence Island, Bering Sea. *Canadian Journal of Zoology*, *64*(3), 611–621. https://doi.org/10.1139/z86-091

Ydesen, K. S., Wisniewska, D. M., Hansen, J. D., Beedholm, K., Johnson, M., & Madsen, P. T. (2014). What a jerk: Prey engulfment revealed by high-rate, super-cranial accelerometry on a harbour seal (Phoca vitulina). *Journal of Experimental Biology*, *217*(15). https://doi.org/10.1242/jeb.111070

Zucchini, W., MacDonald, I. L., & Langrock, R. (2016). *Hidden Markov Models for time series* (2nd ed.). New York: CRC Press.

Appendices

Appendix A: Selecting data streams for Hidden Markov Models

Histograms of the movement metrics were examined to determine the variables that can be used to differentiate between dive types and therefore would be appropriate to include in the Hidden Markov Models (HMMs) as data streams to help identify different broad states (e.g., forage, search, transit).

Both dive duration and maximum depth are helpful dive characteristics that can be used to classify broad state. Dive duration appears to have multiple peaks at approximately 25, 75, and 175 seconds. Maximum dive depth also appears to have a strongly bimodal distribution. It is expected that foraging dives will be longer duration and deeper than transiting dives, with search behaviour having intermediate duration and depth (Stelle et al., 2008; Wursig et al., 1986).

Surface recovery period and the ratio of surface to dive time both reflect the animal's recovery following a dive. The surface recovery period metric has a distribution with clearer modes, likely indicating it is the more useful metric to consider when constructing an HMM. Surface recovery periods are the shortest for foraging and the longest for traveling during focal follows (Stelle et al., 2008), although it is unclear if PCFG grey whales incur an oxygen debt during subsequent foraging dives that then requires a longer surface interval (Castellini, 2012). Additionally, other focal follow studies have found no significant differences between surface period between different behavioural contexts (Mallonee, 1991). The uncertainty in the biological relevance of the surface recovery period led to its exclusion from the model.

Dive tortuosity and change in heading both approximate the sinuosity of the animal's path. Dive tortuosity has clearer breaks in the distribution, which should make it more helpful when classifying different broad states. Transiting dives are expected to have lower tortuosity as they represent directed movement, while foraging dives are expected to have higher tortuosity (Barraquand and Benhamou, 2008).

The proportion of time spent in roll events during a dive is likely an indication of the foraging effort during a dive, given that foraging ecology studies have shown that grey whales roll on their sides to feed (Nerini, 1984; Torres et al., 2018; Woodward and Winn, 2006). The distribution of the proportion of dive time spent rolled is heavily skewed towards 0; when the dives with 0% of time spent rolled are excluded, the distribution is relatively uniform. Therefore,

an alternative metric indicating whether a roll event was present during a dive was used in the HMM. It is expected that only forage and search dives will have roll events present, as these roll events are associated with foraging behaviour.

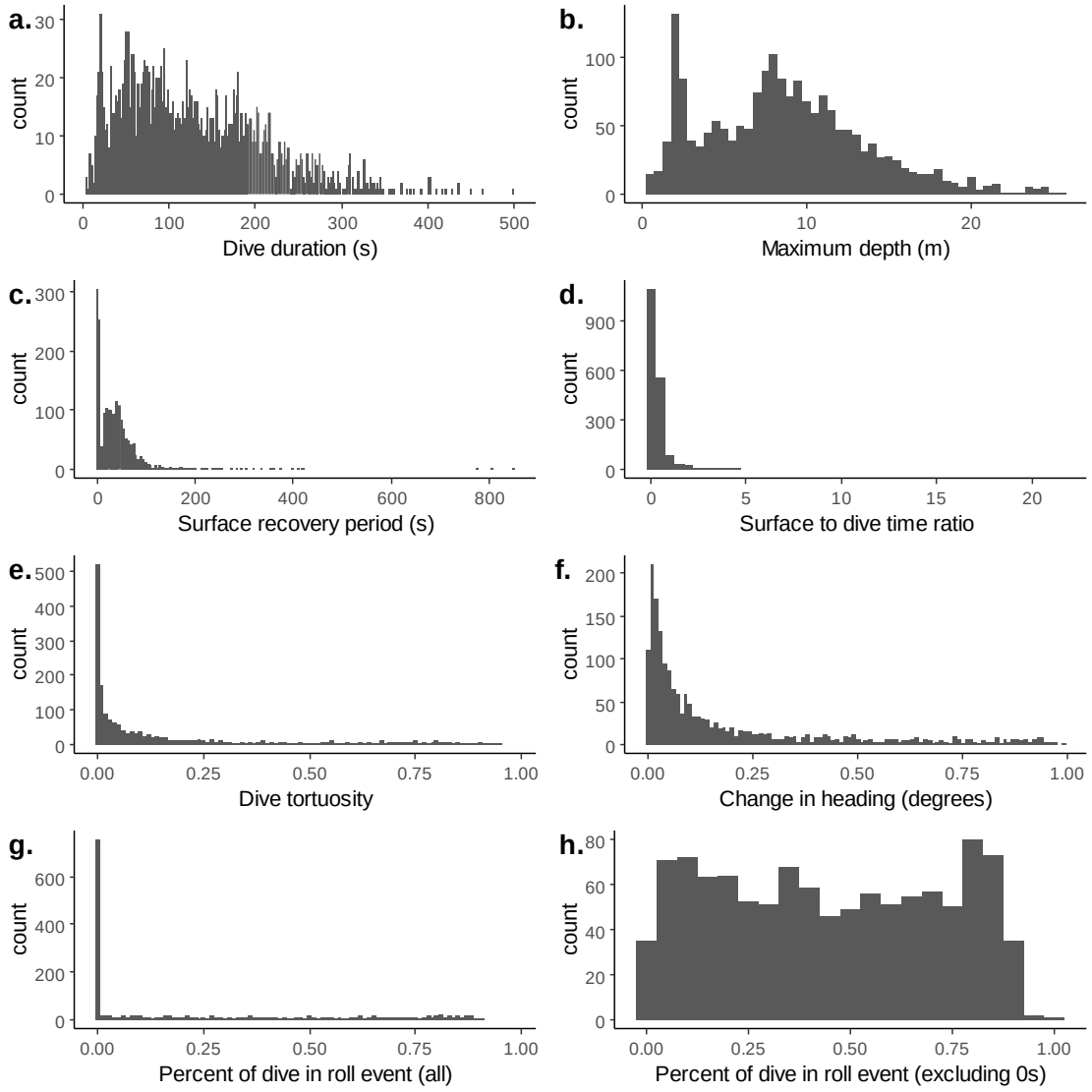

Figure A1. Histograms for the movement metrics summarized over each dive (n = 1,856) from ten CATS tag deployments on PCFG grey whales, representing potential data streams for the Hidden Markov Models (HMMs). Dive duration (a) is the time from dive start to dive end in seconds. Maximum depth (b) is the deepest depth in meters recorded during the dive. Surface recovery period (c) is the time in seconds spent at the surface after the dive is complete and before the next dive starts. The ratio of surface to dive time (d) is the surface recovery period of the dive divided by the dive duration. Dive tortuosity (e) is the ratio of actual distance traveled to the distance between the start and end points of the dive with a value of 0 corresponding to straight line movement and 1 corresponding to extremely circuitous movement. Change in heading (f) was calculated as the difference in heading between the start and end points of the dive. Percent of the dive spent in roll events (g) was used to indicate potential foraging and was zero-dominated so was also examined with the zero-values excluded (h).

Appendix B: Preliminary Hidden Markov Models including maximum depth

In the initial attempt to classify forage, search, and transit behaviour using HMMs, all data streams included in existing cetacean HMMs (DeRuiter et al., 2017) were included in the PCFG grey whale models. Maximum depth showed a clear bimodal distribution and was thought to be helpful to distinguish between forage, search, and transit behaviours due to the benthic foraging ecology of grey whales (Nerini, 1984). However, further analysis showed that the models with maximum depth included, while identifying three states, failed to meet the objective of classifying forage, search and transit behaviours. The preliminary models with maximum depth are expanded upon here, while the final model without maximum depth is reported in the main text as it met the research objective.

HMMs were constructed using turn angle (radians; von Mises distribution) dive duration (s; gamma distribution), maximum dive depth (m; gamma distribution), dive tortuosity (beta distribution), and presence of roll events (Bernoulli distribution) and compared between two- and three-states to attempt to define forage, search, and transit states in the dive data from 10 biologging tag deployments of PCFG grey whales (n = 1,856 dives). The state-dependent distributions showed reduced variation in the three-state HMM, suggesting that three reasonably distinct and biologically significant states are present in PCFG dive behaviour (**Table B1**).

State 1 showed a surface foraging behaviour (**Figure B1**). The dives classified as State 1 were the shallowest and shortest dives, with intermediate turn angles and dive tortuosity. State 1 dives had intermediate roll presence. This behaviour was likely linked to surface foraging on porcelain crab larvae (Darling et al., 1998) and was found in only one deployment (I22).

State 2 indicated a benthic foraging behaviour (**Figure B1**). State 2 dives were the deepest and longest dives, and had the highest turn angles, although there is high variation in these data streams. State 2 dives also had the highest dive tortuosity and roll event presence.

State 3 suggested a non-foraging transit behaviour (**Figure B1**). State 3 had the lowest turn angle, dive tortuosity, and roll event presence. State 3 had an intermediate dive duration and maximum dive depth compared to States 1 and 2.

The transition probability matrix showed that a whale was mostly likely to remain in the current state (**Table B2**). State 1 surface foraging behaviour was least likely to be transitioned to from both State 2 benthic foraging behaviour and State 3 non-foraging transit behaviour. The

most likely transition from State 1 surface foraging behaviour was to State 2 benthic foraging behaviour.

There was no search state found in the best HMM when maximum dive depth was included in the model. To determine if search behaviour could be classified in addition to the surface foraging behaviour, two other models were constructed. First, a four-state HMM was constructed to determine if the addition of another state would lead to search behaviour being recognized by the model. However, when a fourth state was added, the model still failed to isolate a search state. Second, the three-state HMM was reconstructed with the deployment (I22) removed to see if the three-state model with depth was able to classify a search behaviour when the known surface foraging behaviour was excluded from the input data. The model fit without the data from I22 failed to identify a third state. In other words, the state density distribution for the third state across all data streams was equal to zero. As a result, we excluded the maximum depth data stream in all subsequent models.

Table B1. State-dependent distribution parameters of the data streams estimated by the Hidden Markov Model (HMM) for the three states included in the deployments of CATS tags on PCFG grey whales (n = 1,856 dives).

Data stream	Distribution	State	Distribution parameters
Turn angle (radians)	von Mises	1	$\mu = -0.38$; $\kappa = 1.23$
		2	$\mu = 0.08$; $\kappa = 1.11$
		3	$\mu = -0.01$; $\kappa = 17.87$
Dive duration (s)	gamma	1	$\mu = 37.5$; $\sigma = 24.4$
		2	$\mu = 169.8$; $\sigma = 88.2$
		3	$\mu = 102.1$; $\sigma = 48.4$
Maximum dive depth (m)	gamma	1	$\mu = 2.11$; $\sigma = 0.84$
		2	$\mu = 11.24$; $\sigma = 3.86$
		3	$\mu = 7.08$; $\sigma = 3.69$
Dive tortuosity	beta	1	$\alpha = 0.53$; $\beta = 5.40$
		2	$\alpha = 0.60$; $\beta = 1.39$
		3	$\alpha = 0.56$; $\beta = 126.48$
Roll presence	Bernoulli	1	$p = 0.96$
		2	$p = 0.81$
		3	$p = 0.01$

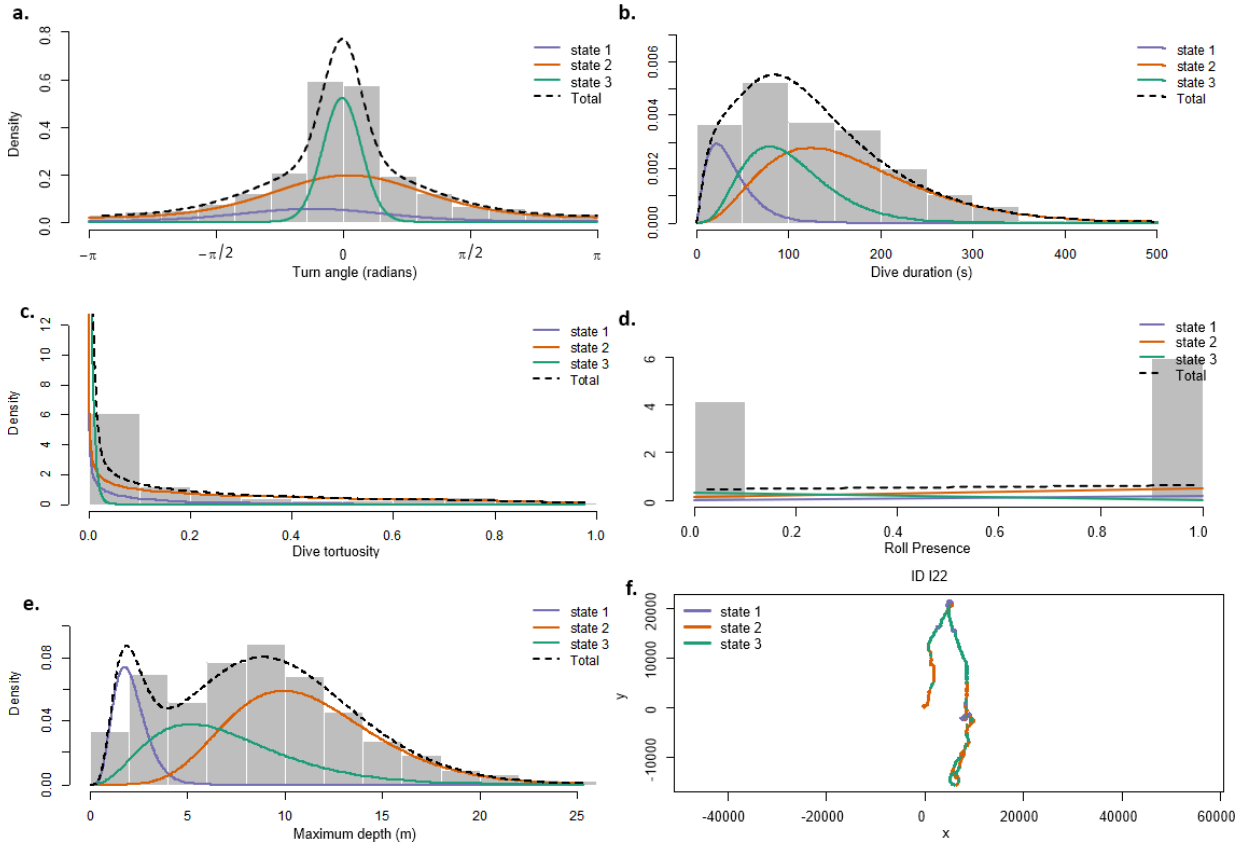

Figure B1. Hidden Markov Model (HMM) state-dependent distributions for all dives (n = 1,856) recorded on CATS tag deployments on PCFG grey whales based on (a) turn angle, (b) dive tortuosity, (c) dive duration, (d) roll event presence, (e) dive depth. (f) Viterbi algorithm state assignments for one deployment's pseudotrack.

Table B2. Transition probability matrix for the three states estimated by the Hidden Markov Model (HMM) based on dives (n = 1,856) recored on CATS tag deployments on PCFG grey whales. Rows indicate the current state and columns indicate the proximate state.

	State 1	State 2	State 3
State 1	0.962	0.025	0.013
State 2	0.005	0.912	0.083
State 3	0.009	0.148	0.843

Appendix C: Preliminary two-state Hidden Markov Model

A two-state HMM was constructed using turn angle (von Mises distribution), dive duration (s; gamma distribution), dive tortuosity (beta distribution), and presence of roll events (Bernoulli distribution) (**Table C1**) to compare to the three-state HMM with the same data streams reported on in the main text. State 1 was interpreted as non-foraging transit behaviour with low turn angle, dive tortuosity and low presence of roll events (**Figure C1**). Dive duration for State 1 was longer than State 2 on average, although with high variation. State 2 was interpreted as forage behaviour with higher turn angle, tortuosity, and roll presence. There was a lower probability of transitioning from State 2 forage behaviour to State 1 transit behaviour than from State 1 transit behaviour to State 2 forage behaviour (**Table C2**). Note the high variation in the state-dependent distributions (especially turn angle and dive duration), which was reduced when a three-state HMM was fitted as described in the main text of Chapter 2 (**Figure 2**), leading to a clearer distinction among the classified states. Moreover, the pseudo-residuals of the two-state model showed a greater deviation from normality compared to the three-state model (**Figure C2**).

Table C1. State-dependent distribution parameters of the data streams estimated by the Hidden Markov Model (HMM) for the two states included in the deployments of CATS tags on PCFG grey whales (n = 1,856 dives).

Data stream	Distribution	State	Distribution parameters
Turn angle (radians)	von Mises	1	$\mu = -0.00$; $\kappa = 26.88$
		2	$\mu = -0.03$ $\kappa = 1.12$
Dive duration (s)	gamma	1	$\mu = 106.2$; $\sigma = 50.6$
		2	$\mu = 139.7$; $\sigma = 103.3$
Dive tortuosity	beta	1	$\alpha = 0.60$; $\beta = 160.15$
		2	$\alpha = 0.51$; $\beta = 1.48$
Roll presence	Bernoulli	1	$p = 0.02$
		2	$p = 0.83$

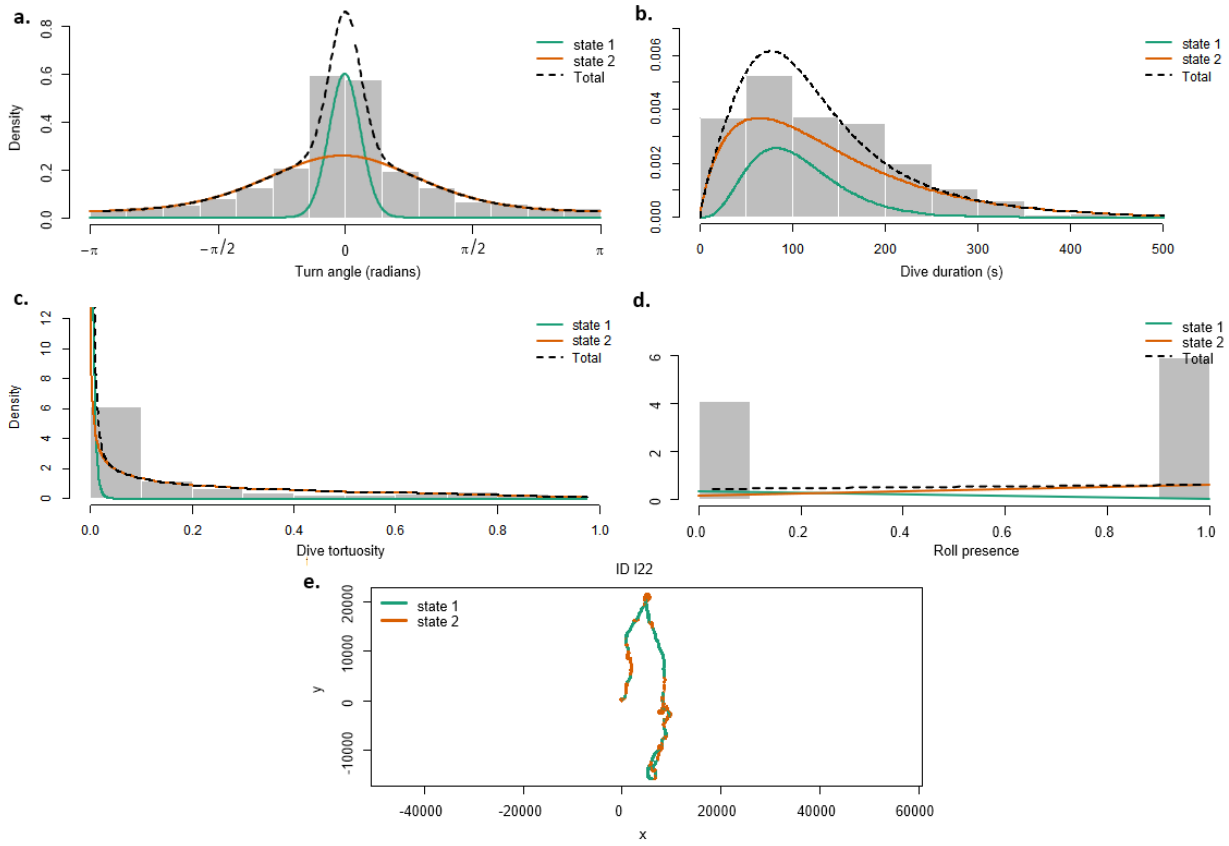

Figure C1. Hidden Markov Model (HMM) state-dependent distributions for all dives (n = 1,856) recorded on CATS tags deployments on PCFG grey whales based on (a) turn angle, (b) dive tortuosity, (c) dive duration, and (d) roll event presence. (e) Viterbi algorithm state assignments for one deployment's pseudotrack.

Table C2. Transition probability matrix for the two states estimated by the Hidden Markov Model (HMM) based on dives (n = 1,856) recorded on CATS tag deployments on PCFG grey whales. Rows indicate the current state and columns indicate the proximate state.

	State 1	**State 2**
State 1	0.847	0.153
State 2	0.063	0.937

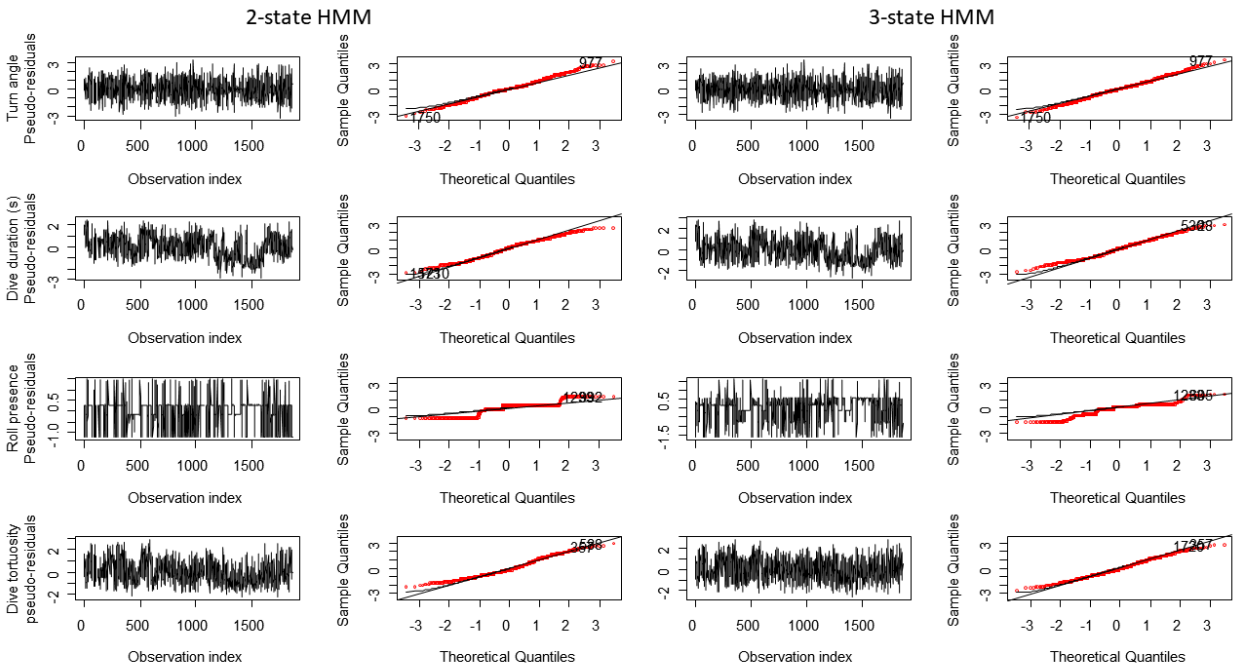

Figure C2. Comparison of the pseudo-residuals for the two- (left) and three-state (right) Hidden Markov Models (HMMs) constructed using dives (n = 1,856) recorded on CATS tag deployments on PCFG grey whales based on turn angle, dive tortuosity, dive duration, and roll presence data streams. The observation index columns show the pseudo-residual values through all data points (n = 1,856 dives). The theoretical quantile columns show the pseudo-residual values (red dots) in relation to normal distribution (black line). A better fit model will have a smaller magnitude of pseudo-residuals more equally distributed above and below 0 (observation index column) and a more normal distribution (theoretical quantiles column) of pseudo-residuals (Zucchini et al., 2016)**.**

Appendix D: Calculating relative speed

The speed (m/s) derived from tag jiggle (Cade et al., 2021) was converted to a relative speed to compare between deployments. Relative speed was determined by choosing a minimum threshold for each deployment to act as a floor speed. The floor speed threshold was determined to be the halfway point between the minimum tag jiggle speed and the 1st quartile tag jiggle speed of the deployment. Values of tag jiggle speed higher than the floor speed were set to 1, indicating forward-moving foraging tactic, while values of tag jiggle speed less than or equal to the floor speed were set to 0 indicating a stationary foraging tactic.

Appendix E: Visual validation of foraging tactics

A random subset of roll events was taken from the data set. Each of the randomly selected events was then viewed to define into a foraging tactic by using TrackPlot to visualize body orientation. TrackPlot is initially viewed from above (mirroring drone footage) and then can be viewed from the side to help aid in assigning a foraging tactic. Foraging tactics are from previously defined PCFG grey whale foraging behaviours **(Table D1)**. Detailed descriptions for assigning each roll event to foraging tactic using the TrackPlot visual data are below.

Table D1. Ethogram that can detect in tag data with body orientation variables. Behaviour names and definitions come from Torres et al. (2018). The *benthic dig (e.g., side dig)* behaviour is included in the *headstand* behaviour in Torres et al. (2018) but for the purpose of my analysis, will be kept separate to use to compare to the 'traditional' foraging tactic of Arctic feeding grey whales (Nerini, 1984)**.**

Behaviour	Definition
Headstand	Whale positioned head down-flukes up (or if in water depths less than whale body length (~12m) whale may be more horizontal in water column; with both body positions the whale is observed pushing head/mouth region into substrate
Side swim (stationary)	Whale observed swimming on its side, but not moving forward
Side swim (forward)	Whale observed swimming on its side, moving forward
Benthic dig	*Whale head is below the fluke, with the head/mouth region in the substrate; whale body position is more horizontal than a headstand, even in deep water*
Upside-down swimming	Whale observed swimming upside down

Headstand

If the whale is diving in deep water (> ~10m), from the top, the whale looks vertical with their fluke up in the air. This visual cue is more obvious in some deployments than others, given that different whales pitch themselves downwards in varying degrees.

When the water is shallower, the whale is not able to be as vertical in the water column. However, the body angle should still look to be at least 45 degrees. The TrackPlot image can be rotated to check the whales body position in relation to the surface height of the dive start to confirm if there is more room in the water column for the whale to be more vertical. The whale's pitch in these shallower water situations can be compared to the pitch of the dive descent/ascent. If the extremeness of the event's pitch matches that of the descent/ascent, the whale is

headstanding (if the pitch of the whale decreases substantially from the descent/ascent body positioning, then the event is likely a benthic dig).

Another hint of a headstand is if from above, the whale does not look to be extremely rolled (e.g., the dorsal side of the whale is still visible) as the whale is pitched in the water column.

Unpublished drone data from C. Bird suggests the following about the headstand foraging tactic. Headstands are assumed to be just pitch and no roll, with a high pitch being the best indicator. Drone observations indicate a high fluke rate but variable. With shallower water and in kelp, the whale is trying not to move its head, the pitch can get more extreme (over 90 degrees in some cases). It seems like when the whale is headstanding in shallower water, the whale's roll is more variable when compared to headstands in deeper water.

Benthic dig

The most common indication of a benthic dig is when the whale looks as if it is positioned horizontally on its side when viewed from above, but upon rotating the TrackPlot frame to be viewed from the side, the whale has its head pitched down to the sediment. This pitch angle is less than 45 degrees, as a benthic dig does not have as extreme a pitch as a headstand.

When watching the duration of the roll event, the whale must stay in this pitched position for the event to be classified as a benthic dig. If the pitch decreases to the point where the whale is horizontal, then the whale would be classified as side swimming.

The whale stays clearly rolled on its side for the whole event duration.

Unpublished drone data from C. Bird suggests the following about benthic digs. The traditional benthic feeding where the whale is thought to be dragging its head, and suctioning the 2m pit as it is moving. The tactic is thought to be a pitch and roll combination, with less extreme pitch than the headstands (about half the pitch angle) and higher, more variable roll. Headstands might look like benthic digs in some cases, and therefore habitat is used to differentiate as headstands usually occur along rocky reefs while benthic digs occur in sandy bottom areas. Benthic digs also seem to be longer than headstands from drone observations.

Side swim (stationary & forward)

This is when the whale is swimming on their side. In the TrackPlot, the whale looks horizontal from above, and from the side does not have the head pitched down into the sediment. Whales are classified as side swimming as long as the head only dips down occasionally such that it appears that the whale is stretching to keep its mouth in a dense prey patch.

Unpublished drone data from C. Bird suggests the following about the side swim foraging tactic. Side swims are periods of high roll and no pitch, where the whale will sometimes swim upside-down between side swim events. The roll is stable throughout the event while pitch can have cyclic variation as it will vary by the habitat the whale is side swimming through. Side swims tend to be as deep as the water column and are possible in shallower waters than headstand and benthic dig tactics. Stationary side swims would be expected to have higher fluke rate and amplitude as well as higher jerk due to vigorous pectoral sculling from drone observations while forward side swimming looks smoother and more graceful than the stationary side swims.

What to do when multiple tactics appear in a single roll event

If multiple foraging tactics appear in a single roll event, note how long each tactic occurs during an event, and then select the tactic that occurs for the longest time. If foraging tactics occur for relatively the same amount of time during the event, both tactics are assigned (e.g., headstand/benthic dig) with the one of higher probability first and make a note explaining my reasoning in the notes section. Roll events with multiple tactics assigned are excluded from the data used to construct the CART model.

Appendix F: Summary metrics to include in classification tree model

Summary metrics of roll events were examined between different foraging tactics that had been visually validated using the TrackPlot (**Figure F1**). Only the metrics that were able to clearly differentiate between tactics were included in the Classification and Regression Tree (CART) model. The summary metrics with the clearest breaks between foraging tactics were the absolute value of the median roll, median pitch, and the depth to body length ratio. Headstands vary between 25^{o} and 75^{o} roll, -80^{o} and -30^{o} pitch, and depth to body length ratio of 0.75-1. Benthic digs vary between 75^{o} and 140^{o} roll, -40^{o} and -10^{o} pitch, and depth to body length ratio of 0.75-1.5. Side swims vary between 80^{o} and 140^{o} roll, -10^{o} and 10^{o} pitch, and depth to body length ratio of 0-0.75. Change in heading, and speed metrics showed too much overlap to be useful for distinguishing between foraging tactics.

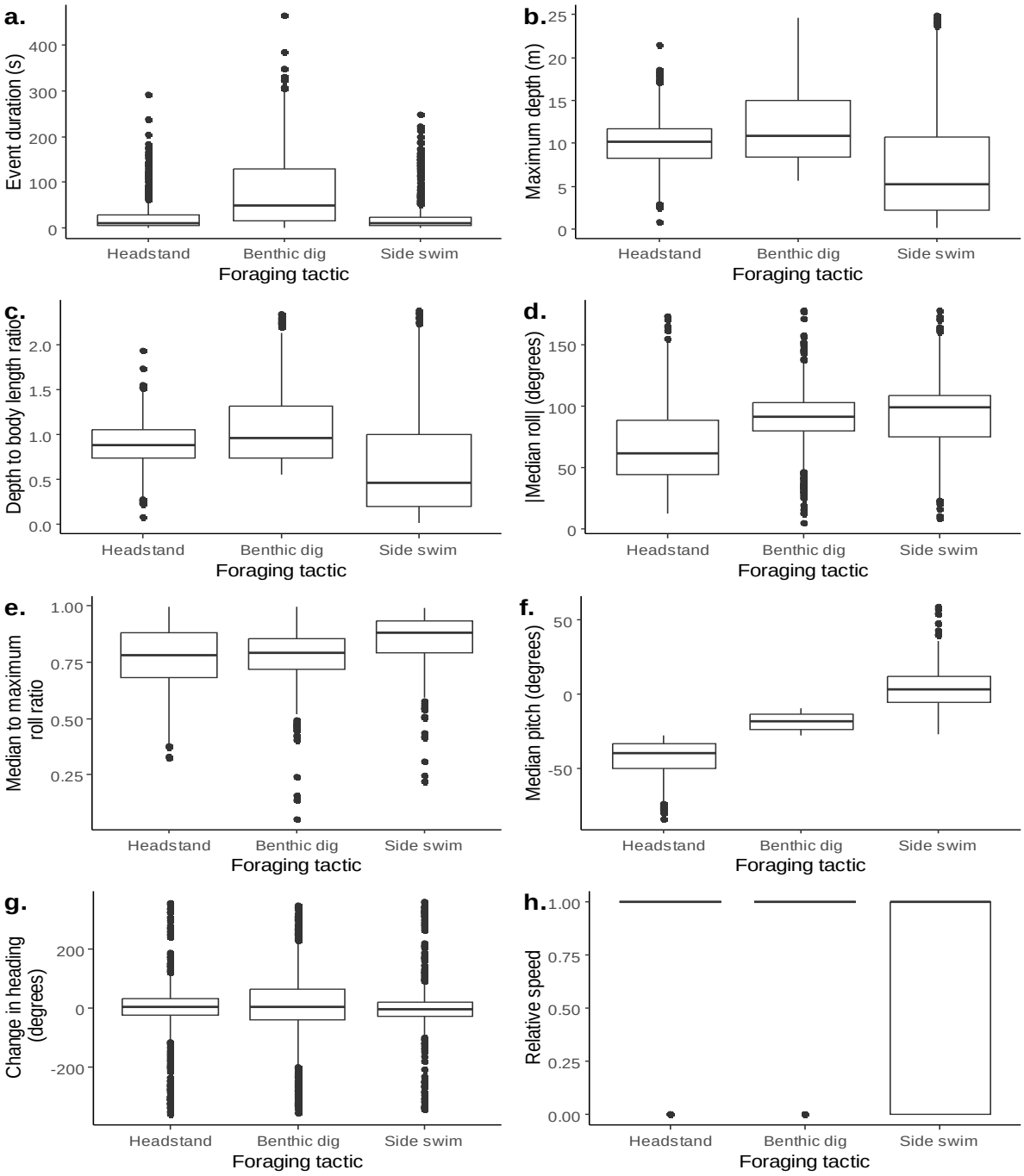

Figure F1. Distributions of each summary metric for foraging tactics from ten CATS tag deployments on PCFG grey whales (n = 1,890 roll events). Event duration (a) is the time in seconds from the start to the end of the roll event. Maximum depth (b) is the deepest depth in meters measured during the roll event. The depth to body length ratio (c) divides the depth of the animal from the CATS tag by the length of the animal from drone photogrammetry. The absolute value of the median roll (d) is the degree to which the animal is rolled onto its side during the roll event. The ratio of the absolute value of the median roll to the maximum roll (e) indicates the variability of the roll during the roll event, with values closer to one showing less difference between the median and the maximum roll. Median pitch (f) shows the degree to which the animal

was vertical in the water column, with a more extreme negative pitch indicating that the whale is more vertical in a head down-fluke up position. The change in heading (g) is the degree of change between the start and end of the roll event. Relative speed (h) shows if the animal was moving forward (1) or was stationary (0) while performing the foraging tactic.

Appendix G: Dominant stroking frequencies and median Overall Dynamic Body Accelerations

Table G1. Dominant stroking frequencies (dsf) and complementary filters from CATS tag deployments on PCFG grey whales. Dsf were calculated on steady swimming bouts in each deployment. Complimentary filters were used when calculating Overall Dynamic Body Acceleration (ODBA; ms^{-2}). Mean and standard deviation (n = 10 deployments) of the dsf and each filter are reported in the last two rows of the table.

		Filter		
Deployment	**Dsf**	**25% dsf**	**50% dsf**	**70% dsf**
A19	0.20	0.05	0.10	0.14
B21	0.07	0.02	0.04	0.05
C21	0.07	0.02	0.04	0.05
D21	0.38	0.09	0.19	0.26
E22	0.18	0.04	0.09	0.13
F22	0.08	0.02	0.04	0.06
G22	0.08	0.02	0.04	0.06
H22	0.28	0.07	0.14	0.20
I22	0.18	0.04	0.09	0.13
J22	0.06	0.01	0.03	0.04
Median	0.13			
Mean	0.16	0.04	0.08	0.11
s.d.	0.10	0.03	0.05	0.07

Table G2. Median Overall Dynamic Body Acceleration (ODBA; ms^{-2}) from CATS tag deployments on PCFG grey whales used to calculate standardized ODBA. Standardization method follows that of (Isojunno and Miller, 2015)**.**

	Median ODBA		
Deployment	**25% dsf**	**50% dsf**	**70% dsf**
All	1.13	0.76	0.61
A19	0.90	0.69	0.57
B21	1.24	0.94	0.83
C21	1.60	1.12	0.92
D21	0.47	0.27	0.22
E22	1.05	0.67	0.49
F22	1.57	1.12	0.93
G22	1.20	0.80	0.65
H22	1.04	0.71	0.49
I22	1.05	0.74	0.61
J22	1.70	1.22	0.99

Appendix H: Covariate analysis shortcomings

The morphology of an individual affects its behaviour (Beale & Monaghan, 2004; Bird et al. *in prep*). Therefore, body length (m) and body area index (BAI) are thought to be important variables affecting PCFG foraging behaviour, because length is an indicator of individual age and BAI is an indicator of body condition. Whale length and BAI were calculated from drone video footage collected during field tagging efforts or within 15 days of the tagging date according to previously established field methods (**see Chapter 3**).

We considered using body length (m) and Body Area Index (BAI) as co-variates for the proxies of the energetic cost of different behaviours in PCFG grey whales. However, Overall Dynamic Body Acceleration (ODBA; ms^{-2}) and stroke rate (Hz) had to be standardized to account for tag placement and body length, and stroke amplitude could only be compared within a deployment due to its dependence on tag placement and lack of an appropriate standardization method. The standardization method for ODBA adjusted the ODBA values for each deployment so that all 10 deployments had the same median ODBA , and thus making it impossible to detect variation in ODBA due to differences in length and BAI, the latter of which is calculated using body length (**Figure H1a,b**). Further consideration was given to the impact of the deployment duration on the ODBA values for each deployment. However, deployment duration did not impact this energy expenditure proxy (**Figure H1c)**. Stroke rate is known to have a negative relationship to body length (Gough et al., 2021; Sato et al., 2007) and was standardized to explicitly remove the effect of morphology on this energy expenditure metric.

Additionally, the small sample size of individual deployments in the study means we have not captured the full body length and BAI spectrum of the PCFG grey whale population. This further limits this study's ability to detect an effect of morphology on the energetic cost of behaviours. Therefore, while the effects of body length and BAI could not be explicitly analyzed, differences in the relative energetic cost of behaviours between individuals, which likely include residual effects of differences in morphology, were examined in the results and summarized in the main text.

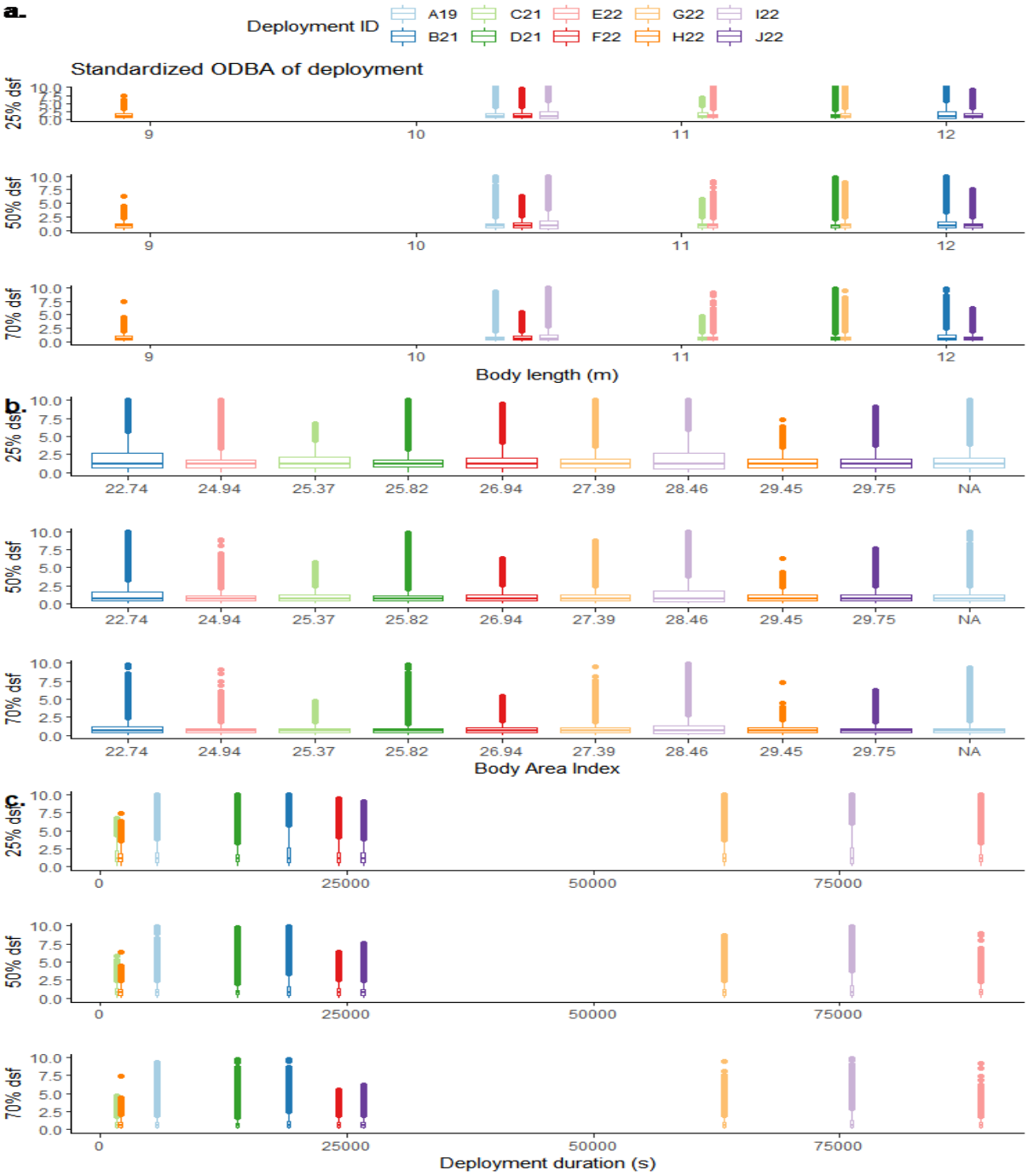

Figure H1. Standardized Overall Dynamic Body Acceleration (ODBA; ms^{-2}) of deployment for each whale compared to body length (m; a), body area index (BAI; b), and deployment duration (s; c). Note that y-axes of all panels were adjusted from a maximum value of 20.0 to 10.0 to better see the box of the box and whisker plot. The standardized ODBA for each deployment has the same median given the standardization method of (Isojunno and Miller, 2015)**. One deployment A19 does not have a BAI measurement from within 15 days of the tagging date and therefore was given a BAI of NA in panel b. Each deployment has many high-value outliers, additionally in the range of values between 10.0 and 20.0 that were excluded from the figure.**